Evaluation of the Deep Geothermal Potential Below Four South Slave Communities, Northwest Territories, Canada

Thesis of 60 ECTS credits submitted to the School of Science and Engineering at Reykjavík University in partial fulfillment of the requirements for the degree of
Master of Science (M.Sc.) in Sustainable Energy Sciences

June 2025

Supervisors:

Jasmin Raymond, Supervisor
Institut national de la recherche scientifique (INRS), Centre Eau Terre Environnement
Juliet A. Newson, Co-Supervisor
Háskólinn í Reykjavík, Iceland School of Energy (HR-ISE)

Examiner:

Samuel Warren Scott, Examiner
Associate Professor, University of Iceland

Evaluation of the Deep Geothermal Potential Below Four South Slave Communities, Northwest Territories, Canada

Michaël Thibault

June 2025

Abstract

The Northwest Territories, Canada, has some of the highest energy costs in the country, which is more than twice the national average. Heating demands account for a significant portion of total energy consumption, with these needs primarily met through imported diesel combustion, leading to high costs and environmental concerns.

In the Southern Northwest Territories, within the South Slave region, the communities of Hay River, Fort Providence, Enterprise, and Kakisa are located along the eastern edge of the Western Canada Sedimentary Basin, within one of Canada's largest high heat flow anomalies. While previous studies have suggested high geothermal potential based on regional assessments, no studies have been carried out at a community-specific scale, leaving the actual localized potential largely unexplored.

This study fills this knowledge gap by providing a comprehensive geothermal assessment for these communities, grounded in specific geological units and rock types found beneath the region. Using laboratory-measured thermal properties from Precambrian basement rocks, this research provides updated temperature estimates to 10 km depth, improving upon previous models that did not account for localized geological variations.

At the top of the Precambrian basement (500 to 750 m depth), temperatures range from 30 to 36 °C, with temperatures reaching 100–156 °C at 3 km depth and 303–511 °C at 10 km depth. The findings show that geothermal gradients vary significantly across the communities, with Hay River exhibiting the highest geothermal potential.

These temperature estimates are essential for evaluating the feasibility of geothermal systems, for space heating and potential power generation, especially heat conduction driven closed-loop systems. This research emphasizes the importance of localized geothermal assessments in remote northern regions, providing a foundation for future exploration and energy planning that could reduce diesel reliance and support sustainable energy solutions, contributing to energy independence and climate change mitigation.

Mat á djúpum jarðhitamöguleikum fyrir neðan fjögur suðurþrælasamfélög, Norðvesturhéruð, Kanada

Michaël Thibault

júní 2025

Útdráttur

Norðvestursvæðin í Kanada, eru með hæsta orkukostnað í landinu, sem er meira en tvöfalt meira en landsmeðaltalið. Þörf fyrir upphitun er stór hluti af heildarorkunotkun, þar sem þessum þörfum er fyrst og fremst mætt með brennslu á innfluttri dísilolíu, sem leiðir til mikils kostnaðar og umhverfisskaða.

Í Suður-norðvestur héruðunum, innan Suðurþrælasvæðisins, eru samfélögin Hay River, Fort Providence, Enterprise og Kakisa staðsett meðfram austurbrún Vestur-Kanadadíska setvatnsbotnsins, innan eins stærsta hluta í háhitaflæði Kanada. Þó að fyrri rannsóknir hafi bent til mikilla jarðhita möguleika á grundvelli svæðisbundinna mats, hafa engar rannsóknir verið gerðar á sértækum samfélags mælikvarða, sem gerir raunverulegan staðbundna möguleika að mestu ókannaða.

Þessi rannsókn fyllir þennan þekkingarskort með því að leggja fram yfirgripsmikið jarðhitamat fyrir þessi samfélög, byggt á tilteknum jarðfræðilegum einingum og bergtegundum sem finnast undir svæðinu. Með því að nota rannsóknir til að mæla eiginleika hitauppstreymis í forkambríum kjallarabergi, gefa þessar rannsóknir uppfært hitamat á 10 km dýpi, sem bætir við fyrri líkön sem tóku ekki tillit til jarðfræðilegra staðbundinna breytinga.

Efst í forkambríukjallaranum (500 til 750 m dýpi) er hiti á bilinu 30 til 36 °C, hiti nær 100–156 °C á 3 km dýpi og 303–511 °C á 10 km dýpi. Niðurstöðurnar sýna að jarðhitahallinn er mjög breytilegur eftir samfélögum, þar sem Hay River sýnir hæsta jarðhitagetuna.

Þessar áætlanir um hita eru nauðsynlegar til að meta hagkvæmni jarðhitakerfa, til húshitunar og hugsanlegrar orkuöflunar, sérstaklega fyrir lokað varmaleiðingar drifnu kerfi. Þessar rannsóknir leggja áherslu á mikilvægi staðbundins mats á jarðhita á afskekktum norðlægum svæðum, sem leggur grunn að framtíðarrannsóknum og orkuskipulagi sem gæti dregið úr neyslu á dísilolíu og stutt sjálfbærar orkulausnir, stuðlað að orkusjálfstæði og jákvæðum loftslagsbreytingum.

Evaluation of the Deep Geothermal Potential Below Four South Slave Communities, Northwest Territories, Canada

Michaël Thibault

Thesis of 60 ECTS credits submitted to the School of Science and Engineering
at Reykjavík University in partial fulfillment of
the requirements for the degree of
Master of Science (M.Sc.) in Sustainable Energy Sciences

June 2025

Student:

Michaël Thibault

Supervisor:

Jasmin Raymond

Examiner:

Samuel Warren Scott

2025-05-01

date

Michaël Thibault
Master of Science

I dedicate this to Guizmo, Émilie, all my family, friends, and everyone whas has helped me through my health journey.

Acknowledgements

This research was funded by the Natural Sciences and Engineering Research Council of Canada (NSERC), the Northwest Territoires Geological Survey (NTGS), the Northern Scientific Training Program (NTSP) and the GEM-GeoNorth program of Natural Resources Canada.

I want to acknowledge that this work was conducted on the ancestral territory of the Dehcho First Nations, home of the Dene people, and I sincerely thank them for welcoming us on their land and for their warm hospitality.

I would like to sincerely thank my supervisor, Jasmin Raymond, for your trust, unwavering support, and the incredible opportunities you have offered our team and me. None of this would have been possible without your guidance. Your open-mindedness, generosity, leadership and mindset create an inspiring environment where collaboration thrives, where we feel supported, and where we are encouraged to give our best—not only for ourselves, but for one another. You are not only the best supervisor I could ever had, but above all, a great person. I am deeply grateful for this journey.

Special thanks to Félix-Antoine Comeau and Mirah Rajaobelison for your invaluable help and dedication throughout this project. Your contributions and teamwork have made a real difference.

Viktor Terlaky and S.M. Talha Qadri, I would like to express my gratitude for your belief in this project, your encouragement, and for trusting me from the beginning. I also thank Dr. Rod Smith and Jacek Majorowicz for their valuable discussions and insights.

Thank you to Juliet Newson and the Iceland School of Energy (ISE), its staff, professors, and fellow students for making this program such a meaningful experience in a country I had dreamed of visiting since childhood.

I also want to recognize the inspiration I have drawn from the brilliant women from our team and throughout my academic journey—you are truly impressive and inspiring.

Also thank you to the Office of the Regulator of Oil and Gas Operations (OROGO) and the Geological Survey of Canada (GSC) Core Repository in Calgary (CRC) for providing access to the drilling cores and assistance with sampling. NTGS staff and Tais Pinto for facilitating access to archived samples.

I would like to express my heartfelt thanks to Guizmo, Émilie, and all my family, as well as everyone who has supported me throughout my personal and health journey. You will forever hold a very special place in my heart. Without your presence and support, I wouldn't be where I am today. I will always be grateful to life for having crossed paths with you. The past hasn't been easy. I've come a long way, and what once seemed impossible became a dream I managed to live. I worked very hard, and while it wasn't always smooth, every effort was worth it. I would like to end with a personal quote that helped me through many moments in my life: « Tout est dans la manière de voir les choses ».

Preface

The dissertation is original work by the author, Michaël Thibault and is presented in the manuscript thesis format. Chapter 3 is a copy of an article published in the *Geothermal Rising Conference Transactions*. The Appendix includes a copy of a peer-reviewed journal article to which I contributed as the second author, in collaboration with the lead author. The other chapters provide a more comprehensive context and methodological framework.

Contents

List of Figures

List of Tables

List of Abbreviations

API	American Petroleum Institute units
BHT	Borehole temperature
CB SS	Cretaceous basal sandstone
CRC	Core Repository in Calgary
DBHE	Deep borehole heat exchanger
DST	Drill-stem test
E	Enterprise
EGS	Enhanced geothermal systems
fm.	Formation
FP	Fort Providence
FPIC	Free, Prior and Informed Consent
Ft.	Fort
GR	Gamma Ray
GSC	Geological Survey of Canada
HR	Hay River
INRS	Institut national de la recherche scientifique
ISE	Iceland School of Energy
K	Kakisa or Potassium
LOG	Laboratoire Ouvert de Géothermie
MSc	Masters of Science
N	Normal
NPHFA	Northern Plains Heat Flow Anomaly
NSERC	Natural Sciences and Engineering Research Council of Canada
NSTP	Northern Scientific Training Program
NTGS	Northwest Territories Geological Survey
NWT	Northwest Territories
O	Optimist
OROGO	Office of the Regulator of Oil and Gas Operations
P	Pessimist
sc.	Scenario
TD	Tectonic Domain
Th	Thorium
TVD	True vertical depth
U	Uranium
USA	United States
WCSB	Western Canada Sedimentary Basin

List of Symbols

Symbol	Definition	Units
Latin Symbol		
A	Heat Generation Rate	W m^{-3}
erf	Error function	
g	Geothermal gradient	°C m^{-1}
G	Coefficient of variation	%
IF	Inhomogeneity factor	
n	Number of samples	
P	Percentile	
Q	Heat flow	W m^{-2}
t	Time	s
T	Temperature	°C
z	Depth	m

Greek Symbol		
α	Thermal diffusivity	m^{2} s ^{1}
ρc	Volumetric heat capacity	J m^{-3} K^{-1}
λ	Thermal conductivity	W m^{-1} K^{-1}

Subscript	
amb	Ambient air
cf	Coefficient correction
Eq	Equilibrium
i	Step between glaciations
m	Measured and corrected from drilling disturbance
max	Maximum
min	Minimum
PC	Precambrian basement
sed	Sedimentary sequence
s	Surface
z	Depth

Chapter 1

Introduction

1.1 Context

1.1.1 Geography

The study area is situated in the southern part of the Northwest Territories (NWT), Canada (Figure 1.11.1), and includes four communities within the South Slave administrative region: Hay River (population 3169), Fort Providence (618), Enterprise (75), and Kakisa (39), according to the 2021 Canadian Census (Government of Canada, 2022). These communities are located within the traditional territory of the Dehcho First Nations, with local indigenous groups, including the K'atlodeeche First Nation, the West Point First Nation, the Deh Gáh Got'îê First Nation, and the Ka'a'gee Tu First Nation. The study site is located north of the 60th parallel to the southwest of Great Slave Lake, in a subarctic climate zone (Amani et al., 2019).

Figure 1.1. Study area (outlined in red) within the NWT, shown in green.

1.1.2 Geological Settings

The study area is located at the eastern margin of the Western Canada Sedimentary Basin (WCSB), which is part of the Interior Platform. It is bordered by the Cordilleran Orogen to the west and the Canadian Shield to the east (Figure 1.21.2).

The WCSB is known for its significant oil and gas reserves, underpinned by a complex geological history involving multiple tectonic events and sedimentary processes (Mossop & Shetsen, 1994). In this region, it's composed of a thin sedimentary cover, ranging from 500 to 750 meters in depth consisting of Devonian marine dolostones, limestones, sandstones, and shales (Gal & Jones, 2003).

Underneath lies the basement, made up of Precambrian metasedimentary and crystalline rocks (Ootes et al., 2015). It forms a complex geological structure with limited permeability and variable thermal properties, which significantly influence the geothermal potential of the region (Majorowicz et al., 2014a).

Figure 1.2. Geological regions of Canada, modified from Miall (2015). Orogenic belts are shown in black, the Canadian Shield in salmon, and the interior platforms in pale yellow. WCSB is outlined with dashed lines. Major lakes of the Northwest Territories, including Great Slave Lake, are shown in pale blue. The study area is indicated by a red box.

Previous studies have revealed a high geothermal potential for this region (EBA Engineering Consultants Ltd., 2010; Grasby et al., 2012; Majorowicz & Grasby, 2010a, 2010b). This potential is largely attributed to the elevated high heat flow, which exceeds 100 mW m^{-2} in the area (Rajaobelison et al., 2024). However, the region's deep geothermal potential remains uncertain due to the lack of detailed data on the subsurface thermal regime, including the specific characteristics of the Precambrian basement rocks. The region's complex tectonic history further complicates geothermal exploration, with significant variability in the properties of the basement rocks, such as the Slave Craton, Great Bear Magmatic Zone, and Hottah Terrane (Majorowicz et al., 2014a; Ootes et al., 2015). These domains, each with distinct thermal properties, play a key role in the geothermal assessment of the region.

1.1.3 Energy

The NWT faces some of the highest energy costs in Canada—more than twice the national average (Canada Energy Regulator & Government of Canada, 2023). Space heating represents a major share of total energy demand, particularly during the winter. In the South Slave region, as in other NWT communities, heating needs are met almost exclusively through diesel combustion (Arctic Energy Alliance, 2018; Government of Northwest Territories, 2024; Mahbaz et al., 2020). This heavy reliance on diesel not only results in high energy costs but also contributes significantly to greenhouse gas emissions and poses environmental risks associated with fuel transportation and storage in remote areas.

1.2 Problematic

Despite the recognized geothermal potential of the region (EBA Engineering Consultants Ltd., 2010; J. Majorowicz & Weides, 2014, Grasby), no detailed localized assessment of deep geothermal resources has yet been carried out for the communities in the area. The geological context presents significant challenges for the development of conventional hydrothermal systems. The sedimentary rock sequence is relatively thin and likely has low permeability, limiting the feasibility of fluid-based geothermal circulation (Rajaobelison et al., In press), and the basement is likewise anticipated to have low permeability (Majorowicz et al., 2014b).

Alternative technologies, such as closed-loop Deep Borehole Heat Exchangers (DBHE) and Enhanced Geothermal Systems (EGS), offer promising solutions that rely primarily on conductive or forced convective heat transfer. However, their implementation requires robust thermal modeling, which in turn depends on accurate knowledge of subsurface thermal properties and temperature distributions.

Currently, the thermal properties of the underlying Precambrian basement remain poorly constrained due to a lack of data (Rajaobelison et al., 2024). This uncertainty significantly limits the ability to accurately evaluate the actual potential for geothermal energy uses in the region.

To assess the feasibility and performance of such systems, it is crucial to characterize both the shallow sedimentary sequence (at depths ranging from 525 to 729 meters) and the thermal behavior of the underlying basement. Addressing these knowledge gaps is essential to reduce uncertainties and support the development of effective geothermal energy solutions adapted to the region's heating needs.

1.3 Objectives

The primary objective of this research is to evaluate the deep geothermal potential of the South Slave Region by characterizing the subsurface thermal regime and estimating temperatures at depth. This includes analyzing the thermal properties of both the Devonian sedimentary rocks and the underlying Precambrian basement.

This work builds upon the methodology detailed in the following chapters and leverages the results of the author's previous research, including the paper by Thibault et al. (2024), which serves as the foundation for the geological characterization and thermal modeling conducted in this study.

By focusing on the communities of Fort Providence, Kakisa, Hay River, and Enterprise, this study aims to address current knowledge gaps that will further help provide a more accurate assessment of the geothermal resources available. Ultimately, the goal is to better define the geothermal potential of these remote northern communities and support the development of sustainable, locally adapted energy solutions.

Chapter 2

Methods

This study follows a two-step methodological approach: geological assessment and calculation at depth. The geological assessment involves evaluating the subsurface geology of the four communities through sampling and laboratory analyses as well as lithostratigraphic analyses. Rock samples were collected from historical oil and gas exploration wells and field sampling campaigns. These samples were analyzed in the laboratory to characterize the thermal properties of the lithologies forming the stratigraphic units. Additionally, a detailed lithostratigraphic analysis was conducted, including the construction of stratigraphic columns and the assessment of the lithologic composition of each geological unit to refine the thermal stratigraphy beneath the communities. The calculation at depth section focuses on numerical modeling to estimate subsurface temperature distribution.

2.1 Geological Assesment

2.1.1 Sampling

Soil samples (Quaternary drift deposits), sedimentary rocks, and Precambrian basement rocks were collected through field sampling, core archives, and rock archives to analyze their thermal properties. The goal was to collect a diverse set of rock samples from different geological units encountered below the community stratigraphy. The aim was to create a comprehensive geological profile of the area and evaluating the properties of the underlying subsurface.

Field sampling took place during the 2024 summer campaign, which had to be terminated earlier than expected due to the evacuation of the region because of forest fires. Samples were collected from rock outcrops, primarily accessible by car and forest hikes on the mainland. Additionally, samples were gathered from the coast and islands of the East Arm of the Great Slave Lake, using a boat to reach the outcrops (Figure 2.12.1).

Furthermore, samples were borrowed from the Geological Survey of Canada's (GSC) core repository in Calgary (CRC), which included vintage oil and gas exploration cores. Geological units of interest were sampled as much as possible while adhering to strict guidelines set by the Regulator of Oil and Gas Operations (OROGO) and the GSC CRC.

In 2022 and 2023, split cores from vintage exploration wells in the South Slave region were sampled at the GSC CRC (Figure 2.22.2). The majority of the samples were sedimentary rocks, with a few rare Precambrian basement samples. The core sampling intervals were based on the availability and conditions of the cores, as detailed in the Geothermal Database Compilation by Petrel Robertson Consulting Ltd (2022). The main goal of this work was to sample existing core units stored at the GSC CRC.

Personnel from the GSC CRC, on behalf of OROGO, carefully analyzed each request, formulated recommendations, and provided clear instructions on which intervals were permissible for sampling. According to the authorization, the maximum number of samples allowed per geological formation for each drilled well was two, with each sample not exceeding 20 cm in length. Challenges arose due to the quality and quantity of available material, as most cores had already been partially cut, leaving only halves, thirds, quarters, or smaller fractions of the original cores. To ensure accuracy, the head of the GSC CRC personally authorized every sample selected before the cutting process. Core material was sawed on-site to match the length of the remaining core slabs, ensuring that no more than 50% of the available material was removed for analysis. These core slabs were then borrowed for a fixed period, sent for laboratory analysis at the Laboratoire Ouvert de Géothermie (LOG) in Québec City, and returned under the same conditions as they were sampled.

Additionally, 38 Precambrian basement samples were collected from the NTGS storage archives in Yellowknife, originating from previous field campaigns in the Slave, Bear, and Churchill geological Provinces, and collected by NTGS staff (Figure 2.12.1).

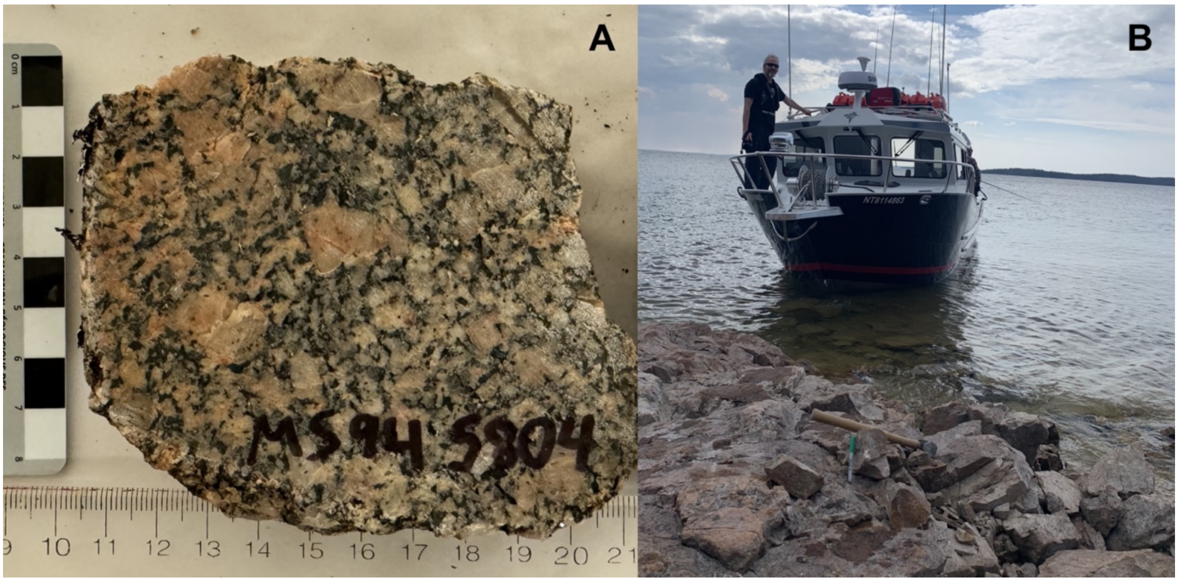

Figure 2.1. A) Monzogranite sample from NTGS archives, sampled by Mike Stubley in 1994 in the Slave Province. B) Sample from the coast of the East Arm of the Great Slave Lake, utilizing a boat to access the outcrop.

Figure 2.2. A) Transition of the Mirage Points red beds and the La Loche (Basal Clastics) sandstone from CS LAFERTE RIVER A-66 vintage well, 536.5 to 554.7 meters depth. B) Mirage Points red beds sample, 548 meters deep, from CS LAFERTE RIVER.

2.1.2 Laboratory measurements

The thermal properties of both unconsolidated sediments and solid rocks (sedimentary rocks and Precambrian basement rocks) were measured at the LOG using two distinct techniques. An optical scanning instrument developed by Popov et al. (2023) was used for rock samples, while a needle probe was employed for soil samples developed by Decagon Devices (2011).

The thermal behavior of geological materials is primarily governed by three key properties: thermal conductivity, which quantifies the ability of a material to conduct heat; thermal diffusivity, which indicates how quickly a material responds to temperature changes; and volumetric heat capacity, which represents the amount of heat a material can store per unit volume. These parameters are critical for assessing heat transfer dynamics in the subsurface (Clauser, 2011).

2.1.2.1 Sample Preparation

All rock samples, whether collected during field campaigns or obtained from archives, underwent preparation before analysis at LOG. Each sample was sawed to obtain a clean, flat surface unaffected by weathering. The cut orientation was selected to maximize the measurement length and to ensure a representative scanning surface for thermal property analysis. Additionally, samples had to meet specific dimensional criteria: a minimum width of 2.4 cm to fit within the scanner and a thickness greater than the width to improve the representativeness of the results. To enhance infrared absorption, the flat sides of the samples were coated with black acrylic paint. The scan lines were carefully positioned to pass through the most characteristic portions of the sample. For samples displaying schistosity, two perpendicular scan lines were prepared—one parallel and one orthogonal to the foliation.

2.1.2.2 Optical Scanning Methodology for Rocks

Thermal conductivity (λ, in W m^{-1} K^{-1}), thermal diffusivity (α, in m^2 s^{-1}), coefficient of variation (G, %), and inhomogeneity factor (IF) were determined using an optical scanning device developed by Popov et al. (2023). This method involves a moving infrared heat source and temperature sensors that measure thermal response along the scan line. To ensure consistent measurement conditions, all samples and reference standards (fused quartz, titanium alloy, or gabbro) were stored at room temperature for at least 24 hours before analysis. The scanning speed was set to 5 mm s^{-1}, with thermal conductivity measurements recorded every 2 mm. Each rock sample was scanned three times to evaluate analytical variability.

The inhomogeneity factor was calculated to quantify the heterogeneity of each sample, following the equation:

$$IF = \frac{2 * (\lambda_{max} - \lambda_{min})}{(\lambda_{max} + \lambda_{min})} \tag{2.1}$$

where λ_{max} and λ_{min} represent the maximum and minimum thermal conductivity values measured along the scan line.

Volumetric heat capacity (ρc, in J m^{-3} K^{-1}) was calculated using the relation:

$$\rho c = \frac{\lambda}{\alpha} \tag{2.2}$$

2.1.2.3 Needle Probe Methodology for Soils

Thermal properties of soil samples were measured using a KD2 Pro portable device (Decagon Devices, 2011), which applies the transient line heat source method. Measurements were conducted at room temperature under in situ and saturated conditions. To preserve natural compaction and moisture content, soil samples were collected using a cylindrical copper tube inserted into the deposits, then sealed with multiple layers of plastic wrap before transport. Measurements were performed in a controlled environment at constant temperature.

Based on regional groundwater well data (Government of Northwest Territories et al., 2023; Mackenzie Valley Land and Water Board, 2023), the quaternary deposits function as an aquifer, with the water table generally between 1 and 5 meters below ground level near the communities. Given these conditions, thermal properties were assessed under full saturation for all sites where sediment thicknesses exceeded 10 meters. For Enterprise, where the soil layer is approximately 4 meters thick, an average of saturated and in situ conditions was used to estimate the mean thermal properties.

For further details on the specific results and compilations of these measurements and additional analyses, refer to the annual internal report prepared for the NTGS (Rajaobelison et al., In press; Thibault et al., 2025). These reports were produced as part of the research collaboration agreement supporting the student's scholarship for the work on this joint project.

2.1.3 Lithostratigraphic analyses

To refine the understanding of the sedimentary strata beneath the studied communities, lithostratigraphic analyses were conducted using regional geological data, formation top records, and stratigraphic columns. These analyses provide a basis for evaluating the geothermal gradient and resource potential in each area.

2.1.3.1 Stratigraphic Columns

Stratigraphic columns were constructed for each community (Figure 2.32.3) based on a combination of literature data (Gal & Jones, 2003; Meijer-Drees, 1993; Morrow, 2012; Mossop & Shetsen, 1994; Rocheleau & Fiess, 2014) and Well History Files from the nearest historical oil and gas wells (three for Fort Providence, four for Kakisa, nine for Hay River, and eight for Enterprise). Wells coordinates were sourced from OROGO Well Status Files (OROGO, 2024), and formation tops were determined using data from Hogue & Gal (2008) and individual Well History Files.

The stratigraphic columns were drawn using Inkscape software, incorporating lithologic symbols from the Federal Geographic Data Committee (2006) and formations color schemes aligned with Gal & Jones (2003) to ensure consistency with previous regional studies. The drill hole analysis indicates that the Precambrian crystalline basement lies at depths of approximately 500 to 700 m, overlain by relatively thin Paleozoic sedimentary rocks and Quaternary deposits. The Quaternary sediments range in thickness from 5 m to 15 m. At Fort Providence, Kakisa, and Enterprise, Paleozoic formations are primarily composed of shales, with a cumulative thickness between 500 and 730 m, while in Hay River, carbonate lithologies dominate the sequence.

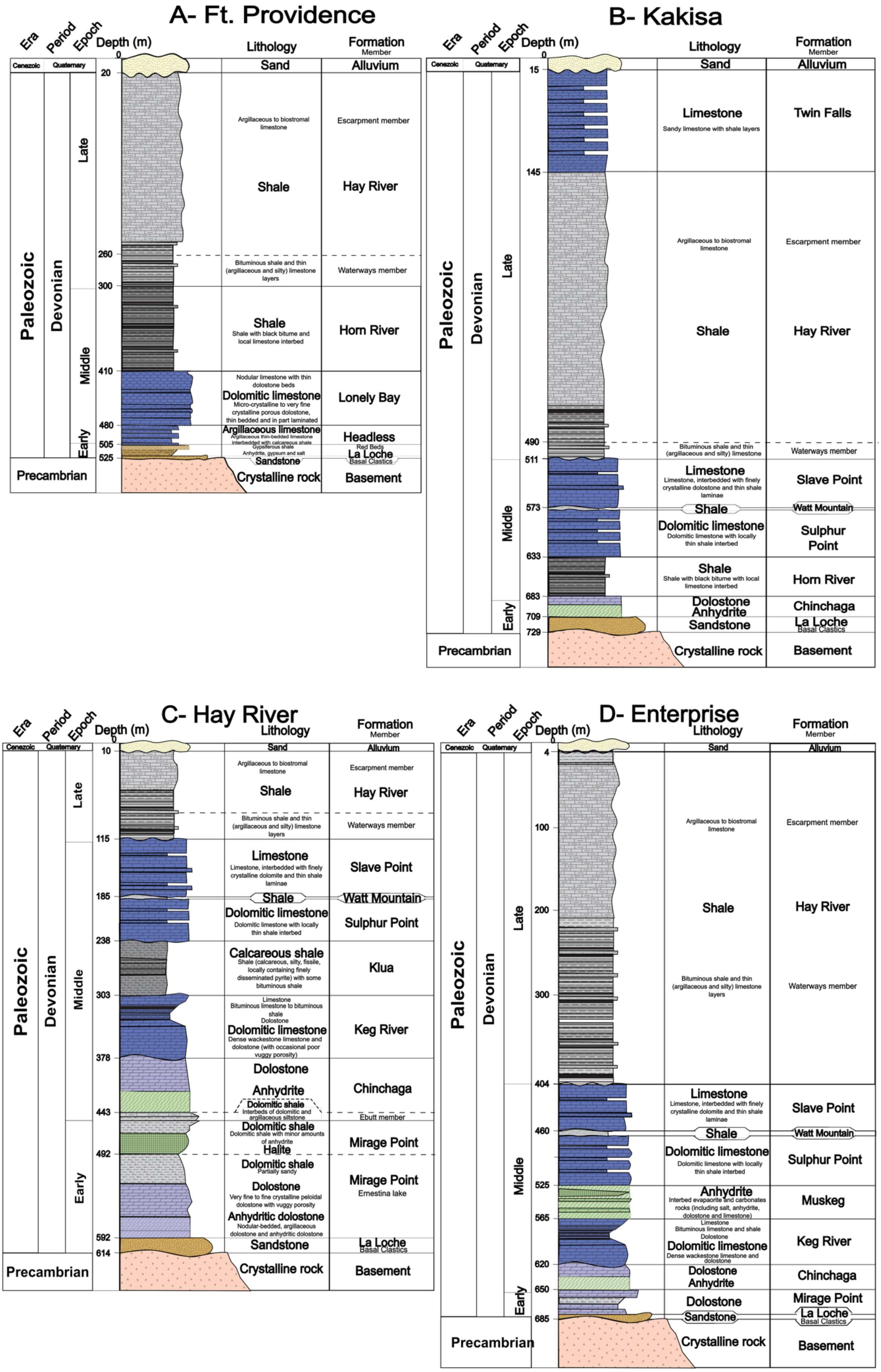

Figure 2.3. Stratigraghic columns at the location of each community.

2.1.3.2 Lithology Composition Evaluation

To complement the lithostratigraphic framework, an assessment of the relative lithological composition of each geological unit was conducted to estimate the average proportion of each rock type. Understanding lithologic composition is crucial for evaluating thermal conductivity in the subsurface, as it directly relates to rock mineralogy.

The relative lithological composition of each unit was then estimated based on information from type section references (Government of Canada & Natural Resources Canada, 2022; Meijer-Drees, 1993), previous core and outcrop descriptions (Gal & Jones, 2003; Morrow, 2012; Mossop & Shetsen, 1994; Rocheleau & Fiess, 2014), and data from Well Files Reports (OROGO, 2024).

Table 2.12.1 provides a general overview of the estimated lithological composition for each geological unit within the communities. The units are organized in ascending order of age, from youngest to oldest, following a left-to-right sequence.

Table 2.1. Lithological composition of geological units of interest.

Geological Unit/ Formation name	Lithology	%
Alluvium	Sand Clay Till	100
Twin Falls	Limestone	95
	Shale	5
Hay River	Shale	92
	Limestone	8
Hay River (Escarpment member)	Shale	90
	Limestone	10
Hay River (Waterways member)	Shale	60
	Limestone	40
Slave Point	Limestone	92
	Shale	4
	Dolostone	4
Horn River	Shale	95
	Limestone	5
Watt Mountain	Shale	92
	Limestone	3
	Sandstone	5
Sulphur Point	Limestone	78
	Dolostone	20
	Shale	2
Muskeg	Anhydrite	90
	Dolostone	10
Klua	Shale	98
	Limestone	2
Keg River	Limestone	90
	Dolostone	10

Geological Unit/ Formation name	Lithology	%
Lonely Bay	Dolostone	50
	Limestone	50
Chinchaga	Anhydrite	43
	Dolostone	30
	Shale	23
	Limestone	2
Chinchaga (Ebbutt Member)	Shale	83
	Limestone	10
	Dolostone	5
	Anhydrite	2
Headless	Limestone	50
	Shale	45
	Dolostone	5
Mirage Point	Shale	62
	Dolostone	15
	Halite	15
	Anhydrite	8
Mirage Point (Ernestina Lake)	Dolostone	55
	Anhydrite	25
	Shale	20
La Loche	Sandstone	99
	Shale	1
La Loche (Red Beds)	Sandstone	100
La Loche (Basal Clastics)	Sandstone	100
Precambrian	Igneous and metamorphic mix	100

2.2 Subsurface temperature assessment

The detailed mathematical formulation and governing equations used for subsurface temperature modeling are discussed extensively in the following chapter. Briefly, the methodology begins with the correction of well temperature data for drilling disturbances and paleoclimate effects. Based on these corrected values, the geothermal gradient is estimated, which then allows for the calculation of surface and basement heat flow. Finally, subsurface temperatures are determined using a one-dimensional steady-state conductive model, applied across the sedimentary sequence and the Precambrian basement. These calculations build on previous studies and ensure consistency across all study sites.

As part of this research, two scientific papers were published: a peer-reviewed article by Rajaobelison et al. (2024) in August and a conference paper by Thibault et al. (2024). The first article, in which I contributed as the second author alongside the lead author, a Postdoctoral researcher, focuses on the thermostratigraphic and heat flow assessment of the four South Slave communities. It develops 1D temperature models using historical oil and gas well data to estimate subsurface temperatures within the sedimentary sequence (Rajaobelison et al., 2024). The second paper, presented at a conference, examines temperature distribution in the Precambrian basement, providing insights into deep geothermal conditions beneath the communities (Thibault et al., 2024).

Chapter 3

Manuscript

Title of the paper:
Evaluation of the Precambrian Basement Temperature Below Four South Slave Communities, Northwest Territories, Canada

Authors:
Michaël Thibault[1,2], Félix-Antoine Comeau[1], Jasmin Raymond[1], Mirah Rajaobelison[1], Viktor Terlaky[3], Juliet Newson[2]
[1] Institut national de la recherche scientifique (INRS)
[2] Iceland School of Energy (ISE), Reykjavik University
[3] Northwest Territories Geological Survey (NTGS)

Published:
Thibault, M., Comeau, F.-A., Raymond, J., Rajaobelison, M., Terlaky, V., & Newson, J. (2024). Evaluation of the Precambrian Basement Temperature Below Four South Slave Communities, Northwest Territories, Canada. *GRC Transactions*, *48*, 28.

3.1 Abstract

Fort Providence, Kakisa, Hay River, and Enterprise are four South Slave communities located in the Northwest Territories (Canada). These communities rely on fossil fuels for space and water heating, and could benefit from geothermal systems. The South Slave Region is estimated to have the highest heat flow (>100 mW m^{-2}) in the Western Canadian Sedimentary Basin (WCSB), therefore is a target for geothermal exploration. However, an analysis of the deep geothermal resources has not been undertaken in this region. This research project objective is to fill this knowledge gap by providing a Precambrian basement temperature assessment below the sedimentary basin, around the four communities.

The Devonian sedimentary rock sequence on which the communities lie is thin (500 to 750 m) and has relatively low permeability (on average $<10^{-14}$ m^2). The lack of information on the Precambrian basement below Devonian sedimentary rocks limits the development of deep geothermal energy resources due to high uncertainty and risk. Deep borehole heat exchangers (DBHE) could be an appealing technology for direct use of heat in this geological context. However, a comprehensive assessment requires a detailed understanding of the thermal properties of the rocks. This information is mandatory to model such systems and provide accurate temperature estimates at depth.

A rock sampling campaign focusing on the Precambrian basement rocks was made in summer 2023, during which 91 outcrops and drilling cores were sampled to analyze their

thermal properties. A range of thermal conductivity expected in the Precambrian basement was determined for the location of each community. Then, the results were used to extrapolate the subsurface temperature in the Precambrian basement until 10 km depth. The newly available information confirmed the presence of a significant geothermal potential in these communities.

In the more likely scenario (the normal one), the temperature at the top of the Precambrian basement ranges from 30.5 to 36.5 °C, with a basement surface heat flow of 99 mW m^{-2} to 157.7 mW m^{-2}. At 3 km depth, the temperature ranges from 100.4 to 156 °C; at 10 km depth, the temperature ranges from 303.6 to 511.6 °C for each community. Hay River has the highest values and most promising geothermal potential for deep closed-loop systems.

3.2 Introduction

Energy costs in northern Canada, populated by several indigenous communities, are higher than in the rest of the country. For example, electricity rates in the Northwest Territories (NWT) are more than twice the national average (Canada Energy Regulator & Government of Canada, 2023). The NWT, like many other northern regions, mainly relies on carbon-intensive fossil fuels such as oil to meet its electricity, space heating, and water heating needs. The Government of the NWT aims to ensure a balance between energy security, affordability, and reduction of greenhouse gas emissions in its 2030 Energy Strategy (Government of Northwest Territories, 2018). Key initiatives include replacing diesel with renewable energy solutions by exploring the potential of technologies such as deep geothermal resources in areas that have been identified as having high geothermal potential (EBA Engineering Consultants Ltd., 2010). These areas have yet to be defined and characterized.

This research project focuses on the geothermal potential of four communities in the southern part of the NWT with the intent of characterizing its deep geothermal resources. The communities (Figure 3.13.1) are located within the South Slave administrative region, part of the Dehcho First Nations: Hay River (Xátł'odehchee, K'atlodeeche First Nation and Ts'ueh Nda, West Point First Nation), Fort Providence (Zhahti Kų́ę́, Deh Gáh Got'îê First Nation), Enterprise, and Kakisa (K'ágee, Ka'a'gee Tu First Nation). Due to their close vicinity, Hay River Town and Hay River Dene (Katlodeeche First Nation Reserve) are referred to as "Hay River" in the study.

These four communities are situated within the largest high heat flow anomaly in Canada, known as the Northern Plains Heat Flow Anomaly (NPHFA) or Northern Anomaly (Majorowicz, 1996; Majorowicz & Weides, 2014). This anomaly is approximately 300 km wide and stretches 500 km from north to south. The geothermal gradient and heat flow in the research areas are significantly higher compared to other Precambrian platform locations worldwide (Majorowicz & Jessop, 1981). Several hypotheses have been proposed to explain the thermal anomalies in this region. Bachu (1993) suggested that the unusually high temperatures measured could be related to hydrogeological effects which can disturb heat flow patterns. Majorowicz (1996) suggested the presence of an increased mantle upflow beneath the region which aligns with other heat flow anomalies along the western margin of the North American Craton. Despite these hypotheses, Majorowicz (2018) concluded that the exact cause of the heat flow anomaly remains speculative.

Rajaobelison et al. (In press) measured thermophysical properties on the NWT South Slave's sedimentary rocks. Then, Rajaobelison et al. (2024) created 1D temperature models based on temperature data from vintage oil and gas wells to evaluate the geothermal potential in the sedimentary sequence of NWT South Slave's communities.

Due to the generally low permeability and porosity inferred for the matrix of the sedimentary rocks analyzed in these studies and the shallow depth of the basement (525 to 729 m), the potential technologies that can be envisioned to produce geothermal energy are closed-loop DBHE relying on conduction to extract heat from rock formations and/or enhanced geothermal systems (EGS) requiring stimulation of potential reservoir formation to extract heat by forced convection.

A temperature model for the Precambrian basement, which lies below the sedimentary sequence, could not be made in previous studies due to a lack of information on the basement thermal properties. Very little information and data exist about the basement below the communities, representing a limitation when it comes to understanding and assessing the geothermal resources of the region. To reach higher temperatures below the sedimentary cover (>37 °C, Rajaobelison et al., 2024), Precambrian basement depth must be considered.

Therefore, this study objective is to assess the temperature at depths within the basement rock beneath the communities. To achieve this goal, we intend to determine a range of thermal properties for each tectonic domain (i.e., the Precambrian bedrock underlying each community). Additionally, we wish to extend previous work on sedimentary sequences (Rajaobelison et al., 2024) by incorporating new data from previously unsampled formations. This will help reduce uncertainties related to the rock thermal properties and temperature calculation at depth.

3.3 Geological Settings

The four NWT communities are located on the eastern edge of the WCSB. It is positioned between the Cordilleran Orogen to the west and the Canadian Shield to the east (Figure 3.23.2). Significant oil and gas exploration activities have taken place since the 1950s, with over 400 exploration wells drilled, most of which are now abandoned (OROGO, 2024) but has contributed to the identification of the high geothermal potential in the area (Figure 3.13.1).

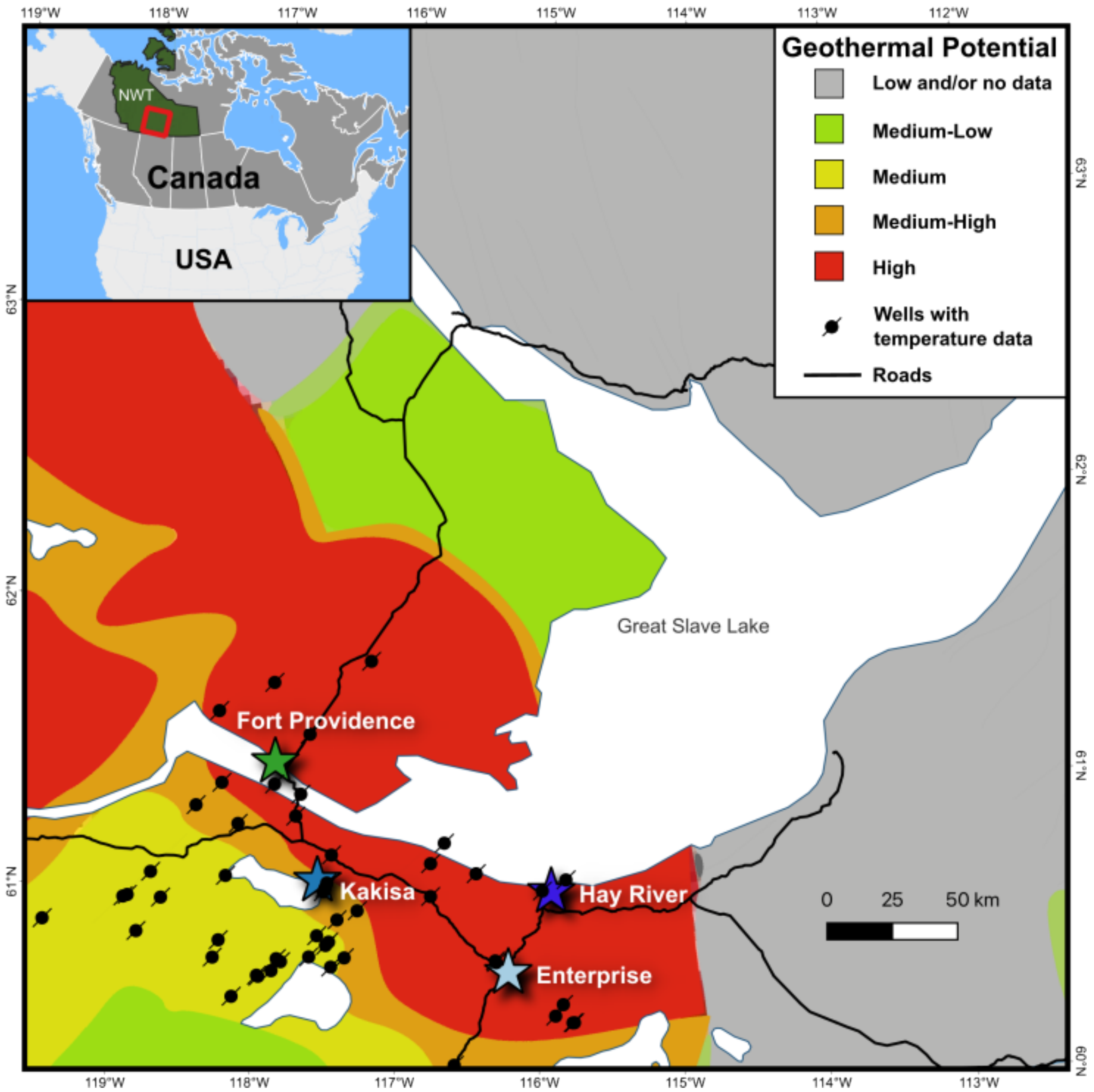

Figure 3.1. Geothermal potential map based on temperature (adapted from EBA Engineering Consultants Ltd., 2010) showing wells (abandoned) with temperature data and community locations.

The Quaternary glacial sediment, often called soil or alluvium, is between 4 m and 20 m thick at the community's location. It was deposited unconformably over the Paleozoic-Cenozoic sedimentary rock formations.

The sedimentary rocks lie on the top of a Precambrian crystalline basement that is part of the Canadian Shield. The sedimentary strata gradually thicken from east-northeast to west-southwest, ranging from about 500 m to 715 m in thickness at the community's locations. Furthermore, the geological formations in the region exhibit low porosity and permeability, implying a limited potential for hot sedimentary aquifers, as noted by Rajaobelison et al. (In press). The anticipated permeability is expected to be mostly influenced by fault and fracture networks rather than the intrinsic porosity of the formations. Conduction is the dominant mechanism for geothermal heat flow in the region (Bachu, 1993; Gray et al., 2012; Majorowicz et al., 1999; 2012), which is the focus of the present study.

The Precambrian basement underlying the sedimentary cover consists of a poorly known mix of igneous and metamorphic rocks. It is characterized and subdivided by tectonic domains (Figure 3.23.2). The domains in the study area, listed from east to west and in chronological order of age are; Slave Craton, Great Bear Magmatic Zone, and Hottah Terrane that is part of Wopmay Orogen accreted terranes (Ootes et al., 2015). All tectonic domains of the Precambrian basement have various compositions, ages and tectonic histories, as well as different thermal properties that are critical for geothermal assessment. Thus, we employ tectonic domain terminology in this study to address basement classification. Hay River and Enterprise are part of the Slave Craton tectonic domain. Fort Providence and Kakisa, on the other hand, are located in Hottah Terrane.

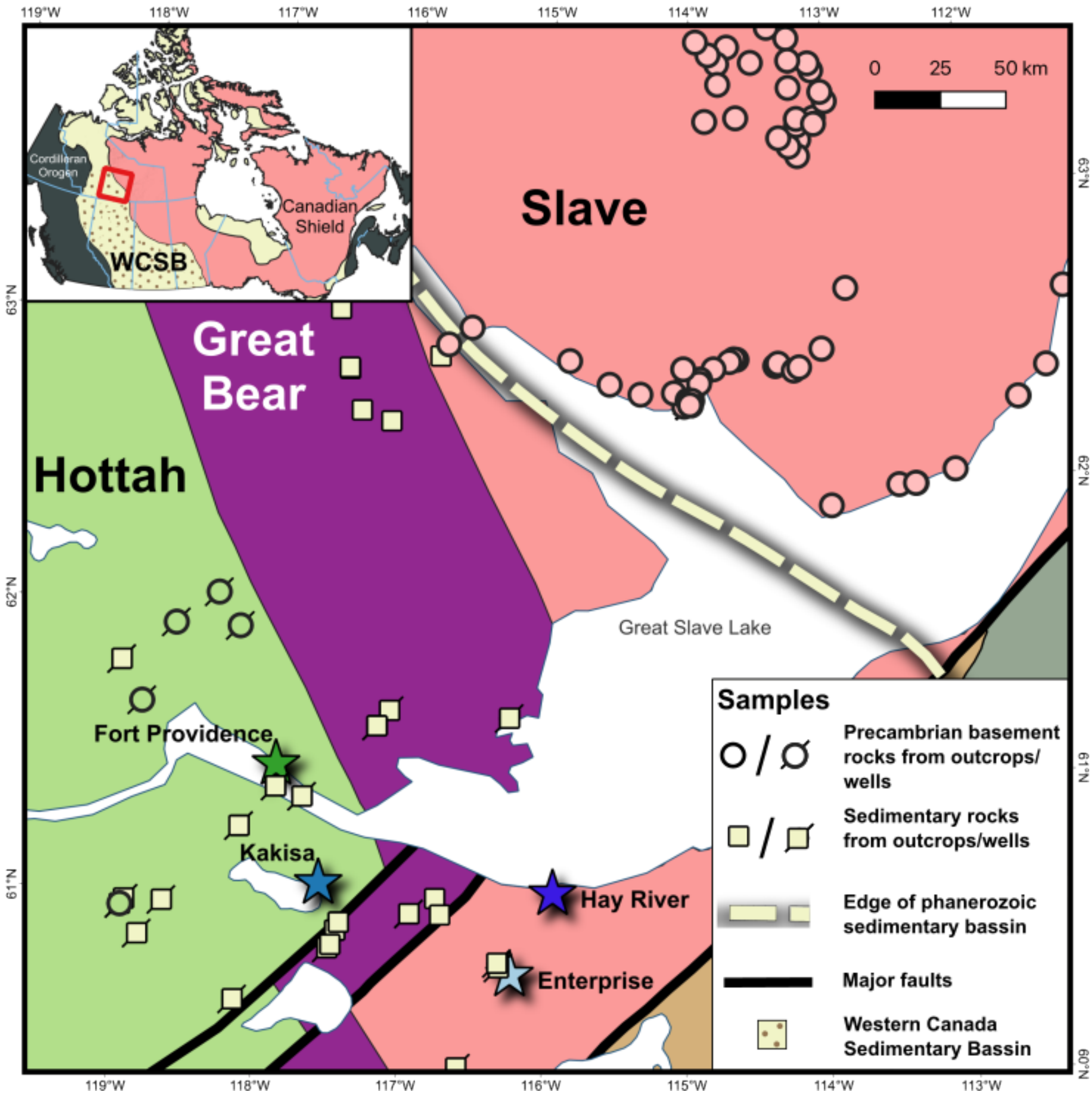

Figure 3.2. Tectonic domain map (based on Ootes et al. (2015) domain division), with samples and community locations.

3.4 Material, Methods and Input Data

To accurately predict temperature at different depths, it was essential to use representative input data that accurately reflected the geological characteristics of the location. Due to the lack of information on thermal properties for geological materials in this area, we conducted extensive sampling and laboratory measurements. Collected data was used as input and is the foundation of subsequent analyses and thermal assessment. We therefore present below an updated thermostratigraphic assessment, providing a new comprehensive dataset for the Precambrian bedrock and enhancing the previous sedimentary rocks sequence data.

This section gives an overview of the sampling process, thermal property analysis, undisturbed ground temperature assessment, input data and scenario examination, and a comprehensive thermostratigraphic assessment. All this information was used to create temperature profiles until the basement's top, 3 km and 10 km depths, which are the main results of this research.

3.4.1 Sampling overview

In 2022, we sampled 84 split core samples from 43 vintage oil and gas exploration wells of the South Slave region. Related descriptions and laboratory results are presented in Rajaobelison et al. (In press). Some sedimentary formations under the communities remained unsampled and thermal conductivity values from literature were assigned based on their lithologic content.

A rock sampling campaign in 2023 allowed the collection of 91 Precambrian basement rock samples, for which we think to have recovered a variety of geological units of each tectonic domain related to each community that could give us a good approximation of the material that can be encountered under these communities (Table 3.13.1). Sedimentary rocks sampling was partial and had to be interrupted due to forest fires and an evacuation order in the area (Figure 3.33.3).

Table 3.1. Sampling overview.

Geological material			Number of samples		
Alluvium					3
Sedimentary Rocks					112
Precambrian Basement Rocks	Igneous	Plutonic	54	66	91
		Volcanic	12		
	Metamorphic	Sedimentary	16	25	
		Plutonic	5		
		Volcanic	4		

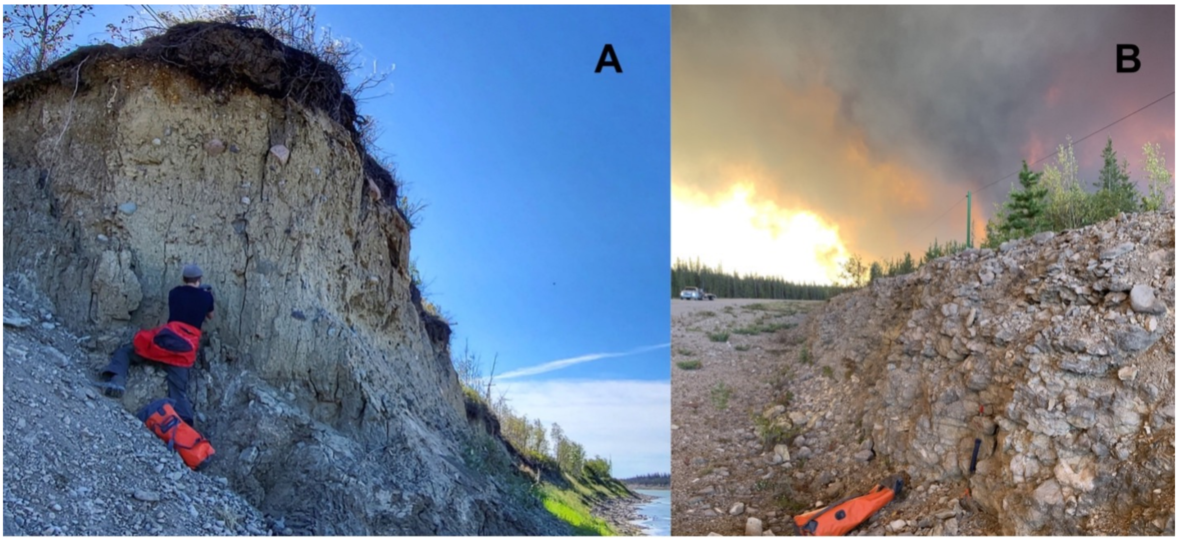

Figure 3.3. A) Soil sampling in Fort Providence on a glacial till cliff along the DehCho Dr road. B) Sedimentary rock outcrop sampling on the roadside of Highway 1 between Kakisa and Enterprise, one of the last samples before the evacuation order.

3.4.2 Thermal Properties

3.4.2.1 Thermal Conductivity

All sedimentary and basement rock samples collected (Table 3.13.1) were analyzed for thermal conductivity. The methodology follows that of Rajaobelison et al. (In press). Transient measurements were made using an optical scanning instrument developed by Popov et al. (2023) under dry conditions (Figure 3.43.4).

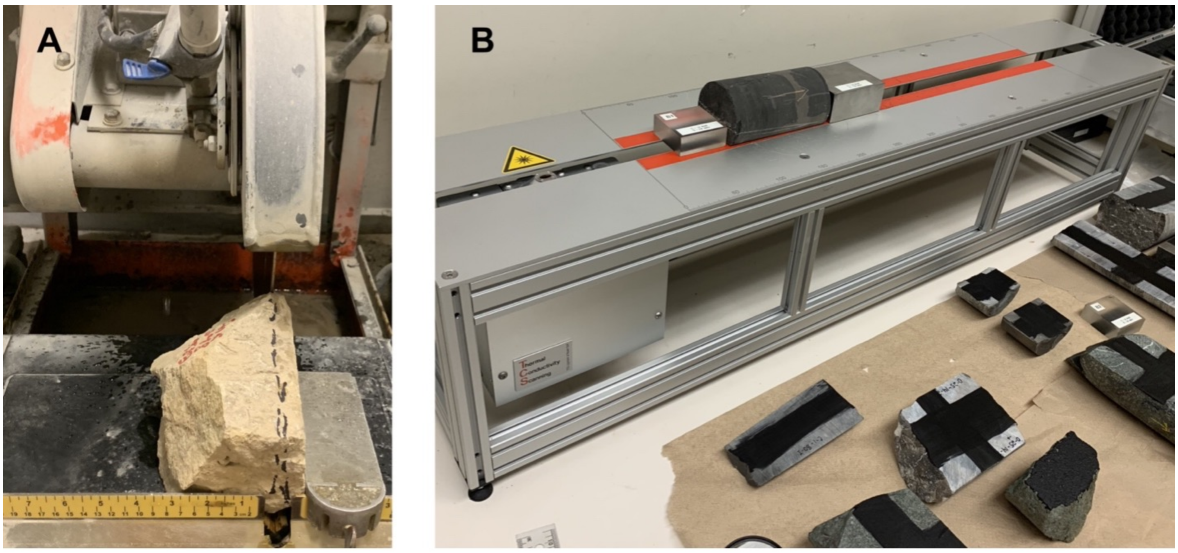

Figure 3.4. Sample preparation and analyses. A) Rock sample saw cutting. B) Thermal property measurement on the optical scanning instrument developed by Popov et al. (2023).

The average thermal conductivity values for all the measured samples, presented by types of material are shown in Figure 3.53.5. The classification of rocks according to their insulating to conductive potential indicated on Figure 3.53.5Figure 3.63.6 is based on Rajaobelison et al. (In press), Sass & Götz (2012) and Sass et al. (1992).

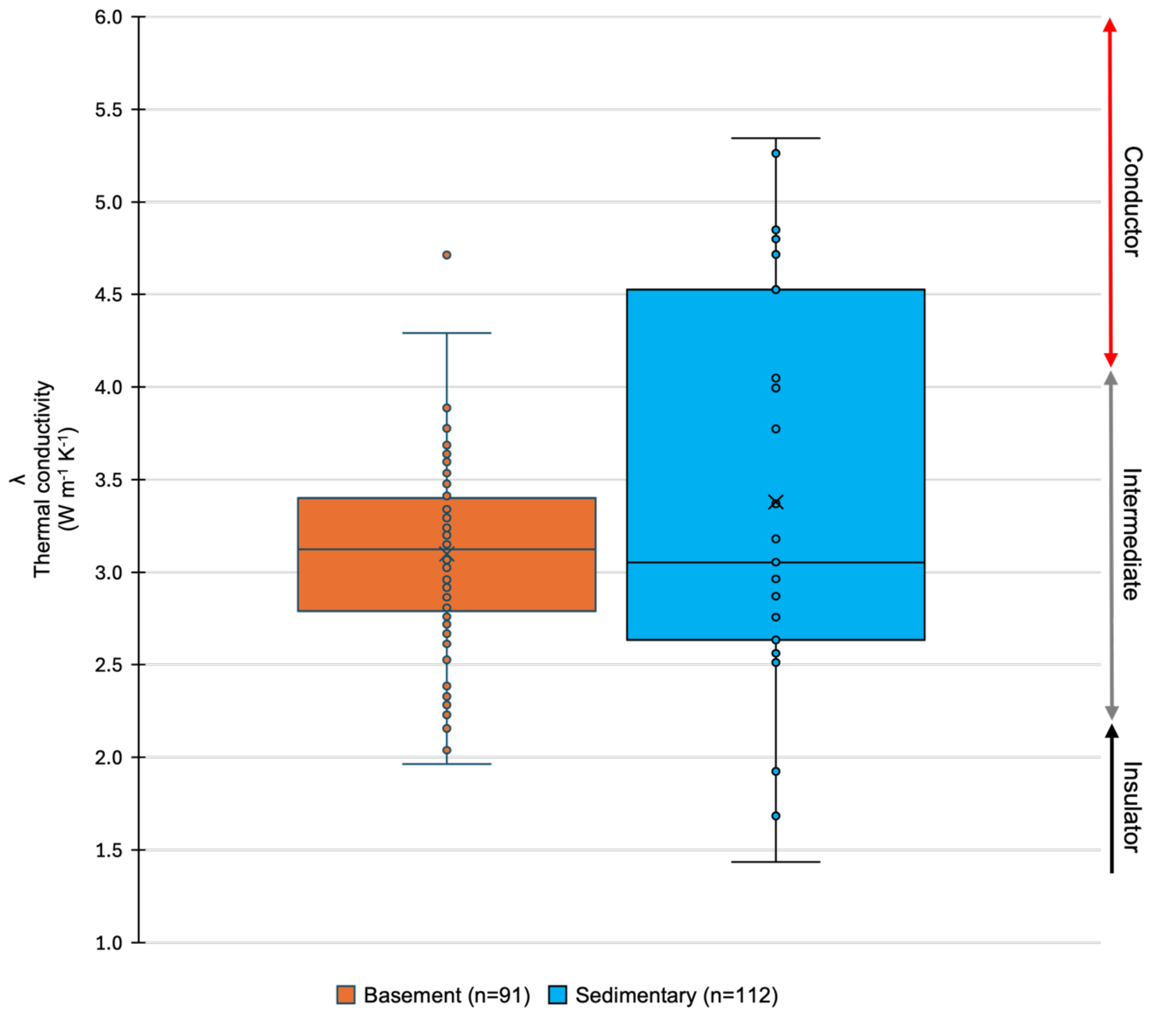

Figure 3.5. Thermal conductivity for the overall sampled Precambrian (PC) basement and sedimentary rocks.

In this study, we treat each tectonic domain (Figure 3.23.2) as a uniform thermal unit. Sixty-six samples from the outcropping Slave Province were analyzed for the Slave Craton tectonic domain, which is associated with the Hay River and the Enterprise Precambrian basement. For the Hottah Terrane tectonic domain (Fort Providence and Kakisa), we sampled eleven core cuttings and surface rocks. We added ten additional previously measured core cuttings from other locations in our data set, which came from Majorowicz et al. (2014). Figure 3.63.6 shows the corresponding thermal conductivity ranges.

The values attributed to the Slave Craton account for a wide range of lithologies that represent practically all geological units visible at the surface of the Slave Province, from which these Precambrian structures extend beneath the sedimentary layer (Ootes et al., 2015). The Hottah Terrane has slightly higher thermal conductivity values, a broader spread, and fewer samples.

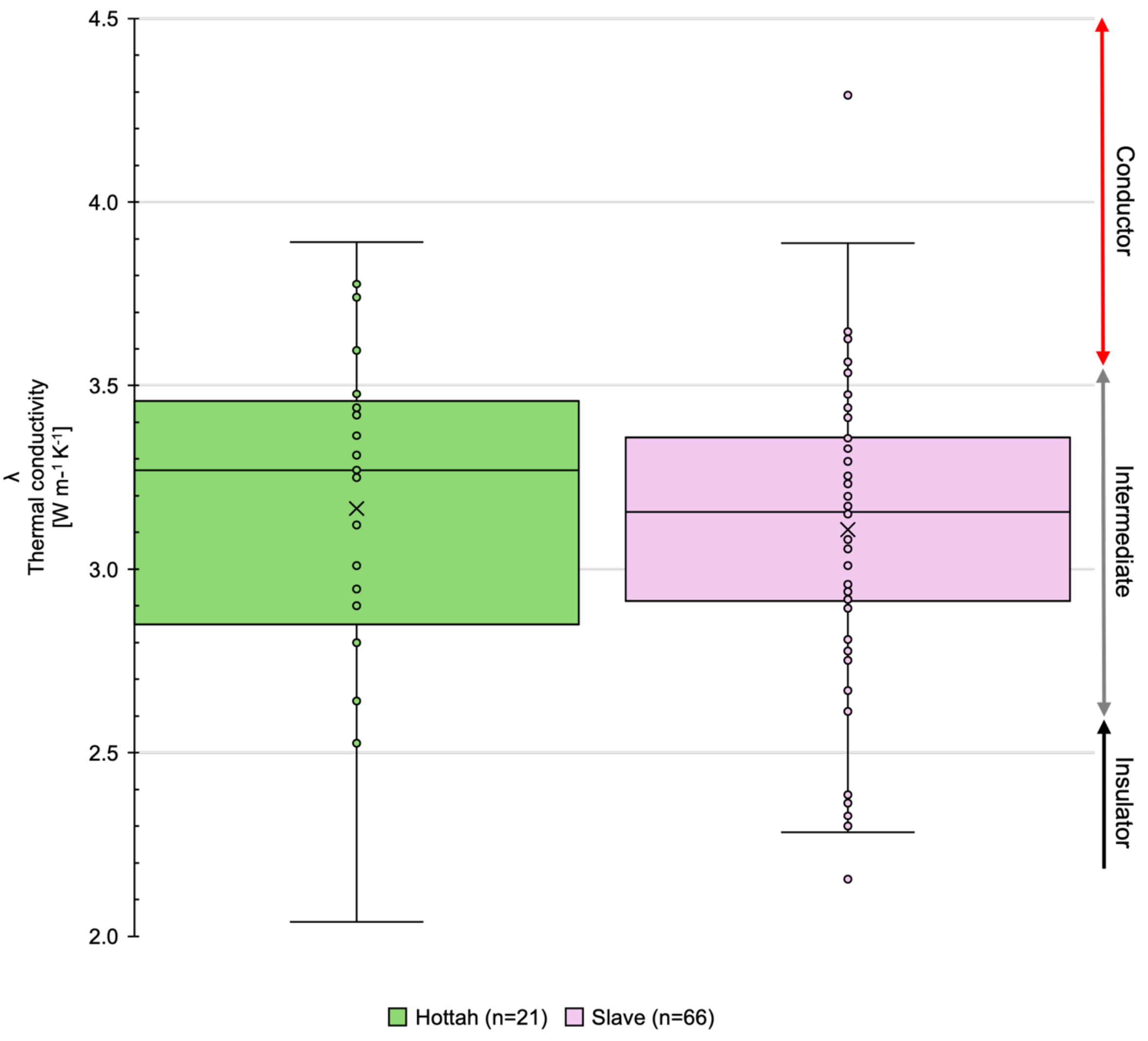

Figure 3.6. Thermal conductivity for basement domain related to each community.

3.4.2.2 Heat Generation Rate

Table 3.33.3 shows the heat generation rate expected for sedimentary units and basement domain. The sedimentary formations values were obtained from Rajaobelison et al. (2024). The basement heat generation rate was determined according to literature values specific to each tectonic domain, including Jessop (1992) for the Hottah Terrane and Perry et al. (2010) for the Slave Craton.

3.4.3 Undisturbed Ground Temperature

The undisturbed ground temperature T_s (K) was estimated using the equation proposed by Ouzzane et al. (2015):

$$T_s = 17.898 + 0.951T_{amb} \tag{3.1}$$

where T_{amb} (K) is the ambient air temperature, which is considered to be -2.5 °C based on the mean annual air temperature from the Hay River-A weather station (Government of Canada & Environment and Natural Resources, 2024). T_s is thus estimated to be 2.1 °C in the South Slave region.

3.4.4 Input Data and Scenarios

In this study, various scenarios were proposed based on the probabilistic distribution of thermal properties. This provides for a normal, pessimistic, or optimistic outlook. These are presented in Table 3.23.2 as input for thermal properties and in Table 3.33.3 as results.

The normal scenario employs the 50th percentile (P_{50}) values of basement thermal conductivity, heat generation rate, as well as the heat flow and geothermal gradient acquired from the corrected well temperature measurements, resulting in a neutral approach. The pessimist scenario uses the 25th percentile (P_{25}) value of heat flow and temperature gradient, the minimum heat generation rate value and the 75th percentile (P_{75}) percentile values for the thermal conductivity, embodying a cautious approach. In contrast, the optimist scenario utilizes P_{75} values for heat flow and temperature gradient, the maximum heat generation rate, and P_{25} values for the thermal conductivity, providing insight into best-case scenarios. These diverse perspectives allowed for a comprehensive analysis of potential outcomes across different scenarios.

Table 3.2. Thermal properties (thermal conductivity and heat generation rate) values assigned to each scenario (normal (N), pessimist (P) and optimist (O)) for each community in the sedimentary sequence and the Precambrian (PC) basement (Hottah Terrane and Slave Craton tectonics domain). The number of samples is denoted by *n*.

			λ Thermal Conductivity (W m^{-1} K^{-1})				A Heat Generation Rate (µW m^{3})			
			n	N	P	O	*n*	N	P	O
				P_{50}	P_{75}	P_{25}		P_{50}	min	max
Sedimentary		Fort Providence	80	2,5	2,8	2,4	80	0,5		
		Kakisa		2,3	2,7	2,2		0,4		
		Hay River		2,8	3,1	2,5		0,4		
		Enterprise		2,6	2,8	2,4		0,4		
PC basement	Hottah	Fort Providence, Kakisa	21	3,3	3,4	2,9	7	2,1	1	3,6
	Slave	Hay River, Enterprise	66	3,1	3,4	2,8	20	2,3	1	4,8

3.4.5 Thermostratigraphic Assesment

Temperature was calculated at the base of each sedimentary rock units and at each 500 m intervals in the basement. To be consistent with previous work, we used for each community the same well temperature data listed in the assessment of Rajaobelison et al. (2024), where well temperature measurements from drill-stem tests (DST) and borehole temperature (BHT) were corrected for drilling disturbance and paleoclimate effects. This temperature assessment of the sedimentary basin served as inputs for the present temperature assessment in the Precambrian basement.

3.4.5.1 Paleoclimate corrections

Past glaciations in Canada lowered subsurface temperatures at shallow depths, due to both the cooling effects of lower surface temperatures and crustal compression induced by the weight of ice sheets that covered the land. These paleoclimate effects persist today to consideradable depth, necessitating paleoclimate corrections in temperature assessments for accurate deep geothermal estimations out of shallow wells temperature measurements (Jessop, 1992). The effects of past glaciations in Canada can be significant to the depth of two kilometres or more (Bédard et al., 2016; Majorowicz et al., 2012, 2014a). While this influence diminishes with depth, it's essential to account for paleoclimate corrections, particularly for this area where temperature measurements from old oil and gas exploration wells are mainly less than a thousand metres deep. Beyond a certain depth, temperatures tend to reach equilibrium, reflecting the long-term geothermal gradient of the region. In this study we consider a depth of 3 km, from which climatic variations no longer have a significant impact on temperature and that we consider as equilibrium temperature. The 3 km cut-off value for the South Slave region seems reasonable, considering that northern Alberta estimates are 2200 m based on the first heat flow measurement in a well that reached the basement under the WCSB below the depth of the paleoclimatic influence (Majorowicz, Chan, et al., 2014; Majorowicz et al., 2012). In areas where paleoclimates have a deeper influence, such as the St. Lawrence Lowlands sedimentary basin in Quebec (Bédard et al., 2016; Chapelet, 2022), the influence on temperatures and heat flow are minimal below 3 km depth. The equilibrium temperature at depth $T_{z\,(\mathrm{eq})}$ is calculated with the following paleoclimate correction equation (Jessop, 1990; Rajaobelison et al., 2024):

$$T_{z(eq)} = T_m + \sum_i (T_i) \left[erf\left(\frac{z}{2\sqrt{\alpha\, t_1}}\right) - erf\left(\frac{z}{2\sqrt{\alpha\, t_2}}\right)\right] \quad (3.2)$$

where T_m (°C) represents the temperature measured at a certain depth z (m), corrected from drilling disturbance and T_i (°C) is the temperature step between glaciations. The error function is represented by erf, α ($m^2\ s^{-1}$) is the mean thermal diffusivity of the rocks, t_1 (s) represents the end of the ice age, while t_2 (s) represents the beginning of the ice age. Specific information regarding the values employed can be found in the laboratory and thermostratigraphic studies conducted by Rajaobelison et al. (2024).

Thus, to estimate the actual subsurface temperature at a depth of less than 3 km, the paleoclimatic correction ((3.23.2) was removed such that temperature is characteristic of the value that can be measured (i.e., affected by glaciation). However, the paleoclimate correction was applied to calculate temperature until 10 km depth since glaciations are expected to have a low impact at great depth.

3.4.5.2 Geothermal Gradient

The geothermal gradient g (°C m^{-1}) refers to the rate at which temperature increases with depth below the Earth's surface. It can be stated by the following:

$$g = \frac{\Delta T}{\Delta z} = \frac{T_z - T_s}{z} \tag{3.3}$$

where ΔT (°C) is the difference between the temperature at the depth being assessed T_z (corrected measured temperature are from Rajaobelison et al., 2024) and the undisturbed ground temperature (T_s = 2.14 °C), and z (m) is the depth of the corrected temperature assessed.

3.4.5.3 Surface Heat Flow

Heat flow in the context of geothermal energy refers to the movement of thermal energy from the Earth's interior toward the surface, often used to assess the potential for geothermal energy extraction. Surface heat flow Q_0 (W m^{-2}) quantifies the rate at which this heat energy is transferred per unit area over the Earth's surface. The following equation (Bédard et al., 2016; Jessop, 1990; Rajaobelison et al., 2024) is used to compute surface heat flow in a sedimentary basin:

$$Q_0 = \lambda_{sed} g + A_{sed} \frac{z}{2} \tag{3.4}$$

λ_{sed} (W m^{-1} K^{-1}) denotes the effective thermal conductivity of the sedimentary sequence, determined by calculating the weighted harmonic mean of the λ for the different lithologic units that make up the sedimentary rock cover at each location, g (°C km^{-1}) refers to the geothermal gradient determined from temperature measurements as described previously, A_{sed} (W m^{-3}) is the effective heat generation obtained from the weighted arithmetic average in the sedimentary rock sequence and z (m) is the rock sequence thickness between the measured temperature depth and the ground surface.

3.4.5.4 Basement Heat Flow

The basement top heat flow Q_{PC} (W m^{-2}) is defined here as the heat flow at the boundary between the sedimentary layers and the underlying Precambrian basement rocks. It is calculated by removing the heat generation effects A_{sed} within the sedimentary rocks from the surface heat flow through the sedimentary sequence, according to the following equation (Bachu, 1993; Bédard et al., 2016; Majorowicz, Nieuwenhuis, et al., 2014; Majorowicz & Grasby, 2010b):

$$Q_{PC} = Q_0 - A_{sed}\frac{z_{sed}}{2} \tag{3.5}$$

where z_{sed} is the thickness of the sedimentary rocks sequence, which is the depth between the top of the Precambrian basement and the ground surface.

3.4.5.5 Temperature at Depth in the Sedimentary Rocks Sequence

Each sedimentary rock formation has a distinct effective thermal conductivity λ, hence the temperature at depth $T_{z(\text{sed})}$ (°C) was calculated at their boundaries. It was computed analytically under steady-state condition, taking into account conductive heat transfer using a one-dimensional approach (Rajaobelison et al., 2024; Stein, 1995):

$$T_{z(sed)} = T_s + \frac{Q_0\, z}{\lambda} - A\frac{z^2}{2\lambda} \tag{3.6}$$

where Ts (°C) is the temperature at the base of the sedimentary formation, z (m) the formation thickness and λ (W m^{-1} K^{-1}) the formation effective thermal conductivity.

3.4.5.6 Temperature at Depth in the Precambrian Basement

The temperature at any depth in the Precambrian basement $T_{z(\text{PC})}$was calculated at each 500 m intervals, using the same relationship mentioned above for $T_{z(\text{sed})}$:

$$T_{z(PC)} = T_{PC} + \frac{Q_{PC}\, z_{PC}}{\lambda_{PC}} - A_{PC}\frac{{z_{PC}}^2}{2\lambda_{PC}} \tag{3.7}$$

where T_{PC} (°C) is the temperature at the top of the basement, Q_{PC} (W m^{-2}) is the basement heat flow, z_{PC} (m) is the depth from the top of the basement, λ_{PC} (W m^{-1} K^{-1}) the thermal conductivity of the basement and A_{PC} (W m^{-3}) is the heat generation of the basement rocks.

3.5 Results

3.5.1 Input data

Table 3.33.3 presents the calculated geothermal gradient and surface heat flow for the sedimentary sequence, which were used in the temperature calculations.

Table 3.3. Geothermal gradient and heat flow assigned to each scenario (normal (N), pessimist (P) and optimist (O)) for each community (Fort Providence (FP), Kakisa (K), Hay River (HR) and Enterprise (E)) in the sedimentary sequence.

		g Geothermal Gradient (°C km^{-1})			g_{eq} Equilibrium (°C km^{-1})			Q_0 Surface Heat Flow (mW m^{-2})			$Q_{0(eq)}$ Equilibirum (mW m^{-2})		
		N	P	O	N	P	O	N	P	O	N	P	O
		P_{50}	P_{25}	P_{75}	P_{50}	P_{25}	P_{75}	P_{50}	P_{25}	P_{75}	P_{50}	P_{25}	P_{75}
Sedimentary	FP	53	43	56	56	47	58	133	104	158	141	112	166
	K	43	39	44	45	41	46	99	85	118	105	90	125
	HR	56	46	61	59	50	64	158	115	186	167	124	195
	E	41	37	43	44	39	46	106	88	120	113	93	129

3.5.2 Temperature in the Sedimentary Rocks Sequence

Each temperature point used for calculations in the sedimentary rock sequence corresponds to the top of each sedimentary formation (fm.; Figure 3.73.7). The calculated temperature is based on heat flow assessed in wells near the communities. The profiles represent an estimate of the current temperature found in the sedimentary rocks, thus affected by glaciations and uncorrected for paleoclimates.

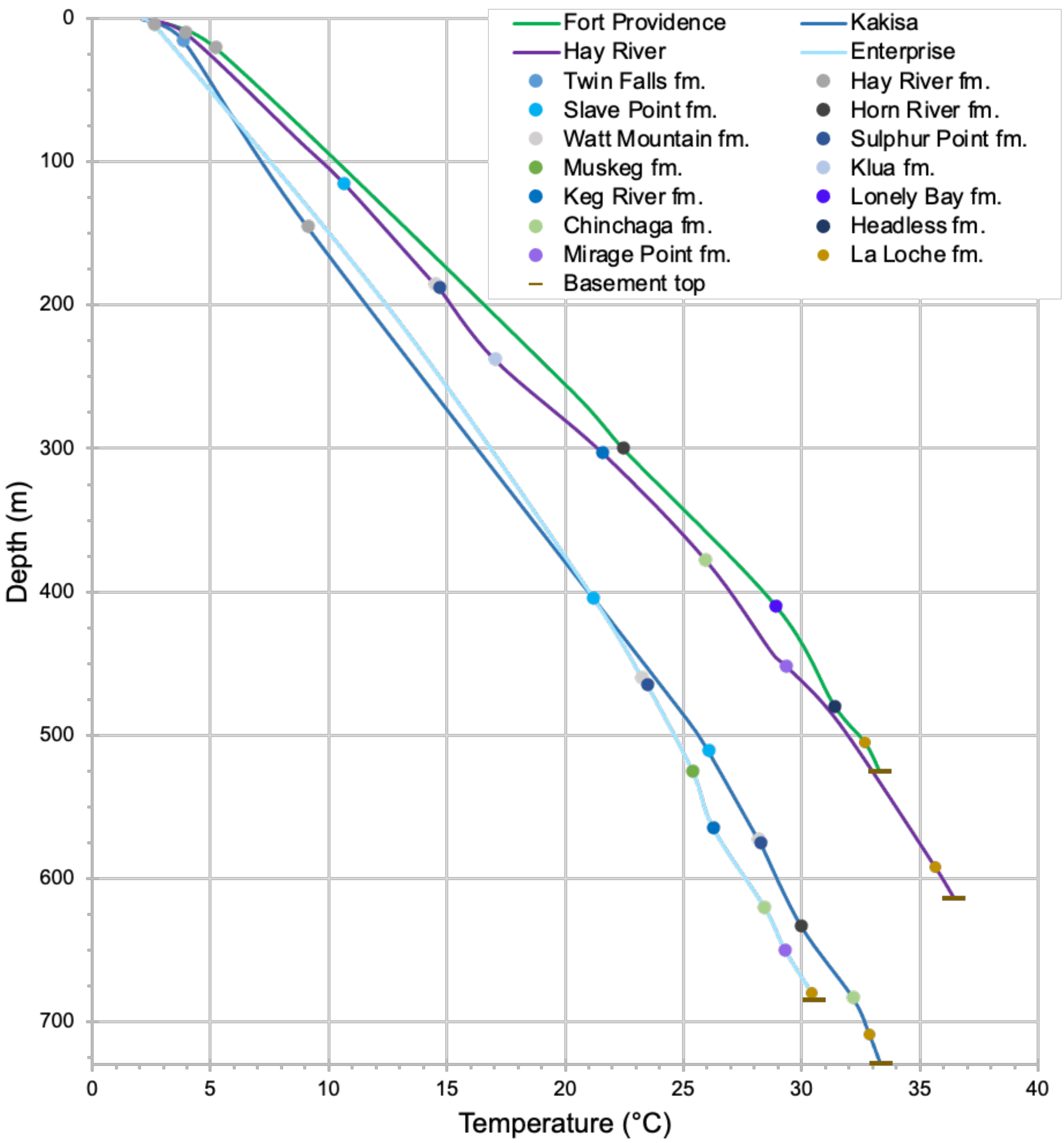

Figure 3.7. Temperature at depth in the sedimentary sequence, with normal scenarios, considering heat flow uncorrected for paleoclimates. Each community is represented by a distinct coloured line, and each geological (fm.) top is represented by a specific coloured circle.

3.5.3 Temperature in the Basement until 3 km depth

The temperature calculated until 3 km depth (Figure 3.83.8Figure 3.93.9Figure 3.103.10Figure 3.113.11, Figure 3.123.12) incorporates uncertainty scenarios. The calculated temperatures represent an estimate of expected and current temperatures found in the basement, thus affected by glaciations and uncorrected for paleoclimates.

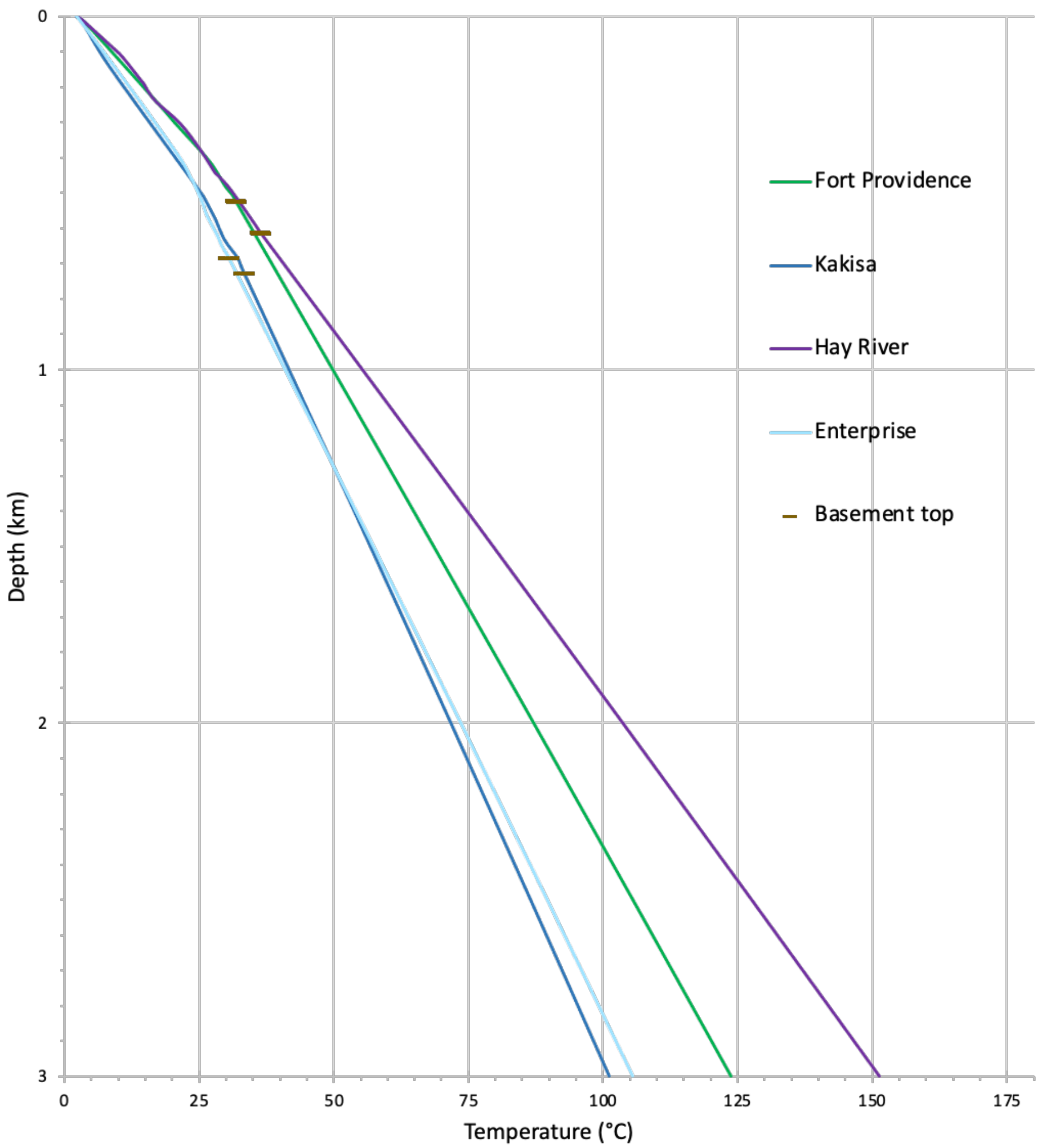

Figure 3.8. Temperature until 3 km depth, with normal scenarios, considering heat flow uncorrected for paleoclimates. Each community is represented by a distinct coloured line.

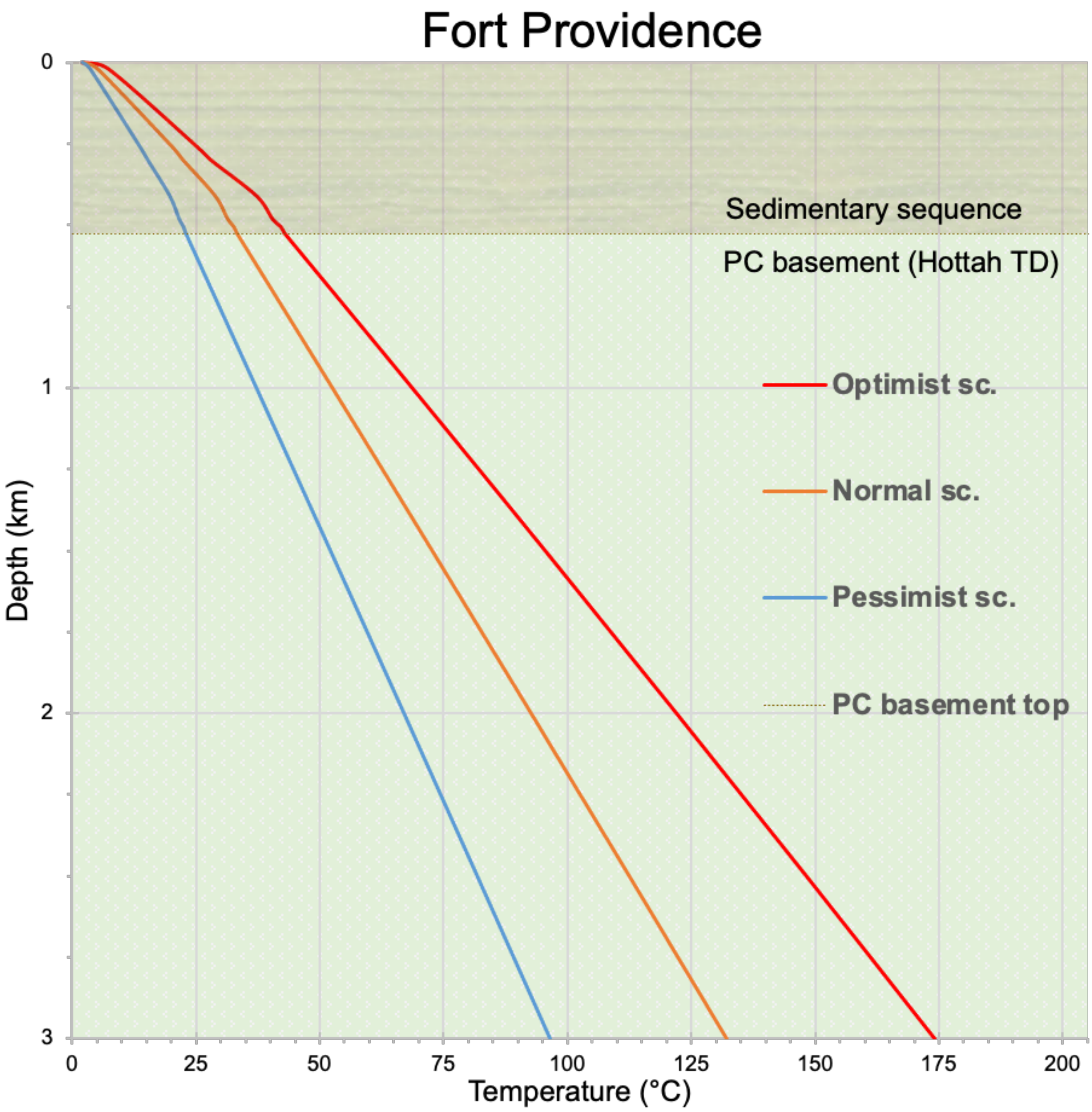

Figure 3.9. Temperature until 3 km depth for Fort Providence, with optimist, normal and pessimist scenarios, considering heat flow uncorrected for paleoclimates.

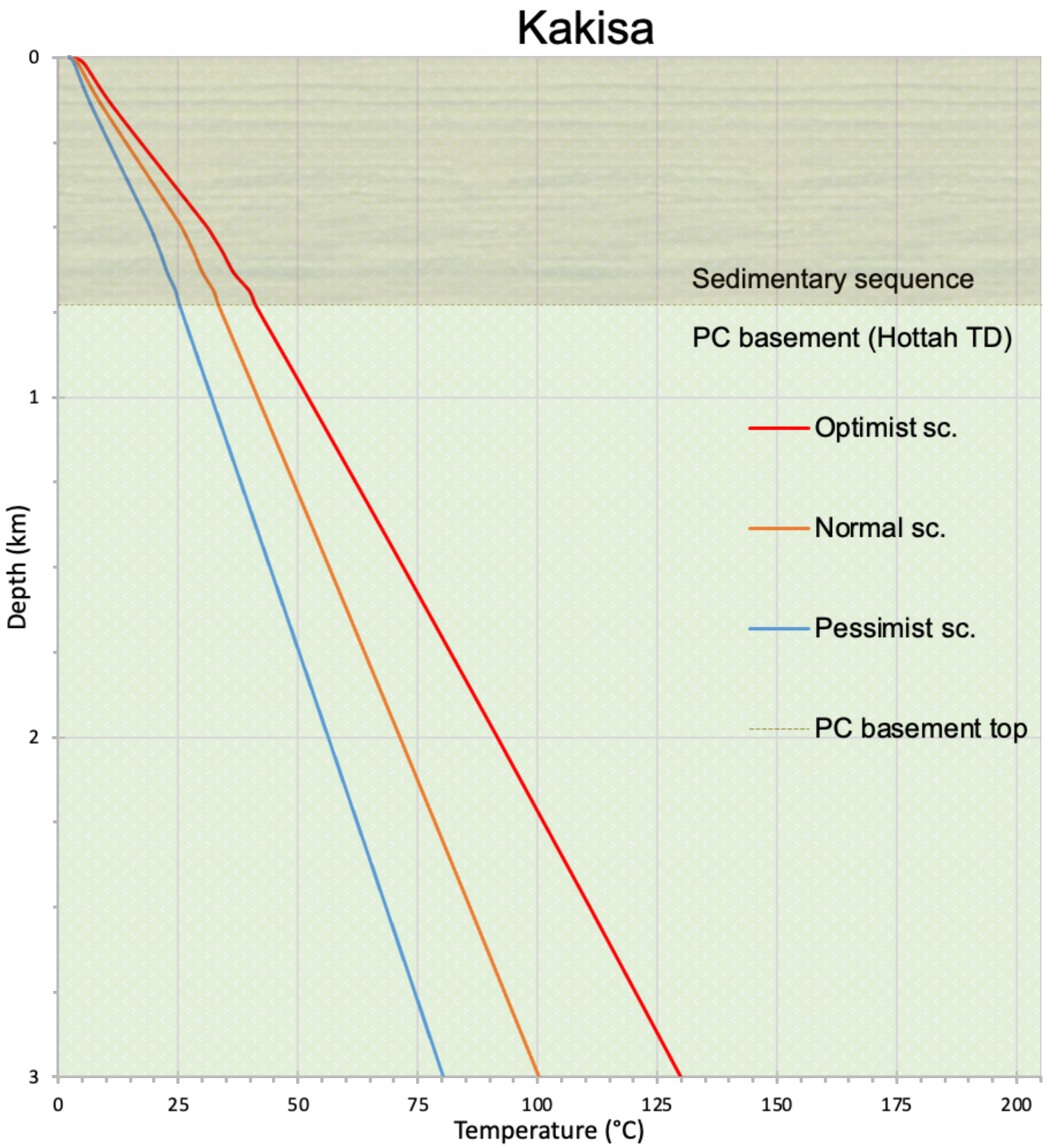

Figure 3.10. Temperatures at depth until 3 km depth for Kakisa, with optimist, normal and pessimist scenarios, considering heat flow uncorredted for paleoclitates.

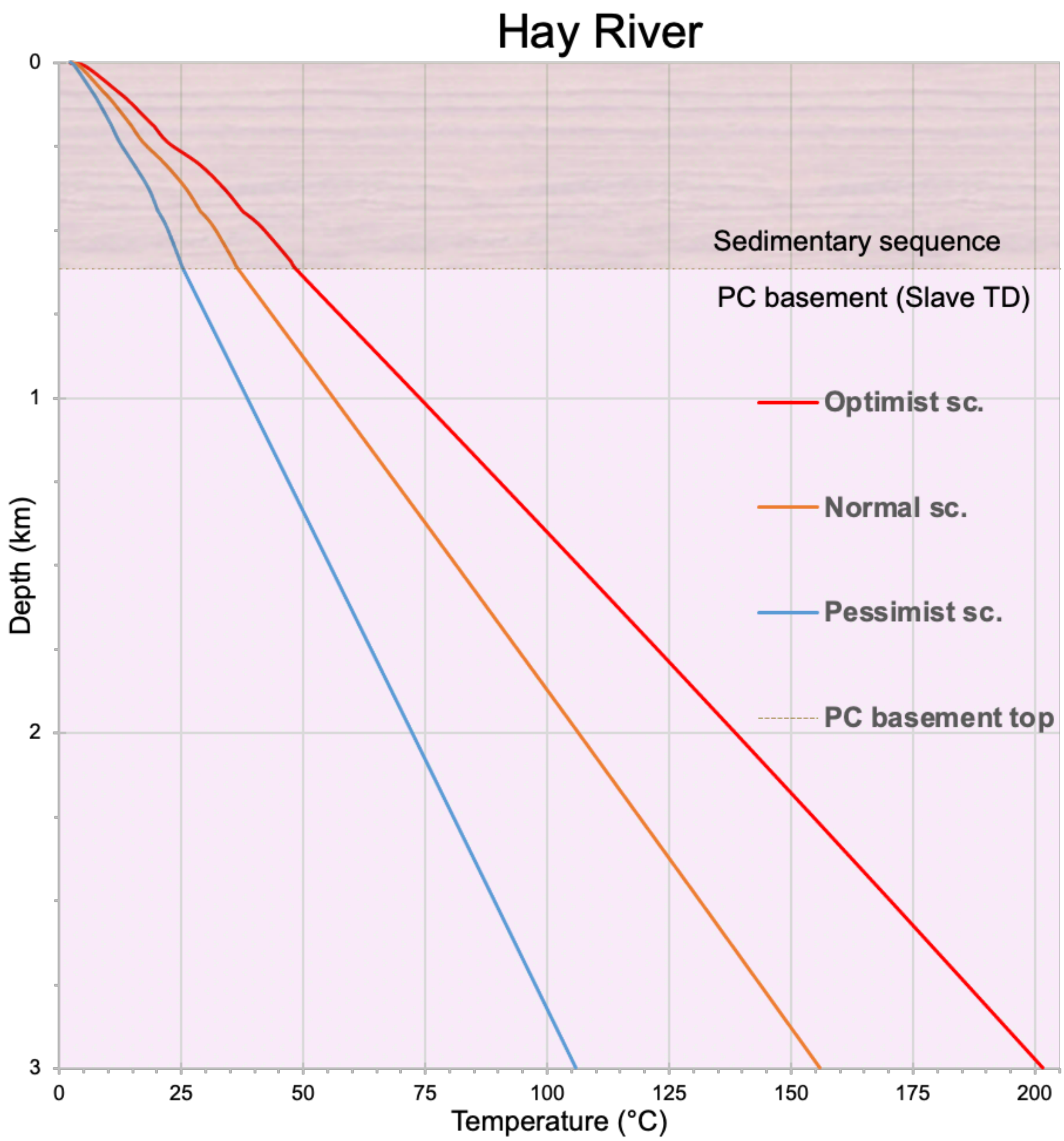

Figure 3.11. Temperatures at depth until 3 km depth for Hay River, with optimist, normal and pessimist scenarios, considering heat flow uncorrected for paleoclimates.

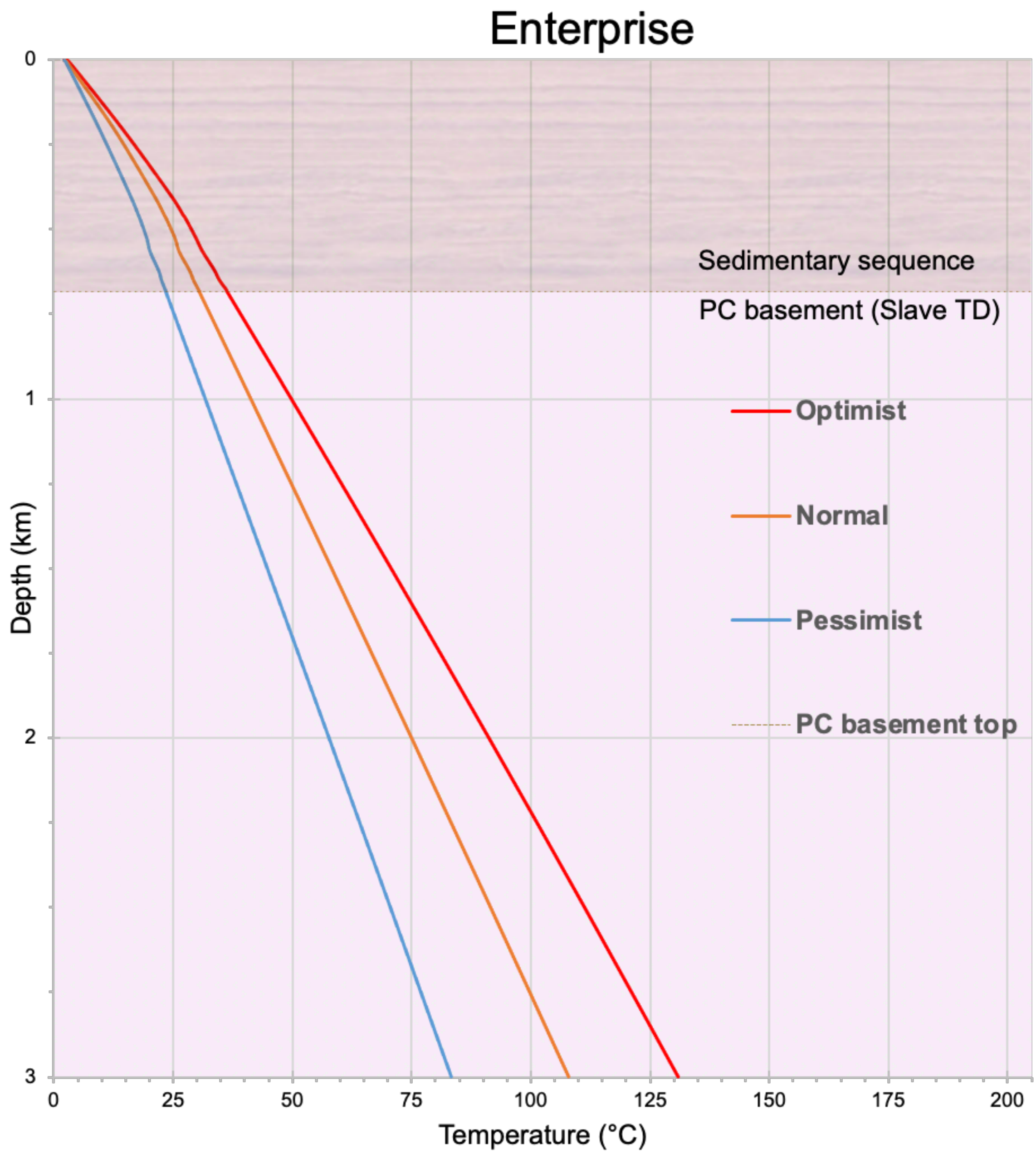

Figure 3.12. Temperatures at depth until 3 km depth for Enterprise, with optimist, normal and pessimist scenarios, considering heat flow uncorrected for paleoclimates.

3.5.4 Temperature in the Basement until 10 km depth

For the sake of clarity, only the normal scenario is considered for the temperature calculated until 10 km depth below each community (Figure 3.133.13). The calculated temperatures represent an estimate of the equilibrium temperature, considering heat flow corrected for paleoclimates.

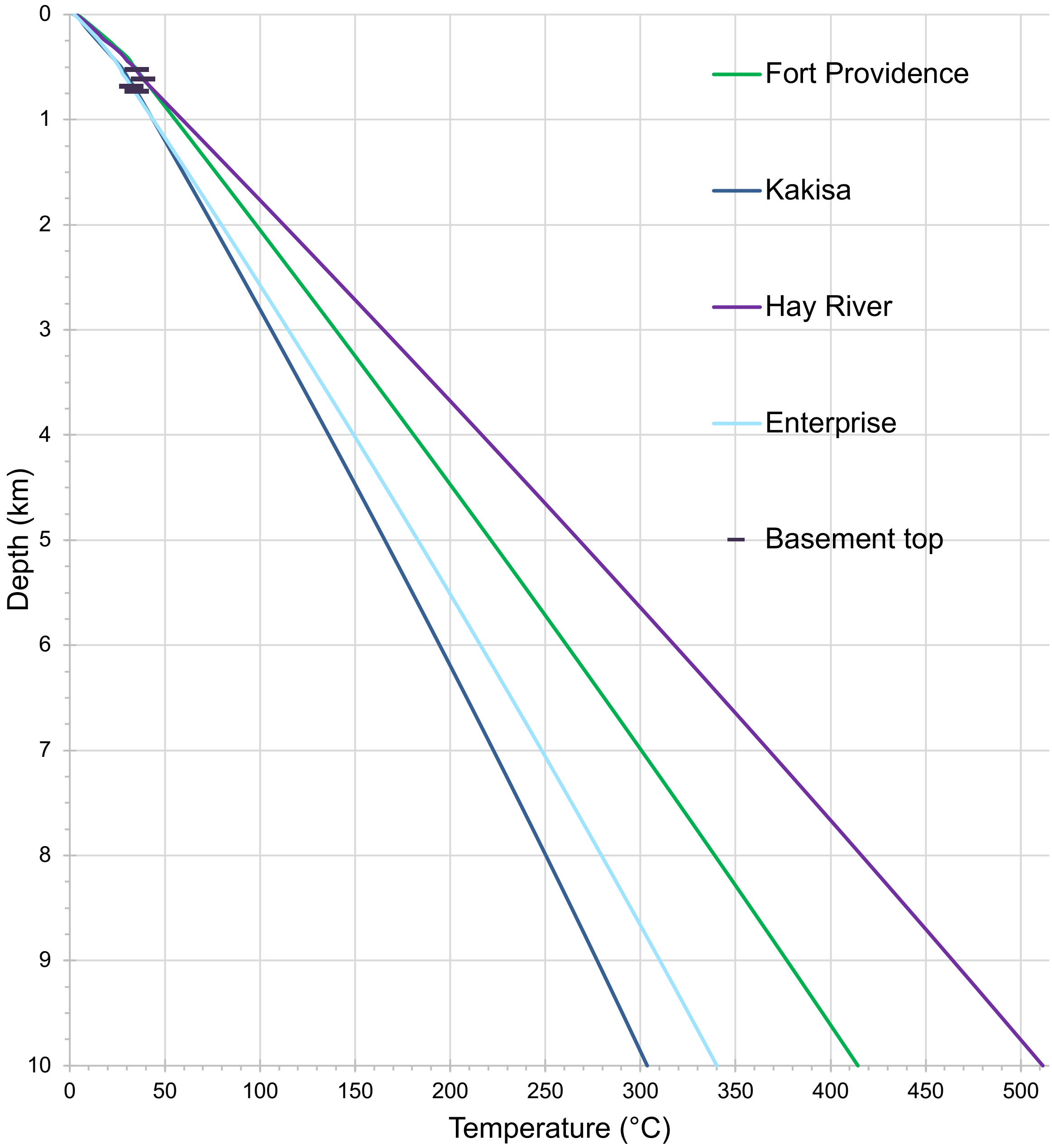

Figure 3.13. Temperature until 10 km depth, with the normal scenario, considering equilibrium heat flow, corrected from paleoclimate effects. Each community is represented by a distinct coloured line.

3.6 Discussion

This basement thermal property assessment allowed to predict temperature at depth below the sedimentary rock cover for the NWT communities of Hay River, Fort Providence, Enterprise, and Kakisa. The new thermal properties data present in this study will be publicly available and can be used for additional subsurface studies in other regions of the WCSB and the Slave Province.

This research builds upon previous studies that focused on the shallow sedimentary sequence (<730 m) (Rajaobelison et al., 2024, In press) by extending the assessment to the deeper Precambrian basement, further demonstrating how oil and gas exploration data can be used for early stage deep geothermal resource assessment.

Thermal conductivity values significantly influence the geothermal gradient. Precambrian basement rocks exhibit higher thermal conductivity than sedimentary rocks, resulting in a slower temperature increase within the basement. In contrast, the sedimentary sequence, with its lower effective thermal conductivity, act as a 'thermal blanket', trapping heat and causing a higher temperature increase with depth.

Our findings indicate that the highest geothermal gradient is expected below Hay River, with temperature increasing more rapidly than in other communities. Conversely, Kakisa has the lowest geothermal gradient, followed closely by Enterprise. The variation in subsurface temperature among these communities, despite their proximity within a 120 km radius, highlights the importance of localized resource assessments rather than relying on extrapolated values from a regional scale assessment.

Temperature at depth for Hay River and Fort Providence reveal a similar profile within the sedimentary sequence, but is significantly different in the Precambrian basement. This disparity can be explained by a lower thermal conductivity and a higher heat flux inside the Slave Craton for Hay River. These factors contribute to a faster increase in temperatures at depth. Similar observations can be made for Enterprise and Kakisa.

Although we would have expected similar temperature due to their proximity, Hay River and Enterprise (approximately 30 km apart and part of the same tectonic domain) show a notable temperature difference at depth. This discrepancy is primarily due to the different heat flow values used in calculations and originating from well temperature measurements that can enclose a high uncertainty (Rajaobelison et al., 2024).

Upon comparing our findings with those of other studies (Grasby et al., 2011; Majorowicz & Grasby, 2010b, 2010a), notable disparities in temperature estimations emerge, particularly in Hay River. Majorowicz & Grasby (2010b) estimate a temperature of approximately 85 °C at 3 km and around 250 °C at 10 km for Hay River. On the other hand, we estimate temperatures slightly above 150 °C at 3 km and 500 °C at 10 km. Moreover, Grasby et al. (2011) report a depth of 3.5 km to reach 150 °C in that region. Also, Majorowicz & Grasby (2010a) estimate a temperature slightly below 350 °C at 10 km for the community locations. However, the temperatures we calculated at depth in Hay River and Fort Providence are much higher than those reported in previous studies. Enterprise and Kakisa values are also higher albeit slightly lower than the other two communities. This is mostly attributed to the utilization of a larger heat flow estimate in our calculations. For example, when using a lower heat flow value, similar to these studies, 95 ± 5 mW m^{-2}, our results align more closely with those of previous studies.

Input temperature is the most influential factor in the estimation of the geothermal gradient and heat flow; therefore, its variability directly affects the results. Noisy or poor-quality data can significantly bias geothermal gradient assessments. The reliability and accuracy of temperature measurements can be influenced by factors such as the method of measurement, quality, depth, season, and the age of the data, as discussed by Majorowicz et al. (1999, 2014b). In this region, the availability of high-quality thermal data is limited, with most drilling reports dating from the 1960s to the 1980s. Also, wells are limited in depth, with only four boreholes exceeding 1000 m and situated at a reasonable distance (<50 km) from the communities. Reconsidering the input values, particularly for unusually high heat flows such as those observed in Hay River and Fort Providence, which may have been overestimated, could lead to more consistent results between communities and with literature values.

Another limitation of the study is that the 1D analytical temperature models do not account for expected decreases in thermal conductivity with increasing temperature and pressure at depth (Clauser, 2011; Majorowicz et al., 2014b). These factors could influence the values obtained by increasing our temperature values at greater depths, especially those predicted to 10 km. Additionally, our results are theoretical predictions that should be interpreted with caution. They heavily depend on the inputs used in calculations, and the uncertainty increases with depth, as highlighted by the optimistic and pessimistic scenarios and in comparison to the literature.

This study is not intended as a regional or large-scale analysis and does not evaluate three-dimensional resource distribution. It does not focus on potential aquifers or consider structural geology impacts, such as faults and fractured patterns on localized resources.

However, one of the strengths of our study is the use of representative thermal properties for the geological formations under the communities. These were obtained from laboratory measurements on the same geological formation rocks that we expect to be found below the communities, rather than from broad literature values, as was done in previous studies. Furthermore, our localized approach ensures relevance to community end users, making our findings directly applicable and reliable for the community's geothermal resource assessment.

Geothermal resources within the sedimentary sequence (<37 °C) could be used for heating applications, most likely requiring the use of a heat pump system. However, for applications requiring temperatures above 40 °C, which can support a wide range of geothermal energy uses, drilling into the Precambrian basement would be necessary to reach such temperature. Specific applications, such as electricity production, necessitate temperatures above 80 °C, below which it becomes uneconomical. However, a high temperature above 150 °C is more commonly employed for power generation (Ahmadi et al., 2020). Based on our 1D models, such temperature is expected at depths about 1500 m and 3000 m for the community of Hay River and around 2250 m and 4500 m for Kakisa. Low permeability crystalline rocks are expected at such depth, which would either require EGS or DBHE.

While our results indicate a great geothermal potential for the South Slave communities, with high temperature at depth, these are theoretical estimates. This potential can only be validated through exploration drilling to confirm the geothermal potential.

3.7 Conclusion

This study provides critical insights into the thermal properties of the Precambrian basement rocks beneath the sedimentary basin in the South Slave communities of the NWT. It was combined with previous temperature assessment in the sedimentary rock cover.

The calculated temperature profiles highlight the importance of local resource assessments for the community's end user, from which geothermal development could potentially contribute to energy independence, reduce greenhouse gas emissions, and promote regional economic development.

The temperature profiles presented in this work can be used as input for future work, focusing on numerical simulations aimed at evaluating the efficiency of heat extraction for each community considering DBHE. Such systems, when coupled with heat pumps, present a promising technology for heating applications in the South Slave Region. Numerical modelling will further assist in defining the thermal output of these systems in locations without deep aquifers. These efforts will provide important information for future decision-making about energy supply in that region as well as any further geoscience study in the area.

3.8 Acknowledgement

We would like to thank the Office of the Regulator of Oil and Gas Operations and the Geological Survey of Canada Core Repository in Calgary for providing access to the drilling cores and assistance with sampling, Northwest Territories Geological Survey (NTGS) staff to provide access and assistance with archive samples and Dr. Jacek Majorowicz and Rod Smith for constructive discussions. This research was funded by a scholarship from the Natural Sciences and Engineering Research Council of Canada to the first author as well as research grants given to INRS under the Northern Scientific Training Program, GEM-GeoNorth program of Natural Resources Canada and the NTGS. The Centre d'études nordiques is also acknowledged for help with logistics.

Chapter 4

Discussion

4.1 Implications

The thermal conductivity measurements obtained for the Precambrian basement rocks significantly impact the geothermal gradient predictions. The thermal conductivity of the basement is higher than that of the sedimentary sequence, resulting in slower temperature increases within the basement. Conversely, the sedimentary rocks, acting as a "thermal blanket," trap heat and exhibit a more rapid temperature rise with depth. These variations in geothermal gradients across the study area, even among neighbouring communities, highlight the necessity of conducting site-specific assessments rather than relying on generalized data from regional studies.

Results allowed predicting temperature at the top of the Precambrian basement (500 to 750 m depth), expected to range from 30 to 36 °C under a surface heat flow between 99 and 157 mW m^{-2}. At 3 km depth, the temperature is expected to vary from 100 to 156 °C, and at 10 km, from 303 to 511 °C.

One of the most notable findings of this study is the significant geothermal gradient observed below Hay River, where subsurface temperatures rise more rapidly than in the other communities. These results indicate that the site potentially exhibits some of the highest geothermal gradient and heat flow in Canada, when compared to heat flow provided in national datasets (Grasby et al 2009, 2011). In contrast, Kakisa and Enterprise show geothermal gradients lower than Hay River, but still important when compared to the Canadian average. These differences are particularly important because they demonstrate that even communities located within a relatively small geographical area (120 km radius) can experience different geothermal conditions, emphasizing the need for localized resource assessments.

The high heat flow anticipated for this area, when compared to other locations in Canada (Grasby et al., 2011; Majorowicz & Grasby, 2010b), is based on non-equilibrium BHT and temperature measurements made during DST, as our models build on data provided by Rajaobelison et al. (2024). Differences in thermal properties specific to the geological units underlying each community, particularly in Hay River and Fort Providence, may also explain differences in geothermal gradient. Although these differences in temperature profiles warrant further examination, they provide valuable insights into the complexities and uncertainty of geothermal resource assessment and the critical role of input data quality.

4.2 Limitations

While this study provides a theoretical framework for estimating deep subsurface temperatures below South Slave communities, several limitations must be acknowledged.

Firstly, the interpretation of thermal anomalies is still unclear and remains outside the scope of this study. Furthermore, the model assumes constant thermal conductivity and radiogenic heat production with depth, despite known vertical variations in these properties. Moreover, the assumption that conduction is the only mode of heat transfer may oversimplify local thermal dynamics. Additionally, the reliance on basic 1D models in this study constrained the comprehensive assessment of unpredictability and uncertainty quantification, relative to what could be achieved with more sophisticated methods. Finally, the sparse and uneven distribution of well data limits model calibration and reduces confidence in deep temperature predictions.

4.2.1 Thermal Anomaly

The high surface heat flow values and elevated subsurface temperatures estimated in this study are particularly striking given that the area lies on the edge of the stable Precambiran Canadian Shield. These estimates significantly exceed the average heat flow typically observed across the Canadian and USA Precambrian shields (~40 mW m^{-2}; Blackwell et al., 1990; Jessop, 1992) as well as those of similar cratonic platforms worldwide (Majorowicz & Jessop, 1981). Such elevated values are more commonly associated with tectonically and/or volcanically active regions (Pollack, 1982), such as rift zones or volcanic provinces, for example, Iceland (Flóvenz & Saemundsson, 1993) or the Basin and Range Province in the USA (Blackwell, 1983).

This anomaly is part of the broader NPHFA, a >300 km wide feature extending over 500 km along the western craton margin (Majorowicz, 1996; Majorowicz & Weides, 2014), with possible alignment to high heat flow zones further south in the USA and Mexico (Blackwell et al., 1990).

According to Majorowicz et al. (2014b), the thermal regime of the sedimentary succession is mainly governed by heat conducted upward from the underlying Precambrian basement, with limited input from mantle heat flow. This conductive regime is further supported by the availability of equilibrium temperature profiles in the Cameron Hills region (Rajaobelison et al., 2024), which are characteristic of conductive heat transfer. Regional groundwater flow may also redistribute heat within the sedimentary basin, as proposed by Bachu (1993), a mechanism observed east of the Rockies in the USA (Blackwell et al., 1990). Other hypotheses involve deeper lithospheric processes, such as basal heat flux from ancient mantle upwelling beneath the craton margin (Gough, 1984; Majorowicz, 1996) or elevated radiogenic heat production in the upper crust, which appears uncorrelated with tectonics domains distribution (Majorowicz, 1996). However, no significant crustal thinning has been observed with seismic data for the NPHFA (e.g., Lithoprobe SNORCLE profiles) and no strong correlation exist between crustal radiogenic heat production and observed surface heat flow (Majorowicz, 2018; Majorowicz & Weides, 2014). Structural features such as the Keg River barrier, previously identified as a conduit for fluid and heat flow (Majorowicz, 1996) may play a localized role, but their influence at the regional scale remains uncertain. As concluded by Majorowicz (2018), the exact cause of the NPHFA anomaly still remains speculative.

Furthermore, identifying the root cause of the NPHFA anomaly lies beyond the scope of this study made with a community approach rather than a regional assessment, and which focuses on a small part of the northernmost extent of the NPHFA. Although this work reveals significant variations in heat flow values between nearby communities located within the same regional anomaly, it does not attempt to explain their origin. Instead, these findings underscore the complexity of the anomaly and highlight the need for further investigation. Nonetheless, these high values raise concerns about potential overestimation due to limitations in legacy datasets. This highlights the need for more data to better understand these anomalies and validate the high estimates. These data could include modern equilibrium temperature logs, thermal conductivity measurements, deep boreholes, geophysical imaging, thermochronology and radiogenic heat production data.

4.2.2 Thermal Conductivity and Lithological Considerations

Although the contrast in thermal conductivity between sedimentary layers and basement rock was addressed in Chapter 3, a more detailed analysis of lithological trends, heterogeneities, and properties assignments for each formation is presented in Rajaobelison et al. (2024) and the forthcoming NTGS report (Rajaobelison et al., In press; Thibault et al., 2025, Submitted). The work of Rajaobelison et al. (2024) specifically provides insights into how thermal conductivity values were assigned based on specific lithological content and include measured petrophysical properties, such as porosity and permeability, for selected sedimentary units. This lithological classification and data interpretation were developed collaboratively with contributions from the master's thesis work and the broader geological characterization effort. Although the complete datasets remain confidential at this stage, it is expected to be made publicly available by the NTGS in the near future.

According to Clauser (2011), increasing porosity and permeability can influence the effective thermal conductivity of rocks, particularly when comparing in situ conditions to dry laboratory measurements. In porous media, the presence of air or water within pore spaces alters the overall thermal conductivity, air significantly reduces it, while water has a more moderate impact due to its higher conductivity compared to air. However, based on visual inspection of core samples, laboratory measurements, and literature and well data from the region (Rajaobelison et al., 2024, In press, In press; Thibault et al., 2025), porosity and permeability in the subsurface are expected to be significantly low. Consequently, their impact on thermal conductivity is considered limited. For the sake of model simplicity, this influence is not explicitly incorporated in this study, although its presence is acknowledged.

An important limitation is the assumptions of constant thermal conductivity among units. Thermal conductivity in rocks diminishes with increasing temperature, particularly at greater depths where temperature and pressure are heightened (Clauser, 2011; Wu et al., 2023). Accounting for this temperature dependence would reduce the efficiency of heat conduction at depth, thereby increasing predicted subsurface temperatures (Majorowicz et al., 2014a). While this study aimed to establish an initial temperature profile using a simple linear solution, more advanced approaches, such as the non-linear heat conduction model proposed by Clauser (2011) or fully numerical simulations (Miranda et al., 2021), could offer more realistic results. Although not pursued here due to the preliminary scope of the study that aimed at providing an initial temperature assessment below the studied South Slave Communities, future studies could implement these methods using platforms like Python, MATLAB, or COMSOL to better capture temperature-dependent thermal conductivity and subsurface heat transfer dynamics.

4.2.3 Radiogenic Heat Production Assumptions

In this study, constant radiogenic heat production values were assumed for each geological unit, including the basement, based on representative values from corresponding tectonic domains. While practical for simplified and preliminary modelling, this assumption overlooks the natural vertical variability of radiogenic heat production within the crust. In crystalline basement rocks in particular, heat production typically decreases approximately exponentially with depth due to compositional changes and the distribution of radioactive isotopes (Blackwell et al., 2007).

Models incorporating exponential decay of heat production with depth, such as that proposed by Blackwell et al. (2007) and used by Bédard et al. (2018), could be integrated in future works. This would reduce the estimated radiogenic contribution at greater depths and consequently, lower temperature estimates in the deeper part of the models. This correction becomes increasingly important for deep extrapolations (e.g., down to 10 km), where cumulative radiogenic heat influences thermal profiles. However, at shallower depths (~3 km or less), which are more realistic targets for preliminary geothermal exploration, the impact on temperature estimates is expected to be minor, as shown by Bédard et al. (2016).

Future work may benefit from implementing depth-dependent heat production, particularly in crustal-scale models or when evaluating deep geothermal reservoirs. Such refinements can be integrated even with low-complexity modelling environments (e.g., spreadsheet-based tools), without requiring advanced numerical simulations. For models extending beyond ~3 km depth, this approach could reduce overestimated temperatures by accounting for the lower radiogenic heat contribution at depth. However, while it can help explore a broader range of thermal scenarios, it may not necessarily improve prediction accuracy. The absence of direct measurements at depth makes it difficult to confirm whether a constant or exponentially decreasing heat production assumption is more realistic. Therefore, although depth-dependent models may refine the conceptual understanding of subsurface heat flow, they do not eliminate the underlying uncertainties associated with radiogenic heat distribution. For practical purposes, especially in early stages resource assessment or for models limited to the upper crust, assuming constant radiogenic heat production may provide a reasonable approximation, given current data limitations.

4.2.4 Modelling Framework and Uncertainty Treatment

This study adopted a scenario-based approach by evaluating optimistic, normal, and pessimistic cases, each constructed using plausible percentile variations in key input parameters. This method offers a straightforward way to explore how variations in input values influence subsurface temperature predictions.

However, this approach remains limited compared to probabilistic methods such as Monte Carlo simulations, which provide a more rigorous framework for uncertainty quantification (Miranda et al., 2020). These methods involve running thousands of simulations by randomly sampling input parameters from defined probability distributions. This produces a statistical distribution of outcomes, enabling the estimation of confidence intervals, the identification of the most influential parameters, thus improving confidence in resource assessments (Bacon et al., 2024; Miranda et al., 2020). Such techniques are particularly valuable in regions with sparse data and high geological heterogeneity, as is the case in this study, where scenario-based models revealed wide temperature ranges between optimistic and pessimistic cases for each community. It is important to note, however, that while probabilistic methods can better characterize uncertainty, they do not reduce it. The fundamental limitations, such as the absence of direct temperature measurements or uncertainties in thermal properties, remain, regardless of the method used.

Implementing such probabilistic methods was beyond the scope and timeframe of this master's thesis. Nonetheless, future work should prioritize such approaches to improve the robustness and reliability of geothermal resource assessments.

4.2.5 Well Data

The present study builds upon and integrates findings from prior collaborative efforts (Rajaobelison et al., 2024, In press), which provided an initial thermal assessment of the shallow sedimentary sequence.

A key limitation of the present work, shared with the earlier study, lies in the reliance on sparse, shallow, and legacy well temperature data, primarily BHT and DST. These point-based measurements are often unequilibrated and subject to drilling-related disturbances, introducing significant uncertainty in subsurface temperature estimates (Rajaobelison et al., 2024). Such conditions may result in the over- or underestimation of equilibrium subsurface temperatures, particularly in areas where advective heat transport or fluid migration may occur (Bachu, 1993).

A central simplifying assumption of this study is that it only considers conductive heat transfer. This assumption is based on the expected and measured low permeability and porosity of the sedimentary formations and basement rocks at the regional scale (Rajaobelison et al., 2024, In press; Thibault et al., 2025, Submitted), which also facilitated model simplification in light of the limited availability of detailed, site-specific subsurface data. Support for this assumption also comes from recent equilibrium temperature profiles acquired at Cameron Hills, which indicates a linear geothermal gradient consistent with conductive heat transfer (Rajaobelison et al., 2024). However, the profile's depth is limited, and its representativity for deeper sections or other locations remains uncertain. Nonetheless, this assumption may overlook localized phenomena that could enhance advective heat transport, such as faulting, fracturing, hydrothermal alteration, or tectonic activity (Grasby et al., 2012). A relevant example is the Pine Point Mine area, located about 60 km east of Hay River, where such localized effects have been documented, including increased permeability and porosity (Meijer-Drees, 1993; Rhodes et al., 1984). Although such phenomena are plausible, their presence directly beneath the studied communities cannot be confirmed with current data. Even if present, quantifying their influence on local heat flow would be challenging without targeted hydrogeological and petrophysical measurements. For this reason, their exclusion from the model represents both a necessary simplification and a limitation that could affect the validity of temperature predictions.

Moreover, the limited spatial coverage and legacy nature of available well data constrain the ability to resolve thermal gradients confidently or to assess localized variations. The reliance on discrete, unequilibrated temperature measurements and the assumption of purely conductive heat transfer, while practical, may oversimplify the subsurface system, particularly in geologically complex settings. Altogether, these limitations underscore the need for improved data acquisition. Future studies would benefit from dedicated drilling campaigns, modern equilibrium temperature logging, and detailed hydrogeological characterization to refine thermal models and better account for subsurface heterogeneities in this data-scarce region.

4.3 Contribution

The strength of this research lies in its localized approach and the use of site-specific thermal data, derived from laboratory measurements on rocks expected to be found below the communities. This contrasts with the use of generalized literature values in previous studies (EBA Engineering Consultants Ltd., 2010), making our results more applicable and relevant to the communities of the South Slave Region, which are the potential beneficiaries of that heat resource.

This research advances the understanding of geothermal potential in the South Slave Region by focusing on the deep geothermal resources beneath the communities of Hay River, Fort Providence, Enterprise, and Kakisa. Although the region had previously been recognized as part of the NPHFA (Majorowicz, 1996; Majorowicz & Weides, 2014) and classified by EBA Engineering Consultants Ltd. (2010) for its potentially high geothermal potential, no prior study had assessed this potential at a community-specific level. Previous assessments grouped these communities within a broad regional classification, relying on averaged values that overlooked local geological variations and did not provide temperature estimates at depth tailored to each community. As a result, the potential end users of geothermal energy lacked relevant localized data to support informed energy planning and development.

This study represents the first geothermal assessment in the region grounded in specific geological units and rock types that characterize the local subsurface. Previous studies relied mostly on generalized literature values and regional averages, without accounting for the geological heterogeneity and stratigraphic distribution of subsurface formations. By incorporating laboratory-measured thermal properties from rock samples representative of the same geological formations found beneath the communities, this work improves the accuracy and reliability of temperature estimations at depth and provides a more realistic picture of the geothermal resource potential.

By first providing a detailed analysis of the local geology beneath each community—contributing to the understanding of the shallow sedimentary sequences—this study places particular emphasis on the thermal properties of the underlying Precambrian basement. These properties are critical for accurately estimating deep geothermal resources, especially considering that the basement depth is relatively shallow in this area. The results offer a clearer picture of subsurface temperatures beneath the South Slave communities and highlight the importance of localized assessments in geothermal exploration, while averaged regional-scale estimates may not reflect site-specific conditions.

4.3.1 Implications for Geothermal Exploration

The results of this study offer the first assessment of subsurface temperature profiles below South Slave communities and helped identify both where prospective geothermal resources may exist and which technologies are best suited to harness them. This localized modelling approach yields results that are directly relevant for future geothermal resource evaluations and can help guide strategic decision-making for community-scale energy planning.

Geothermal exploration in northern Canada presents unique logistical and economic challenges. Communities are often small, remote, and dispersed over vast territories, meaning that geothermal development must be targeted near actual energy demand centers (Majorowicz & Grasby, 2021a, 2021b). Conducting regional-scale exploration in areas devoid of consumers is not economically viable (Grasby et al., 2012). The high cost of constructing long-distance pipelines or power lines could quickly outweigh the potential benefits of the geothermal resource, making projects economically unfeasible if the source is located more than approximately 10 to 30 km from the community it is intended to serve (Ammar et al., 2012; Kapil et al., 2012; Majorowicz & Grasby, 2021b). Given these constraints, a community-based exploration strategy is more appropriate than a broad regional assessment. This approach ensures that geothermal assessments are concentrated in areas where development could realistically proceed and deliver tangible benefits for residents. In addition to technical and economic factors, the success of geothermal initiatives in northern communities should involve social acceptability (Friser et al., 2024), and ideally be grounded in meaningful collaboration with local populations and authorities, guided by their interests, values.

In terms of practical applications, the predicted thermal gradients and temperature profiles indicate promising opportunities for direct-use geothermal systems. In the sedimentary sequence, temperatures below 37 °C suggest that geothermal heat could be used for space heating, particularly when combined with heat pump technologies (Grasby et al., 2012). For Hay River and Kakisa, deeper drilling into the Precambrian basement is needed to reach higher temperatures. Our models estimate that temperatures exceeding 150 °C, suitable for power generation (Ahmadi et al., 2020), could be reached at depths of 1500–3000 m for Hay River and 2250–4500 m for Kakisa. At these depths, the geological context consists of low-permeability crystalline rocks, which would require the implementation of EGS or closed-loop systems such as DBHE that relies on conductive heat transfer.

In areas like Hay River, where the highest subsurface temperatures coincide with the presence of nearby communities, closed-loop systems, particularly DBHEs, appear to be a practical and scalable solution. These systems are not dependent on the presence of aquifers or fractures, and pose fewer environmental and social concerns compared to open-loop or EGS technologies (Kolo et al., 2024). Their deployment within communities minimizes surface infrastructure and heat loss, making them especially attractive for heating networks. The evaluation and optimization of such systems will form the next phase of this research project, through site-specific numerical modelling in the context of future work.

In contrast, if the objective is to explore higher-enthalpy resources or evaluate electricity production potential, exploration would need to focus on deeper targets potentially associated with regional fault zones. These structures, although not well characterized, could host fluid circulation or localized permeability enhancements favourable to EGS. However, the current lack of structural and hydrogeological data limits our ability to assess this potential. More detailed geophysical surveys and deep exploration drilling would be necessary to evaluate the viability of such systems.

For now, the simplicity, adaptability, and compatibility with local heating needs make closed-loop systems the most promising near-term option for geothermal development in the South Slave region. Nevertheless, continued efforts to improve geological knowledge and quantify geothermal resources, such as estimating energy in place or recoverable heat volumes, as demonstrated by Bédard et al. (2020) in the St. Lawrence Lowlands, could be essential to guide long-term geothermal energy strategies in the northern part of the WCSB.

4.4 Conclusion

In conclusion, this study provides the first localized assessment of deep geothermal potential in the South Slave communities, based on modelled temperature profiles at depth. The results suggest the presence of relatively high temperatures and heat flow, which would be associated with a favourable geothermal potential. As such, geothermal energy could play a meaningful role in enhancing regional energy security, reducing reliance on diesel, and supporting climate mitigation efforts. However, these estimates remain theoretical and are subject to significant uncertainty due to the limited availability of subsurface data in the region. Exploration drilling would therefore represent the next essential step to reduce this uncertainty through direct temperature measurements at depth. Although such drilling involves substantial costs, the promising results of this study help justify its consideration. By delivering a preliminary temperature evaluation directly beneath the communities, this work fulfills its objective of supporting informed decisions about whether or not to proceed with further geothermal exploration.

A key next step in this research would be to conduct a probabilistic resource calculations to provide a more detailed assessment of the geothermal potential. This includes estimating the amount of extractable heat and energy capacity. Future work could enhance the evaluation by incorporating numerical simulations to assess the performance and efficiency of geothermal systems, such as DBHE. These simulations would offer valuable insights into the system's capabilities in these specific geological settings and help quantify the region's geothermal potential.

Given the applied nature of this research, it is also important to reflect on what these findings could mean in a practical context for the communities involved. For those interested in developing geothermal energy as part of their local energy strategy, the next step would typically involve drilling an exploration well to validate the estimated temperatures at depth (Aragón-Aguilar et al., 2019). This would allow for accurate resource calculations and support decisions about the feasibility and scale of geothermal heating systems.

Beyond the technical evaluations, successful implementation also depends on understanding the specific energy needs, priorities, and values of each community. This includes assessing current and future heating demands, ensuring social acceptability, and considering the long-term vision for sustainable development. While deeper geothermal systems may require substantial investments, alternative or hybrid approaches, such as shallow geoexchange systems, could offer more accessible solutions in the short term. In all cases, collaboration among local governments, Indigenous organizations, residents, engineers, and policymakers will be essential to advance geothermal development in a way that reflects community aspirations and realities.

Importantly, this research takes place on Indigenous traditional territories, and care must be taken not to repeat colonial patterns. It is therefore essential that Indigenous communities have the right to Free, Prior and Informed Consent (FPIC) as recognized by the United Nations (OHCHR, 2013), enabling them to lead decision-making processes regarding whether geothermal development aligns with their visions, values, and long-term aspirations. Respecting Indigenous sovereignty and governance is crucial to ensuring that geothermal projects are developed in a manner that truly reflects community priorities and supports self-determination.

Ultimately, these efforts could guide the development of sustainable energy solutions tailored to local communities' needs and support broader goals of regional economic development and energy independence.

Bibliography

Ahmadi, A., Assad, M. E. H., Jamali, D. H., Kumar, R., Li, Z. X., Salameh, T., Al-Shabi, M., & Ehyaei, M. A. (2020). Applications of geothermal organic Rankine Cycle for electricity production. *Journal of Cleaner Production*, *274*, 122950. https://doi.org/10.1016/j.jclepro.2020.122950

Amani, M., Mahdavi, S., Afshar, M., Brisco, B., Huang, W., Mirzadeh, S. M. J., White, L., Banks, S. N., Montgomery, J., & Hopkinson, C. (2019). Canadian Wetland Inventory using Google Earth Engine: The First Map and Preliminary Results. *Remote Sensing*, *11*, 842. https://doi.org/10.3390/rs11070842

Ammar, Y., Joyce, S., Norman, R., Wang, Y., & Roskilly, A. P. (2012). Low grade thermal energy sources and uses from the process industry in the UK. *Applied Energy*, *89*(1), 3–20. https://doi.org/10.1016/j.apenergy.2011.06.003

Aragón-Aguilar, A., Izquierdo-Montalvo, G., Aragón-Gaspar, D. O., & Barreto-Rivera, D. N. (2019). *Renewable Geothermal Energy Explorations*. BoD – Books on Demand.

Arctic Energy Alliance. (2018). *ENERGY PROFILE Where we get energy and how we use it FORT PROVIDENCE*.

Augustine, C., Tester, J., Anderson, B., Petty, S., & Livesay, B. (2006). A comparison of geothermal with oil and gas well drilling costs. *31st Workshop on Geothermal Reservoir Engineering*, 5–19.

Bachu, S. (1993). Basement heat flow in the Western Canada Sedimentary Basin. *Tectonophysics*, *222*(1), 119–133. https://doi.org/10.1016/0040-1951(93)90194-O

Bacon, Y., Miranda, M. M., Raymond, J., Newson, J., Wigston, A., & Minnick, M. (2024). The deep geothermal energy potential of Baker Lake (Nunavut, Canada): Initial resource assessment from Monte Carlo analysis. *GRC Transactions*, *48*, 2443–2465.

Beach, R. D. W., Jones, F. W., & Majorowicz, J. A. (1987). Heat flow and heat generation estimates for the churchill basement of the western canadian basin in Alberta, Canada. *Geothermics*, *16*(1), 1–16. https://doi.org/10.1016/0375-6505(87)90075-7

Beardsmore, G. R., & Cull, J. P. (2001). *Crustal Heat Flow: A Guide to Measurement and Modelling*. Cambridge University Press.

Bédard, K., Comeau, F.-A., Millet, E., Raymond, J., Malo, M., & Gloaguen, E. (2016). *Évaluation des ressources géothermiques du bassin des Basses-Terres du Saint-Laurent.* (Rapport de recherche No. 1659; Issue R1659). Institut national de la recherche scientifique, Centre Eau Terre Environnement. https://espace.inrs.ca/id/eprint/4845/

Bédard, K., Comeau, F.-A., Raymond, J., Gloaguen, E., Malo, M., & Richard, M.-A. (2020). Deep geothermal resource assessment of the St. Lawrence Lowlands sedimentary basin (Québec) based on 3D regional geological modelling. *Geomechanics and Geophysics for Geo-Energy and Geo-Resources*, *6*(3), 46. https://doi.org/10.1007/s40948-020-00170-0

Bédard, K., Comeau, F.-A., Raymond, J., Malo, M., & Nasr, M. (2018). Geothermal Characterization of the St. Lawrence Lowlands Sedimentary Basin, Québec, Canada. *Natural Resources Research*, *27*(4), Article 4. https://doi.org/10.1007/s11053-017-9363-2

Beltrami, H., Gosselin, C., & Mareschal, J. C. (2003). Ground surface temperatures in Canada: Spatial and temporal variability. *Geophysical Research Letters*, *30*(10). https://doi.org/10.1029/2003GL017144

Birch, A. F. (1948). *The effects of Pleistocene climatic variations upon geothermal gradients*. *246*, 729–762.

Blackwell, D. D. (1983). *HEAT FLOW IN THE NORTHERN BASIN AND RANGE PROVINCE* (Special Report No. 13; The Role of Heat in the Development of Energy and Mineral Resources in the Northern Basin and Range Province, pp. 81–93). Geothermal Resources Council.

Blackwell, D. D., Negraru, P. T., & Richards, M. C. (2007). Assessment of the Enhanced Geothermal System Resource Base of the United States. *Natural Resources Research*, *15*(4), 283–308. https://doi.org/10.1007/s11053-007-9028-7

Blackwell, D. D., Richards, M. C., & Stepp, P. (2010). *Texas Geothermal Assessment for the I35 Corridor East* (No. CM709). Huffington Department of Earth Sciences, Southern Methodist University. https://www.smu.edu/-/media/site/dedman/academics/programs/geothermal-lab/documents/smu_seco_cm709_texasgeothermalreport.pdf

Blackwell, D. D., & Steele, J. L. (1992). *Geothermal Map of North America* [Map]. Geological Society of America. https://doi.org/10.1130/DNAG-CSMS-v6

Blackwell, D. D., Steele, J. L., & Carter, L. C. (1990). *Heat flow patterns of the North American continent: A discussion of the DNAG Geothermal Map of North America*. DOEEEGTP (USDOE Office of Energy Efficiency and Renewable Energy Geothermal Tech Pgm). https://doi.org/10.2172/896322

Bücker, C., & Rybach, L. (1996). A simple method to determine heat production from gamma-ray logs. *Marine and Petroleum Geology*, *13*(4), 373–375. https://doi.org/10.1016/0264-8172(95)00089-5

Burrus, J., & Foucher, J. P. (1986). Contribution to the thermal regime of the Provençal Basin based on Flumed heat flow surveys and previous investigations. *Tectonophysics*, *128*(3), 303–334. https://doi.org/10.1016/0040-1951(86)90299-4

Canada Energy Regulator & Government of Canada. (2023, November 28). *Market Snapshot: Explaining the high cost of power in northern Canada* [Governmental website]. Canada Energy Regulator. https://www.cer-rec.gc.ca/en/data-analysis/energy-markets/market-snapshots/2017/market-snapshot-explaining-high-cost-power-in-northern-canada.html

Cermak, V., & Rybach, L. (1982). Thermal Conductivity and Specific Heat of Minerals and Rocks. In *Physical Properties of Rocks* (Vol. 1A, pp. 305–343). Springer. https://doi.org/10.1007/10201894_62

Chapelet, M. (2022). *Chapelet, M. (2022). Évaluation du potentiel des anomalies géothermiques du bassin sédimentaire des basses-terres du Saint-Laurent (Québec, Canada)* [Master's thesis, Institut national de la recherche scientifique]. https://www.proquest.com/openview/3ffdbacd59fcde3cdc69e7c98d58fd28/1?pq-origsite=gscholar&cbl=18750&diss=y

Clauser, C. (2011). Thermal Storage and Transport Properties of Rocks, I: Heat Capacity and Latent Heat. In H. K. Gupta (Ed.), *Encyclopedia of Solid Earth Geophysics* (pp. 1423–1431). Springer Netherlands. https://doi.org/10.1007/978-90-481-8702-7_238

Clauser, C., & Huenges, E. (1995). Thermal conductivity of rocks and minerals. In *Rock physics and phase relations: A handbook of physical constants* (Vol. 3, pp. 105–126). American Geophysical Union.

Crowell, A. M., & Gosnold, W. (2011). Correcting Bottom Hole Temperatures: A Look at the Permian Basin (Texas), Williston Basin (North Dakota), Anadarko and Arkoma Basins (Oklahoma). *GRC Transactions*, *35*, Article GRC1029323. https://www.osti.gov/biblio/1137031

Crowell, A. M., Ochsner, A. T., & Gosnold, W. (2012). Correcting Bottom-Hole Temperatures in the Denver Basin: Colorado and Nebraska. *Geothermal Resources Council Annual Meeting*, *36*.

Da Silva Carvalho, H., & Vacquier, V. (1977). Method for determining terrestrial heat flow in oil fields. *GEOPHYSICS*, *42*(3), 584–593. https://doi.org/10.1190/1.1440729

Davenport, P. H. (2001). *Exploration Areas of the NWT, Yukon and Nunavut; ESRI* [ESRI ArcView® GIS Shapefiles; Shapefiles]. Geological Survey of Canada.

Decagon Devices. (2011). *KD2 Pro Thermal Properties Analyzer Operator's Manual Version 10*. Decagon Devices, Inc. https://www.catec.nl/uploads/pdf/DEC-KD2-Pro-manual_763.pdf

Deming, D., & Chapman, D. S. (1988). Heat Flow in the Utah-Wyoming Thrust Belt From Analysis of Bottom-Hole Temperature Data Measured in Oil and Gas Wells. *Journal of Geophysical Research: Solid Earth*, *93*(B11), 13657–13672. https://doi.org/10.1029/JB093iB11p13657

Dowdle, W. L., & Cobb, W. M. (1975). Static Formation Temperature From Well Logs—An

Empirical Method. *Journal of Petroleum Technology*, *27*(11), 1326–1330. https://doi.org/10.2118/5036-PA
Dyke, A. S. (2004). An outline of North American deglaciation with emphasis on central and northern Canada. In J. Ehlers & P. L. Gibbard (Eds.), *Developments in Quaternary Sciences* (Vol. 2, pp. 373–424). Elsevier. https://doi.org/10.1016/S1571-0866(04)80209-4
Eaton, D. W., & Hope, J. (2003). *Structure of the crust and upper mantle of the Great Slave Lake shear zone, northwestern Canada, from teleseismic analysis and gravity modelling1 | Canadian Journal of Earth Sciences | GeoScienceWorld*. *40*(9), 1203–1218. https://doi.org/10.1139/e03-038
EBA Engineering Consultants Ltd. (2010). *Geothermal Favourability Map Northwest Territories Report* (Governmental Report No. Y22101146; Northwest Territories Environment and Natural Resources., pp. 1–59). Northwest Territories Environment and Natural Resources. https://www.enr.gov.nt.ca/sites/enr/files/reports/geothermal_favorability_report.pdf
Eppelbaum, L., Kutasov, I., & Pilchin, A. (2014). *Applied Geothermics*. Springer. https://doi.org/10.1007/978-3-642-34023-9
Faulds, J., Coolbaugh, M., Bouchot, V., Moeck, I., & Oguz, K. (2010). Characterizing Structural Controls of Geothermal Reservoirs in the Great Basin, USA, and Western Turkey: Developing Successful Exploration Strategies in Extended Terranes. *World Geothermal Congress*. World Geothermal Congress, Bali, Indonesia. https://brgm.hal.science/hal-00495884/
Federal Geographic Data Committee. (2006). *FGDC Geologic Map Symbol Standard* (Dataset No. FGDC-STD-013-2006). Federal Geographic Data Committee. https://ngmdb.usgs.gov/fgdc_gds/geolsymstd.php
Flóvenz, Ó. G., & Saemundsson, K. (1993). Heat flow and geothermal processes in Iceland. *Tectonophysics*, *225*(1), 123–138. https://doi.org/10.1016/0040-1951(93)90253-G
Förster, A., Merriam, D. F., & Davis, J. C. (1997). Spatial analysis of temperature (BHT/DST) data and consequences for heat-flow determination in sedimentary basins. *Geologische Rundschau*, *86*(2), 252–261. https://doi.org/10.1007/s005310050138
Friser, A., Chapman, F., Miranda, M. M., Gorcy, D., & Raymond, J. (2024). Capturing the social acceptability of geothermal energy in northern Canada: An interdisciplinary initiative involving communities. *European Geologist*, *57*. https://doi.org/10.5281/zenodo.12205625
Gal, L. P., & Jones, A. L. (2003). *Evaluation of oil and gas potential in the Deh Cho territory* (Open File Report Nos. 2003–03; p. 88). C.S. Lord Northern Geoscience Centre. https://www.osti.gov/etdeweb/biblio/20800544
Gough, D. I. (1984). Mantle upflow under North America and plate dynamics. *Nature*, *311*(5985), 428–433. https://doi.org/10.1038/311428a0
Government of Canada & Environment and Natural Resources. (2024). *Historical Climate Data* [Governemental Website]. Weather, Climate and Hazard. https://climate.weather.gc.ca/
Government of Canada & Natural Resources Canada. (2022). *Lexicon of Canadian Geological Names on-line* [Database Governmental Website]. WEBLEX Canada. https://weblex.canada.ca/weblexnet4/LithoSearch_e.aspx
Government of Canada, S. C. (2022). *Population and dwelling counts: Canada, provinces and territories, and census subdivisions (municipalities)*. https://www150.statcan.gc.ca/t1/tbl1/en/tv.action?pid=9810000202
Government of Northwest Territories. (2018). *2030 Energy Strategy* (Governmental Report No. 7272; p. 46). Government of Northwest Territories. https://www.inf.gov.nt.ca/en/services/energy/2030-energy-strategy
Government of Northwest Territories. (2024). *2023-2024 Energy Initiatives Report* (Reporting on Actions under the 2030 Energy Strategy, p. 60) [Information]. Government of Northwest Territories. https://www.inf.gov.nt.ca/en/services/energy/2023-2024-energy-initiatives-report
Government of Northwest Territories, Municipal and Community Affairs, & Goddard, J. (2023). *GNWT water monitoring wells* [Excel sheet].
Grasby, S. E., Allen, D. M., Bell, S., Chen, Z., Ferguson, G., Jessop, A. M., Kelman, M., Ko, M., Majorowicz, J., Moore, M., Raymond, J., & Therrien, R. (2012). *Geothermal energy resource potential of Canada* (Open File No. 6914; p. 322). Geological Survey of Canada. https://doi.org/10.4095/291488
Grasby, S. E., Majorowicz, J., & Fiess, K. (2021). Geothermal Energy Potential of Northwest

Territories, Canada. *World Geothermal Congress 2020+1*, 6. https://www.researchgate.net/publication/354968121_Geothermal_Energy_Potential_of_Northwest_Territories_Canada

Grasby, S. E., Majorowicz, J., & Ko, M. (2009). *Geothermal maps of Canada* (Geological Survey of Canada Open File No. 6167; p. 35). https://doi.org/10.4095/247765

Grasby, S. E., Majorowicz, J., & McGune, G. E. (2013). *Geothermal energy potential for northern communities* (Open File No. 7350; p. 50). Geological Survey of Canada. https://doi.org/10.4095/292840

Gray, A. D., Majorowicz, J., & Unsworth, M. (2012). Investigation of the geothermal state of sedimentary basins using oil industry thermal data: Case study from Northern Alberta exhibiting the need to systematically remove biased data. *Journal of Geophysics and Engineering*, *9*(5), 534–548. https://doi.org/10.1088/1742-2132/9/5/534

Gregory, A. R., Dodge, M. M., Posey, J. S., & Morton, R. A. (1980). *Volume and accessibility of entrained (solution) methane in deep geopressured reservoirs—Tertiary formations of the Texas Gulf Coast. Final report* (Final Report No. DOE/ET/11397-1). Texas Univ., Austin (USA). Bureau of Economic Geology. https://doi.org/10.2172/5282675

Harrison, W. E., Luza, K. V., Prater, M. L., & Cheung, P. K. (1983). *Geothermal resource assessment in Oklahoma* (No. DE-AS07-80ID12172). Oklahoma Geological Survey, Norman (USA). https://doi.org/10.2172/6763329

Hasterok, D., Gard, M., & Webb, J. (2018). On the radiogenic heat production of metamorphic, igneous, and sedimentary rocks. *Geoscience Frontiers*, *9*(6), 1777–1794. https://doi.org/10.1016/j.gsf.2017.10.012

Hogue, B. C., & Gal, L. P. (2008). *NWT Formation Tops for Petroleum Exploration and Production Wells: 60 to 80° N; Northwest Territories Geoscience Office* (Database No. NWT Open Rport 2008-002; pp. 4 and Microsoft Excel spreadsheet). Northwest Territories Geoscience Office.

Jaupart, C., & Mareschal, J.-C. (2010). *Heat Generation and Transport in the Earth*. Cambridge University Press.

Jessop, A. M. (1971). The Distribution of Glacial Perturbation of Heat Flow in Canada. *Canadian Journal of Earth Sciences - CAN J EARTH SCI*, *8*, 162–166. https://doi.org/10.1139/e71-012

Jessop, A. M. (Ed.). (1990). Chapter 3—Analysis and Correction of Heat Flow on Land. In *Developments in Solid Earth Geophysics* (Vol. 17, pp. 57–85). Elsevier. https://doi.org/10.1016/B978-0-444-88309-4.50007-5

Jessop, A. M. (1992). Thermal input from the basement of the Western Canada Sedimentary Basin. *Bulletin of Canadian Petroleum Geology*, *40*(3), 198–206. https://doi.org/10.35767/gscpgbull.40.3.198

Kapil, A., Bulatov, I., Smith, R., & Kim, J.-K. (2012). Process integration of low grade heat in process industry with district heating networks. *Energy*, *44*(1), 11–19. https://doi.org/10.1016/j.energy.2011.12.015

Kolo, I., Brown, C. S., Nibbs, W., Cai, W., Falcone, G., Nagel, T., & Chen, C. (2024). A comprehensive review of deep borehole heat exchangers (DBHEs): Subsurface modelling studies and applications. *Geothermal Energy*, *12*(1), 19. https://doi.org/10.1186/s40517-024-00297-3

Larmagnat, S., Lavoie, D., Rajaobelison, M., & Raymond, J. (2019). *Geothermal assessment of a conventional hydrocarbon reservoir in eastern Quebec: Preliminary field and petrophysical data* (Open File No. 8597). Geological Survey of Canada. https://doi.org/10.4095/315028

Lemmen, D. S., Duk-Rodkin, A., & Bednarski, J. M. (1994). Late glacial drainage systems along the northwestern margin of the Laurentide Ice Sheet. *Quaternary Science Reviews*, *13*(9), 805–828. https://doi.org/10.1016/0277-3791(94)90003-5

Lindal, B. (1973). Industrial and other applications of geothermal energy. *Geothermal Energy*, 135–148.

Mackenzie Valley Land and Water Board. (2023). *MV2019L3-0010—Groundwater Monitoring Program Proposal—Hay River, NT*. Mackenzie Valley Land and Water Board, Town of Hay River. https://mvlwb.com/registry/mv2019l3-0010

Mahbaz, S. B., Dehghani-Sanij, A. R., Dusseault, M. B., & Nathwani, J. S. (2020). Enhanced and integrated geothermal systems for sustainable development of Canada's northern communities. *Sustainable Energy Technologies and Assessments*, *37*, 100565.

https://doi.org/10.1016/j.seta.2019.100565
Majorowicz, J. (1996). Anomalous heat flow regime in the Western margin of the North American Craton, Canada. *Journal of Geodynamics*, *21*(2), 123–140. https://doi.org/10.1016/0264-3707(95)00020-2
Majorowicz, J. (2018). Heat flow–heat production relationship not found: What drives heat flow variability of the Western Canadian foreland basin? *International Journal of Earth Sciences*, *107*(1), 5–18. https://doi.org/10.1007/s00531-016-1352-x
Majorowicz, J., Chan, J., Crowell, J., Gosnold, W., Heaman, L. M., Kück, J., Nieuwenhuis, G., Schmitt, D. R., Unsworth, M., Walsh, N., & Weides, S. (2014a). The first deep heat flow determination in crystalline basement rocks beneath the Western Canadian Sedimentary Basin. *Geophysical Journal International*, *197*(2), 731–747. Geophysical Journal International. https://doi.org/10.1093/gji/ggu065
Majorowicz, J., Garven, G., Jessop, A. M., & Jessop, C. (1999). *Present Heat Flow Along a Profile Across the Western Canada Sedimentary Basin: The Extent of Hydrodynamic Influence* (A. Förster & D. F. Merriam, Eds.; pp. 61–79). Springer US. https://doi.org/10.1007/978-1-4615-4751-8_3
Majorowicz, J., Gosnold, W., Gray, A., Safanda, J., Klenner, R., & Unsworth, M. (2012). Implications of Post-Glacial Warming for Northern Alberta Heat Flow—Correcting for the Underestimate of the Geothermal Potential. In *GRC Transactions* (2012th ed., Vol. 36, pp. 693–698).
Majorowicz, J., & Grasby, S. (2021a). *Geothermal Heat Energy Potential for Small Communities in Alberta, Canada*.
Majorowicz, J., & Grasby, S. E. (2010a). Heat flow, depth–temperature variations and stored thermal energy for enhanced geothermal systems in Canada. *Journal of Geophysics and Engineering*, *7*(3), 232–241. https://doi.org/10.1088/1742-2132/7/3/002
Majorowicz, J., & Grasby, S. E. (2010b). High Potential Regions for Enhanced Geothermal Systems in Canada. *Natural Resources Research*, *19*(3), 177–188. https://doi.org/10.1007/s11053-010-9119-8
Majorowicz, J., & Grasby, S. E. (2021b). Deep Geothermal Heating Potential for the Communities of the Western Canadian Sedimentary Basin. *Energies*, *14*(3), Article 3. https://doi.org/10.3390/en14030706
Majorowicz, J., & Jessop, A. M. (1981). Regional heat flow patterns in the Western Canadian Sedimentary Basin. *Tectonophysics*, *74*(3), 209–238. https://doi.org/10.1016/0040-1951(81)90191-8
Majorowicz, J., Nieuwenhuis, G., Unsworth, M., Phillips, J., & Verveda, R. (2014b). High Temperatures Predicted in the Granitic Basement of Northwest Alberta—An Assessment of the EGS Energy Potential. *Thirty-Ninth Workshop on Geothermal Reservoir Engineering*, 12.
Majorowicz, J., Šafanda, J., & Torun-1 Working Group. (2008). Heat flow variation with depth in Poland: Evidence from equilibrium temperature logs in 2.9-km-deep well Torun-1. *International Journal of Earth Sciences*, *97*(2), 307–315. https://doi.org/10.1007/s00531-007-0210-2
Majorowicz, J., & Weides, S. (2014). Large Scale Geothermal High in the Westernmost North American Covered Craton–Can Heat Flow Vs. Basement Heat Production Be a Reliable Tool in Predicting Deep EGS Geothermal Resource? *Thirty-Ninth Workshop on Geothermal Reservoir Engineering*, 9.
Mareschal, J. C., & Jaupart, C. (2004). Variations of surface heat flow and lithospheric thermal structure beneath the North American craton. *Earth and Planetary Science Letters*, *223*(1), 65–77. https://doi.org/10.1016/j.epsl.2004.04.002
Meijer-Drees, N. C. (1993). *The Devonian succession in the subsurface of the Great Slave and Great Bear plains, Northwest Territories* (Vol. 393). Energy, Mines and Resources Canada, Geological Survey of Canada. https://publications.gc.ca/site/eng/25782/publication.html
Miall, A. D. (2015). Geological Regions. In *The Canadian Encyclopedia*. https://www.thecanadianencyclopedia.ca/en/article/geological-regions
Mielke, P., Bär, K., & Sass, I. (2017). Determining the relationship of thermal conductivity and compressional wave velocity of common rock types as a basis for reservoir characterization. *Journal of Applied Geophysics*, *140*, 135–144. https://doi.org/10.1016/j.jappgeo.2017.04.002
Miranda, M. M., Raymond, J., & Dezayes, C. (2020). Uncertainty and Risk Evaluation of Deep

Geothermal Energy Source for Heat Production and Electricity Generation in Remote Northern Regions. *Energies*, *13*(16), Article 16. https://doi.org/10.3390/en13164221

Miranda, M. M., Velez Márquez, M. I., Raymond, J., & Dezayes, C. (2021). A numerical approach to infer terrestrial heat flux from shallow temperature profiles in remote northern regions. *Geothermics*, *93*, 102064. https://doi.org/10.1016/j.geothermics.2021.102064

Moeck, I. (2012). A new classification scheme for deep geothermal systems based on geologic controls. *EGU General Assembly Conference Abstracts*, 9681. https://ui.adsabs.harvard.edu/abs/2012EGUGA..14.9681M/abstract

Moore, P. F. (1993). Devonian. In D. F. Stott & J. D. Aitken (Eds.), *Sedimentary Cover of the Craton in Canada* (Vol. 5, p. 0). Geological Society of America. https://doi.org/10.1130/DNAG-GNA-D1.150

Morrow, D. W. (2012). *Devonian of the Northern Canadian Mainland Sedimentary Basin (a contribution to the Geological Atlas of the northern Canadian Mainland Sedimentary Basin)* (Oen File No. 6997; p. 88). Geological Survey of Canada. https://doi.org/10.4095/290970

Morrow, D. W., & Geldsetzer, H. H. J. (1988). Devonian of the Eastern Canadian Cordillera. *2nd International Symposium on the Devonian System*, *1*, 85–121. https://archives.datapages.com/data/cspg_sp/data/014/014001/85_cspgsp014a0085.htm

Morrow, D. W., MacLean, B. C., Tzeng, P., & Pana, D. (2002). Subsurface Palaeozoic structure and isopach maps and selected seismic lines in southern Northwest Territories and northern Alberta: Implications for mineral and petroleum potential. *Geological Survey of Canada, Open File*, *4366*.

Mossop, G. D., & Shetsen, I. (1994). *Geological atlas of the Western Canada Sedimentary Basin; Canadian Society of Petroleum Geologists and Alberta Research Council.* Canadian Society of Petroleum Geologists and Alberta Research Council. https://ags.aer.ca/reports/atlas-western-canada-sedimentary-basin

Northwest Territories Geological Survey. (2023). *Geology Map* [Map]. Northwest Territories Geological Survey. https://ntgs-open-data-ntgs.hub.arcgis.com/

OHCHR. (2013). *Consultation and free, prior and informed consent (FPIC)*. OHCHR. https://www.ohchr.org/en/indigenous-peoples/consultation-and-free-prior-and-informed-consent-fpic

Ootes, L., Davis, W. J., Jackson, V. A., & Van Breemen, O. (2015). Chronostratigraphy of the Hottah terrane and Great Bear magmatic zone of Wopmay Orogen, Canada, and exploration of a terrane translation model. *Canadian Journal of Earth Sciences*, *52*(12), 1062–1092. https://doi.org/10.1139/cjes-2015-0026

OROGO. (2024). *Well Status* [Well list; Excel sheet]. OROGO. https://www.orogo.gov.nt.ca/en/resources-0

Ouzzane, M., Eslami-Nejad, P., Badache, M., & Aidoun, Z. (2015). New correlations for the prediction of the undisturbed ground temperature. *Geothermics*, *53*, 379–384. https://doi.org/10.1016/j.geothermics.2014.08.001

Pasquale, V., Verdoya, M., & Chiozzi, P. (2015). Measurements of rock thermal conductivity with a Transient Divided Bar. *Geothermics*, *53*, 183–189. https://doi.org/10.1016/j.geothermics.2014.05.008

Perry, H. K. C., Rosieanu, C., Mareschal, J.-C., & Jaupart, C. (2010). Thermal regime of the lithosphere in the Canadian Shield. *Canadian Journal of Earth Sciences*, *47*, 389–408. https://doi.org/10.1139/E09-059

Peters, K. E., & Nelson, P. H. (2012). Criteria to Determine Borehole Formation Temperatures for Calibration of Basin and Petroleum System Models. In N. B. Harris & K. E. Peters (Eds.), *Analyzing the Thermal History of Sedimentary Basins: Methods and Case Studies* (SEPM SPECIAL PUBLICATION, Vol. 103, pp. 5–15). SEPM Society for Sedimentary Geology. https://doi.org/10.2110/sepmsp.103.ch02

Petrel Robertson Consulting Ltd. (2022). *Geothermal database compilation*. Internal unpublished report.

Pollack, H. N. (1982). The Heat Flow from the Continents. *Annual Review of Earth and Planetary Sciences*, *10*(Volume 10, 1982), 459–481. https://doi.org/10.1146/annurev.ea.10.050182.002331

Popov, Y., Beardsmore, G., Clauser, C., & Roy, S. (2016). ISRM Suggested Methods for Determining Thermal Properties of Rocks from Laboratory Tests at Atmospheric Pressure.

Rock Mechanics and Rock Engineering, *49*(10), 4179–4207. https://doi.org/10.1007/s00603-016-1070-5

Popov, Y., Lippmann, E., & Rauen, A. (2023). *TCS-Manual. Thermal conductivity (TC) and thermal diffusivity (TD) Scanner. Version 15.11.2023.* https://www.schwartech.de/index_en.html#/tcs_en

Rajaobelison, M., Raymond, J., Malo, M., Dezayes, C., & Larmagnat, S. (2022). Understanding heat transfer along extensional faults: The case of the Ambilobe and Ambanja geothermal systems of Madagascar. *Geothermics*, *104*, 102455. https://doi.org/10.1016/j.geothermics.2022.102455

Rajaobelison, M., Thibault, M., Comeau, F.-A., Raymond, J., Smejkal, E. J., & Terlaky, V. (2024). Thermostratigraphic and Heat Flow Assessment of the South Slave Region in the Northwest Territories, Canada. *Energies*, *17*(16), Article 16. https://doi.org/10.3390/en17164165

Rajaobelison, M., Thibault, M., Comeau, F.-A., Raymond, J., & Terlaky, V. (In press). *Laboratory analyses on split core samples from wells to assess the geothermal potential of the South Slave Region, Northwest Territories, Canada* (Open Report Nos. 2023–015). Institut national de la recherche scientifique & Northwest Territories Geological Survey.

Rhodes, D., Lantos, E. A., Lantos, J. A., Webb, R. J., & Owens, D. C. (1984). Pine Point orebodies and their relationship to the stratigraphy, structure, dolomitization, and karstification of the Middle Devonian barrier complex. *Economic Geology*, *79*(5), 991–1055. https://doi.org/10.2113/gsecongeo.79.5.991

Richards, M., & Crowell, A. M. (2012). *Personal Communication*. SMU Geothermal Laboratory.

Rocheleau, J., & Fiess, K. M. (2014). *Northwest Territories oil and gas poster series: Basins and Petroleum resources, table of formations, schematic cross sections* (Open File Nos. 2014–03). Northwest Territories Geoscience Office. https://www.nwtgeoscience.ca/sites/ntgs/files/content/table_of_formations_2014_0.pdf

Sass, I., & Götz, A. E. (2012). Geothermal reservoir characterization: A thermofacies concept. *Terra Nova*, *24*(2), 142–147. https://doi.org/10.1111/j.1365-3121.2011.01048.x

Sass, J. H., Lachenbruch, A. H., Moses Jr., T. H., & Morgan, P. (1992). Heat flow from a scientific research well at Cajon Pass, California. *Journal of Geophysical Research: Solid Earth*, *97*(B4), 5017–5030. https://doi.org/10.1029/91JB01504

Smejkal, E. J., Hickson, C. J., & Collard, J. (2023). Revisiting the geothermal potential of the Dehcho Region in NWT: New data from old wells. *Geoconvention*. Geoconvention, Calgary, AB Canada. https://geoconvention.com/wp-content/uploads/abstracts/2023/91565-revisiting-the-geothermal-potentia.pdf

Smith, I. R., Deblonde, C., Hagedorn, G., & Paulen, R. C. (2022). A drift isopach model for the southwestern Great Slave Lake region, Northwest Territories, Canada. *Journal of Maps*, *0*(0), 1–12. https://doi.org/10.1080/17445647.2022.2147871

Stein, C. A. (1995). Heat Flow of the Earth. In T. J. Ahrens (Ed.), *Global earth physics: A handbook of physical constants* (pp. 144–158). American Geophysical Union. https://doi.org/10.1029/RF001p0144

Stott, D. F., & Klassen, R. W. (1993). Geomorphic Divisions. In D. F. Stott & J. D. Aitken (Eds.), *Sedimentary Cover of the Craton in Canada* (Vol. 5, p. 0). Geological Society of America. https://doi.org/10.1130/DNAG-GNA-D1.31

Tang, B., Zhu, C., Xu, M., Chen, T., & Hu, S. (2019). Thermal conductivity of sedimentary rocks in the Sichuan basin, Southwest China. *Energy Exploration & Exploitation*, *37*(2), 691–720. https://doi.org/10.1177/0144598718804902

Thibault, M., Comeau, F.-A., Rajaobelison, M., Raymond, J., & Terlaky, V. (Submitted). *Laboratory analyses update on split core and field samples to assess the geothermal potential of the South Slave Region in Northwest Territories* (p. 38) [Annual Internal Report]. INRS and NTGS.

Thibault, M., Comeau, F.-A., Raymond, J., Rajaobelison, M., Terlaky, V., & Newson, J. (2024). Evaluation of the Precambrian Basement Temperature Below Four South Slave Communities, Northwest Territories, Canada. *GRC Transactions*, *48*, 28.

Thibault, M., Raymond, J., Comeau, F.-A., Rajaobelison, M., & Qadri, S. M. T. (2025). *Update on the Geothermal Potential Assessment of the South Slave Region, Northwest Territories* (p. 21) [Annual Internal Report]. NTGS.

Turcotte, D. L., & Schubert, G. (2002). *Geodynamics* (3rd ed.). Cambridge University Press.

Waples, D. W. (2002). A New Model for Heat Flow in Extensional Basins: Estimating Radiogenic Heat Production. *Natural Resources Research*, *11*(2), 125–133. https://doi.org/10.1023/A:1015568119996

Westaway, R., & Younger, P. L. (2013). Accounting for palaeoclimate and topography: A rigorous approach to correction of the British geothermal dataset. *Geothermics*, *48*, 31–51. https://doi.org/10.1016/j.geothermics.2013.03.009

Wright, G., McMechan, M., & Potter, D. (1994). Chapter 3—Structure and architecture of the Western Canada sedimentary basin. In *Geological atlas of the Western Canada Sedimentary Basin* (Vol. 4, pp. 25–40). Canadian Society of Petroleum Geologists and Alberta Research Council. https://ags.aer.ca/publications/atlas-western-canada-sedimentary-basin/chapter-3-structure-and-architecture

Wu, H., Liu, Y., Yang, M., Zhang, J., & Zhang, B. (2023). Effect of temperature-dependent rock thermal conductivity and specific heat capacity on heat recovery in an enhanced geothermal system. *Rock Mechanics Bulletin*, *2*(2), 100045. https://doi.org/10.1016/j.rockmb.2023.100045

Yin, Y., Unsworth, M., Liddell, M., Pana, D., & Craven, J. A. (2014). Electrical resistivity structure of the Great Slave Lake shear zone, northwest Canada: Implications for tectonic history. *Geophysical Journal International*, *199*(1), 178–199. https://doi.org/10.1093/gji/ggu251

Appendix

Manuscript

Title of the paper:
Thermostratigraphic and heat flow assessment of the South Slave Region in the Northwest Territories, Canada

Contribution:
The following article was developed in close collaboration with the lead author, a postdoctoral researcher. Although I am not listed as the first author, this work represents a significant part of my research activities during this master's project. I was heavily involved in the development of the manuscript, and the collaboration was an essential and substantial component of my academic journey. My individual contributions included leading the collection of all samples, securing access and permission, and managing all related logistics. I also conducted the Lithostratigraphic analyses and the geological assessment of the region. These tasks formed the basis of several sections of the article and were essential to its overall conclusions.

Authors:
Mirah Rajaobelison[1], Michaël Thibault[1,2], Félix-Antoine Comeau[1], Jasmin Raymond[1], Emily J. Smejkal[3], Viktor Terlaky[4]
[1] Institut national de la recherche scientifique (INRS)
[2] Iceland School of Energy (ISE), Reykjavik University
[3] Terrapin Geothermics
[4] Northwest Territories Geological Survey (NTGS)

Published:
Rajaobelison, M., Thibault, M., Comeau, F.-A., Raymond, J., Smejkal, E. J., & Terlaky, V. (2024). Thermostratigraphic and Heat Flow Assessment of the South Slave Region in the Northwest Territories, Canada. *Energies*, *17*(16), Article 16. https://doi.org/10.3390/en17164165

5.1 Abstract

Despite the elevated heat flow known in the Western part of the South Slave Region (Northwest Territories, Canada), a continuous and equilibrium geothermal gradient was never measured in boreholes below the communities where geothermal energy could be developed. This paper aims to predict the geothermal gradient and assess the Earth's natural heat flow below the communities of Fort Providence, Kakisa, Hay River, and Enterprise. Temperatures from drill-stem test and bottom well logs were corrected for drilling disturbance and paleoclimate. Thermal conductivity and heat generation rate of the geological formations were determined from the literature and with new laboratory measurements. Original 1D models were developed to evaluate subsurface temperature through the sedimentary formations, based on a thermostratigraphic assessment. Results indicate a geothermal gradient that varries from 44.1 ± 10.6 °C km^{-1} to 59.1 ± 14.9 °C km^{-1} and heat flow that varries from 105.5 mW m^{-2} to 160.2 mW m^{-2} below the communities. These estimates are in agreement with the equilibrium geothermal gradients measured in the Cameron Hills, south of the four communities, and used to verify our predictions. The highest geothermal gradient (59.1 ± 14.9 °C km^{-1}) was estimated at Hay River which therefore has the most favourable geological conditions for geothermal development.

5.2 Introduction

Estimating the geothermal gradient and terrestrial heat flow are important steps in assessing the geothermal potential of a region. The geothermal gradient is typically estimated based on an equilibrium temperature profile (e.g., Jessop, 1990; Majorowicz et al., 2008) and the thermal conductivity of the geological materials underlying the region is measured for heat flow assessment. This kind of heat flow assessment is crucial for any geothermal development, but can be expensive, because it usually requires an exploration borehole specifically drilled for geothermal purposes (e.g., Augustine et al., 2006). In remote communities of the Canadian North that have populations of a few hundred to less than four-thousand people, drilling such boreholes is difficult to justify in the early exploration stage. However, 1D models that rely on a thermostratigraphic assessment and corrected downhole temperatures can be used to predict geothermal gradient and heat flow at this stage. (e.g., Bédard et al., 2018; Grasby et al., 2013; Harrison et al., 1983; Jessop, 1990). This approach can better inform decision-making regarding the exploitability of clean and reliable local geothermal heat for such remote communities.

The geothermal potential of the South Slave Region of the Northwest Territories (NWT) is studied using a community-based approach to evaluate the thermal state and properties below - from North to South - Fort Providence, Kakisa, Hay River, and Enterprise (Figure 5.1). The most recent map of heat flow in Canada (Grasby et al., 2021; Majorowicz & Grasby, 2021b), updated from (Grasby et al., 2021), indicates heat flow values in the South Slave region from 40 mW m^{-2} to 100 mW m^{-2}, which is the highest in the Western Canada Sedimentary Basin (WCSB). The work of EBA Engineering Consultants Ltd. (2010) has shown very high geothermal favourability and potential in NWT to the west of Great Slave Lake (Figure 5.1b). To support geothermal research in the South Slave region, Petrel Robertson Consulting Ltd (2022) identified 109 oil and gas wells between 48 m and 1500 m depth that were cored and have publicly available geoscience data that could be further investigated. Historic well files with bottom-hole temperatures (BHT) and drill-stem test (DSTs) records are publicly available for 68 of these wells. Individual Well History Files from the archives of the OROGO (2024) were also consulted to supplement the temperature data. Oil and gas wells were recently abandoned in the Cameron Hills located about 100 km to the southwest of the studied communities. Smejkal et al. (2023) accessed these wells during abandonment activities, and measured an equilibrium temperature profile in six deep wells and evaluated the geothermal gradient.

Terrestrial heat flow estimates from analysis of BHT data exist for several sedimentary basins around the world, including Brazil Da Silva Carvalho & Vacquier (1977), Western Canada (Majorowicz & Jessop, 1981), Eastern Canada (Majorowicz & Jessop, 1981) and the St. Lawrence Lowlands in Québec (Bédard et al., 2018). DST temperature based on flowing oil or water from the producing formation is generally a reliable source of data for the calibration of basin system models (Peters & Nelson, 2012), but are not as common as BHT measurements. On the other hand, BHTs from well log headers are available for most wells, but are biased and usually lower than the equilibrium formation temperature (Deming & Chapman, 1988). Hence, correction for drilling disturbances is necessary and ideally requires multiple BHT measurements at successive times in order to find the equilibrium temperature. The analytical Horner technique is commonly used to correct multiple BHT measurements (Dowdle & Cobb, 1975). Criteria for reliable Horner corrected BHTs include a minimum of three logging runs that record time and temperature for each run, and deviation from the least squares regression line that is less than the measurement uncertainty (i.e. ± 1-3 °C; Peters & Nelson, 2012). Other corrections that do not use mud circulation time include the Förster Correction (Förster et al., 1997), the Harrison Correction (Harrison et al., 1983), subsequently redefined by Blackwell et al. (2010); Blackwell & Steele (1992), and the Kehle Correction (Gregory et al., 1980). These correction schemes were used for correcting BHTs in the Denver Basin of Colorado and in Nebraska (Crowell et al., 2012). However, these empirical corrections are not always appropriate as differences in lithologies and thermal histories may affect the correction (Crowell et al., 2012; Crowell & Gosnold, 2011). Heat flow estimates, especially based on temperature measurements at shallow depth, additionally require corrections for paleoclimate effects (Westaway & Younger, 2013). These effects must be considered in the South Slave Region, which was covered by the Laurentide Ice Sheet during the last glaciation (Late Wisconsinan) ~25–10 ka (Dyke, 2004; Lemmen et al., 1994), resulting in a decrease in subsurface temperature through thermal diffusion.

In this study, our objective is to reevaluate the heat flow and predict the geothermal gradient with original 1D models in the four main South Slave communities that are at an early geothermal exploration stage. This paper provides a widely applicable workflow of local geological assessment that can be used to plan the drilling of exploration boreholes, helping to move to the next step of geothermal development in small and remote communities. Relying on available data, we use a community approach rather than a regional assessment to predict the thermal state and properties below population centers where geothermal energy can be used. We believe it is the most appropriate method for such a remote region where the population is sparse and geothermal energy exportation is hindered by the lack of infrastructure. Our assessment comprises analysis of publicly available data from oil and gas wells nearby the four communities and include BHT and DST data combined with vertical thermal conductivity profiles deduced from core analysis and corresponding lithological profiles beneath the communities. A 1D thermostratigraphic model for each community is developed and is verified with equilibrium temperature data obtained from Cameron Hills.

5.3 Geological setting

The study area defined within the South Slave Region is delineated by the coordinates 60°N, 111°W in the SE to 62°N, 120°W in the NWT (Figure 5.1a). This area is located in the Interior Platform, which constitutes the northern extension of the WCSB, and is bounded by the Canadian Shield to the East and the Mackenzie Mountains of Cordilleran Orogen to the West (Lemmen et al. (1994) and references therein). According to Davenport (2001), the Interior Platform is divided into a number of domains or exploration areas. This subdivision was based on geological history, physiographic and structural characteristics, as well as changes in bedrock geology. The area of interest for this study is in the Great Slave Plain (Figure 5.1a; (Stott & Klassen, 1993).

The geology of the Great Slave Plain comprises Precambrian metasedimentary and crystalline basement rocks overlain by Paleozoic and Mesozoic sedimentary rocks, and Quaternary overburden with variable thickness. The dominant lithologies making up the Paleozoic and Mesozoic sedimentary strata are shale, limestone, marine dolostone, anhydrite and sandstone. Devonian rocks make up the bulk of the sedimentary strata underlying the communities, illustrated by the cross-sections in Figure 5.2b; for a detailed review and description of the Devonian stratigraphy see Meijer-Drees (1993), Moore (1993), Morrow & Geldsetzer (1988), Mossop & Shetsen (1994), among others.

According to the works of Gal & Jones (2003), the local stratigraphy comprises a relatively thin (500 m to 700 m) Paleozoic and Mesozoic sedimentary cover overlying the Precambrian basement (b). This is confirmed by the Phanerozoic isopach map of the WCSB (Wright et al., 1994).

Smith et al. (2022) provides the most recent drift isopach model including the thickness of Quaternary glacial sediment. The drift cover in the South Slave is up to 150 m thick, but has considerable variation; the majority of the cover is less than 10 m thick, and sedimentary rocks outcrop in the area sporadically. At Cameron Hills, the drift thickness is locally up to 400 m thick.

An extensional tectonic regime in the late Precambrian resulted in deep-seated faults and horst and graben block faulting of basement rocks stretching to the Cameron Hills area. This extensional tectonic regime was reactivated and influenced the Phanerozoic sediment cover. The major faults and fault zones that affected the area have a Northeast trend (Figure 5.2; Gal & Jones (2003); Morrow et al. (2002)).

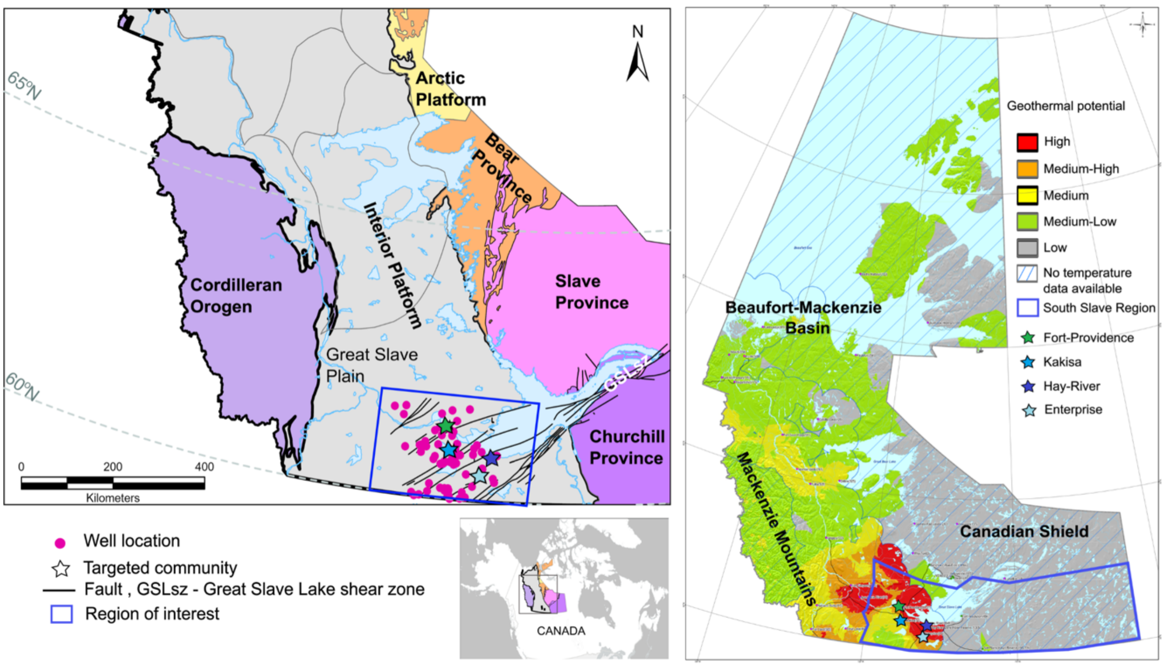

(a) (b)

Figure 5.1. a) The location of the study area outlined in blue. The geological provinces and general simplified tectonic structure lines with the exploration areas are

from base map modified according to Davenport (2001) and Rocheleau & Fiess (2014). Pink dots indicate the location of wells with subsurface temperature information. The well locations are from the map of Petrel Robertson Consulting Ltd (2022). b) Geothermal feasibility map of the NWT modified from EBA Engineering Consultants Ltd. (2010).

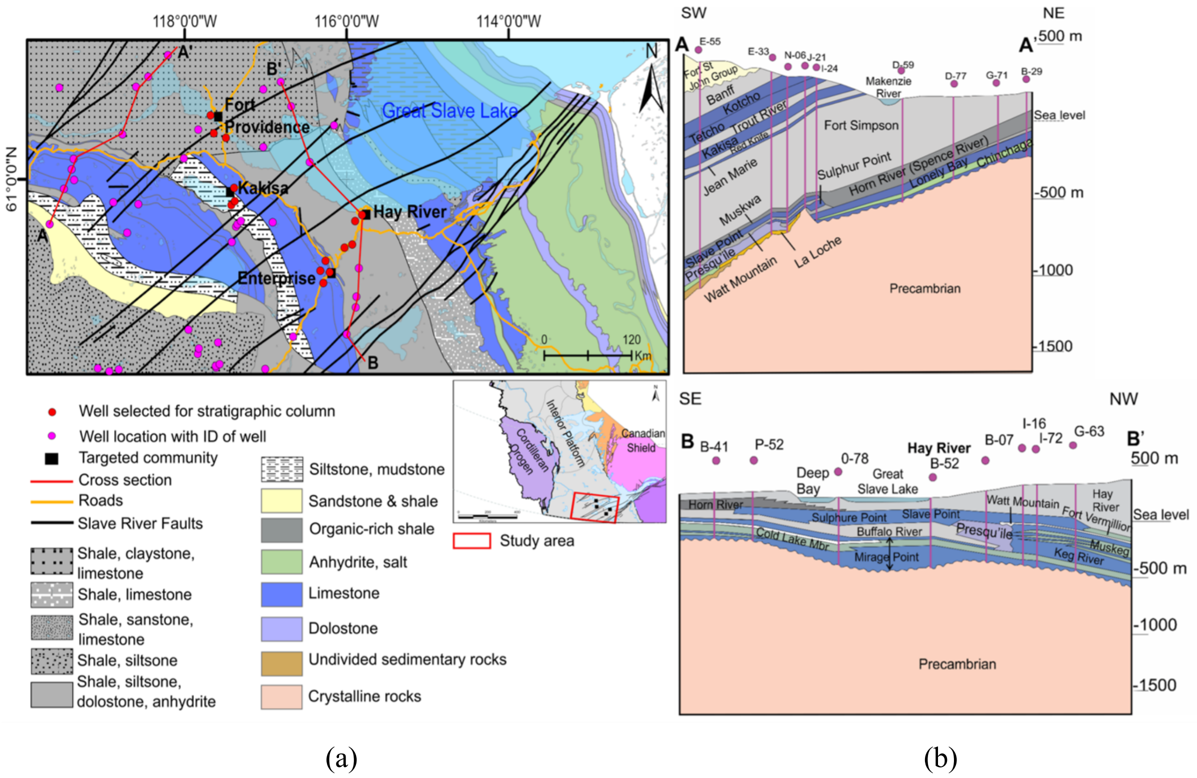

Figure 5.2. a) Geological map of the study area (modified from Morrow et al., 2002). The well locations were taken from the Geothermal Database Compilation Devonian Cores Map from Petrel Robertson Consulting Ltd (2022) and Gal & Jones (2003). b) Cross sections showing stratigraphic and chronological relationships of the dominant lithologies and their corresponding formations in the Great Slave Plain (modified from Gal & Jones, 2003).

5.4 Input Data

The data set consists of information from 75 of the 116 wells in the area of interest (Figure 5.3), which were made available from the Petrel Robertson Consulting Ltd (2022) Excel file and from the Individual Well History Files from OROGO (2024). The wells with DST and/or BHT data were also chosen to be as close as possible to the four main communities. The equilibrium temperature profiles recorded in 2023 from six wells (A-73, E-07, I-10, I-74, L-44, M-49) in the Cameron Hills region are located close enough to the study area (Figure 5.3) to be used for verification purposes.

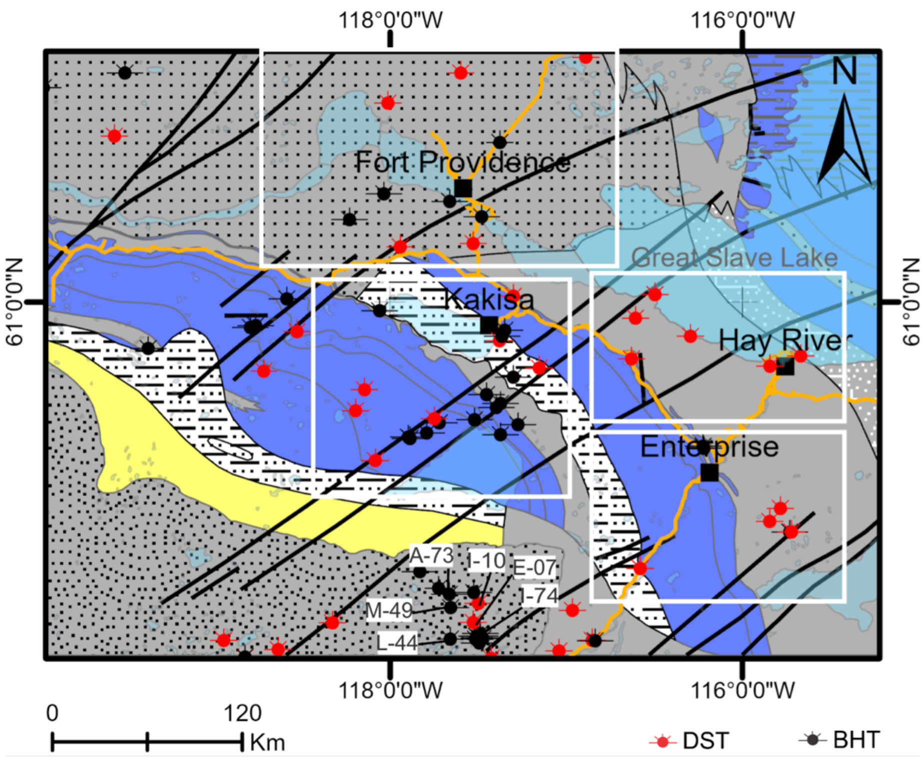

Figure 5.3. Location of the 75 wells with measured DST and BHT. The white boxes delineate the wells se-lected for each community. The wells with ID are those in the Cameron Hills region that have equilibrium temperature data. The geological base map is modified from the Northwest Territories Geological Survey (2023) and has the same legend as Figure 5.2.

5.4.1 Temperature data

5.4.1.1 South Slave Region

A total of 33 of the 75 wells have a DST temperature record. BHTs were measured in 42 wells at depths from 504 m to 1657 m (Table 5.1).

Table 5.1. Temperature data from wells

Data type	Number of wells	Depth *TVD* (m)	Temperature (°C)	Source
DST	20 5	≥ 600-1846 < 600	19-63	Petrel Robertson Consulting Ltd (2022)
	4 3	≥ 600-941 < 600	17-42	OROGO (2024)
BHT	36 5	≥ 600-1657 < 600	26-76	Petrel Robertson Consulting Ltd (2022)
	1 1	≥ 600 < 600	27	OROGO (2024)
No data	41			Petrel Robertson Consulting Ltd (2022)
Total	116	49 -1949	17-76	

Set as the upper boundary condition in our model, the average annual undisturbed ground temperature T_s (°C) was obtained by converting the air -temperature to ground-temperature using an empirical relationship. The following equation developed by Ouzzane et al. (2015) was used for this purpose:

$$T_s = 17.898 + 0.0951 T_{amb} \tag{5.1}$$

where T_s (K) is the undisturbed ground surface temperature and T_{amb} (K) is the annual ambient temperature, which is -2.5 °C for the region. This mean annual air temperature was obtained from the Hay River-A weather station (Government of Canada & Environment and Natural Resources, 2024). T_s was consequently estimated to be 2.1 °C.

5.4.1.2 Cameron Hills

The equilibrium temperature data from wells in the Cameron Hills were chosen because the stratigraphy shares similarities with that of the South Slave communities. These similarities were confirmed with gamma ray (*GR*) log (Smejkal et al., 2023). The stratigraphic formations and corresponding lithology were taken from the Table of Formation tops established by Hogue & Gal (2008) and Rocheleau & Fiess (2014). In the Cameron Hills, T_s was evaluated from the temperatures measured at the top of the Cretaceous basal sandstone (CB SS unit) marking the base of the clastic Cretaceous section underlying the Devonian carbonates, since continuous temperature profiles were available at this geological formation at depth around 500 m (Smejkal et al., 2023).

5.4.2 Thermal conductivity and heat generation rate

5.4.2.1 South Slave Region

Thermostratigraphic logs were initially created for the four South Slave communities combining the stratigraphic column that approximates the thickness of the main stratigraphic formations, with the corresponding subsurface thermal conductivity (Table 5.2; Figure 5.4; Rajaobelison et al. (In press)). The average thermal conductivity per formation was calculated using the weighted harmonic mean related to bedded lithologies, assuming perpendicular heat flow (Clauser, 2011). These local stratigraphic columns gave an extended and refined geological model under each community, showing that the Precambrian basement lies at a shallow depth of 500 m to 700 m. Shale is the dominant lithology over the total thickness of sedimentary rocks (~600 m) in Fort Providence, Kakisa, and Enterprise. Carbonate rocks is 600 m thick and the shale cover is approximately 100 m thick at the Hay River location. Near-surface, quaternary sediments overlying the Paleozoic rocks are less than 10 m thick, and are omitted, because the sedimentary deposits do not contribute enough to heat transfer when calculating the geothermal gradient and heat flow from deep rocks (e.g., Beardsmore & Cull, 2001; Jaupart & Mareschal 2010). Laboratory assessment of the thermal conductivity was completed on 84 split core samples from 33 wells that cover seven geological formations. Measurements were carried out at the LOG at the INRS in Canada using an optical scanning instrument following the methodology of Popov et al. (2016). For some formations no core was available for measurement; the thermal conductivity were therefore taken from literature (e.g., Grasby et al., 2012 and references therein, Clauser & Huenges, 1995; Eppelbaum et al., 2014 and references therein, Cermak & Rybach, 1982; Larmagnat et al., 2019; Mielke et al., 2017; Pasquale et al., 2015; Tang et al., 2019) and used in the weighted harmonic mean thermal conductivity calculation of the formation.

The average heat generation rate A (W m^{-3}) for lithological formations below the South Slave Communities was evaluated using the empirical equation of Bücker & Rybach (1996), which relates heat generation to the concentration of uranium *(U)*, thorium *(Th)* and potassium *(K).* The concentration of these radiogenic elements was determined by means of inductively coupled plasma analyses at INRS geochemical Laboratory (Rajaobelison et al., In press). Although laboratory measurements were made on available core material, this was insufficient to cover all geological formations. Consequently, heat generation rates were assumed by analogy with lithologically similar formations where it was evaluated. Additionally, literature values of heat generation rate (e.g.,Hasterok et al., 2018; Waples, 2002) and references therein) were assigned to the sedimentary rock type for formations with no core.

Table 5.2. Thermal conductivity and heat generation rate for South Slave Communities.

Formation	Lithology	%	*n*	Heat Production A (W m^{-3})	Thermal conductivity λ (W m^{-1} K^{-1})		
					Measured	Literature*	Average
Alluvium	Sand	100		0.73×10-6		1.4	1.4
Twin Falls	Limestone	95		0.19×10-6		2.5	2.5
	Shale	5		0.53×10-6		2.1	
Hay River	Shale	92		0.53×10-6		2.1	2.1
	Limestone	8		0.19×10-6		2.5	
Hay River (Escarpment)	Shale	90		0.53×10-6		2.1	2.1
	Limestone	10		0.19×10-6		2.5	
Hay River (Waterways)	Shale	60		0.53×10-6		2.1	2.2
	Limestone	40		0.19×10-6		2.5	
Slave Point	Limestone	92	25	0.19×10-6	2.9±0.25		2.9
	Shale	4		0.53×10-6		2.1	
	Dolostone	4	4	0.11×10-6	4.6±0.55		
Horn River	Shale	95		0.53×10-6		2.1	2.1
	Limestone	5		0.19×10-6		2.5	
Watt Mountain	Shale	92		0.53×10-6		2.1	2.2
	Limestone	3	6	0.19×10-6	3.1±0.18		
	Sandstone	5		0.73×10-6		3.4	
Sulphur Point	Limestone	78	13	0.19×10-6	3.4±0.63		3.5
	Dolostone	20	7	0.11×10-6	4.4±0.64		
	Shale	2		0.53×10-6		2.1	
Muskeg	Anhydrite	90	1	0.08×10-6	5.0±0.17	3.4	4.4
	Dolostone	10	6	0.11×10-6	5.6		
Klua	Shale	98		0.53×10-6		2.1	2.1
	Limestone	2		0.19×10-6		2.5	
Keg River	Limestone	90		0.19×10-6		2.8	3
	Dolostone	10	8	0.11×10-6	4.9±0.47		
Lonely Bay	Dolostone	50		0.11×10-6		3.8	3
	Limestone	50		0.19×10-6		2.5	

n : number of sample; *Sources (e.g., Grasby et al., 2012 and references therein, Clauser & Huenges, 1995; Eppelbaum et al., 2014 and references therein, Cermak & Rybach, 1982; Larmagnat et al., 2019; Mielke et al., 2017; Pasquale et al., 2015; Tang et al., 2019)

Table 2 (continued)

Formation	**Lithology**	**%**	***n***	**Heat Production** *A* **(W m**$^{-3}$**)**	**Thermal conductivity** *λ* **(W m**$^{-1}$ **K**$^{-1}$**)**		
					Measured	**Literature***	**Average**
Chinchaga	Anhydrite	43	2	0.08×10-6	4.8±0.77		3.6
	Dolostone	30	4	0.11×10-6	4.2±0.80		
	Shale	23		0.53×10-6		2.1	
	Limestone	2		0.19×10-6		2.5	
Chinchaga (Ebutt Member)	Shale	83		0.53×10-6		2.1	3.6
	Limestone	10		0.19×10-6		2.5	
	Dolostone	5		0.11×10-6		3.8	
	Anhydrite	2		0.08×10-6		4.3	
Headless	Limestone	50		0.19×10-6		2.5	2.3
	Shale	45		0.53×10-6		2.1	
	Dolostone	5		0.11×10-6		3.8	
Mirage Point	Shale	62		0.53×10-6		2.1	2.6
	Dolostone	15		0.11×10-6		3.8	
	Halite	15		0.08×10-6		5	
	Anhydrite	8		0.08×10-6		4.3	
Mirage Point (Ernestina Lake)	Dolostone	55		0.11×10-6		3.8	3.3
	Anhydrite	25		0.08×10-6		4.3	
	Shale	20		0.53×10-6		2.1	
La Loche	Sandstone	99		0.73×10-6		3.4	3.4
	Shale	1		0.53×10-6		2.1	
La Loche (Red Beds)	Sandstone	100		0.73×10-6		3.4	3.4
La Loche (Basal Clastics)	Sandstone	100		0.73×10-6		3.4	3.4
Precambrian	Granite	100				3	

n : number of sample; *Sources (e.g., Grasby et al., 2012 and references therein, Clauser & Huenges, 1995; Eppelbaum et al., 2014 and references therein, Cermak & Rybach, 1982; Larmagnat et al., 2019; Mielke et al., 2017; Pasquale et al., 2015; Tang et al., 2019)

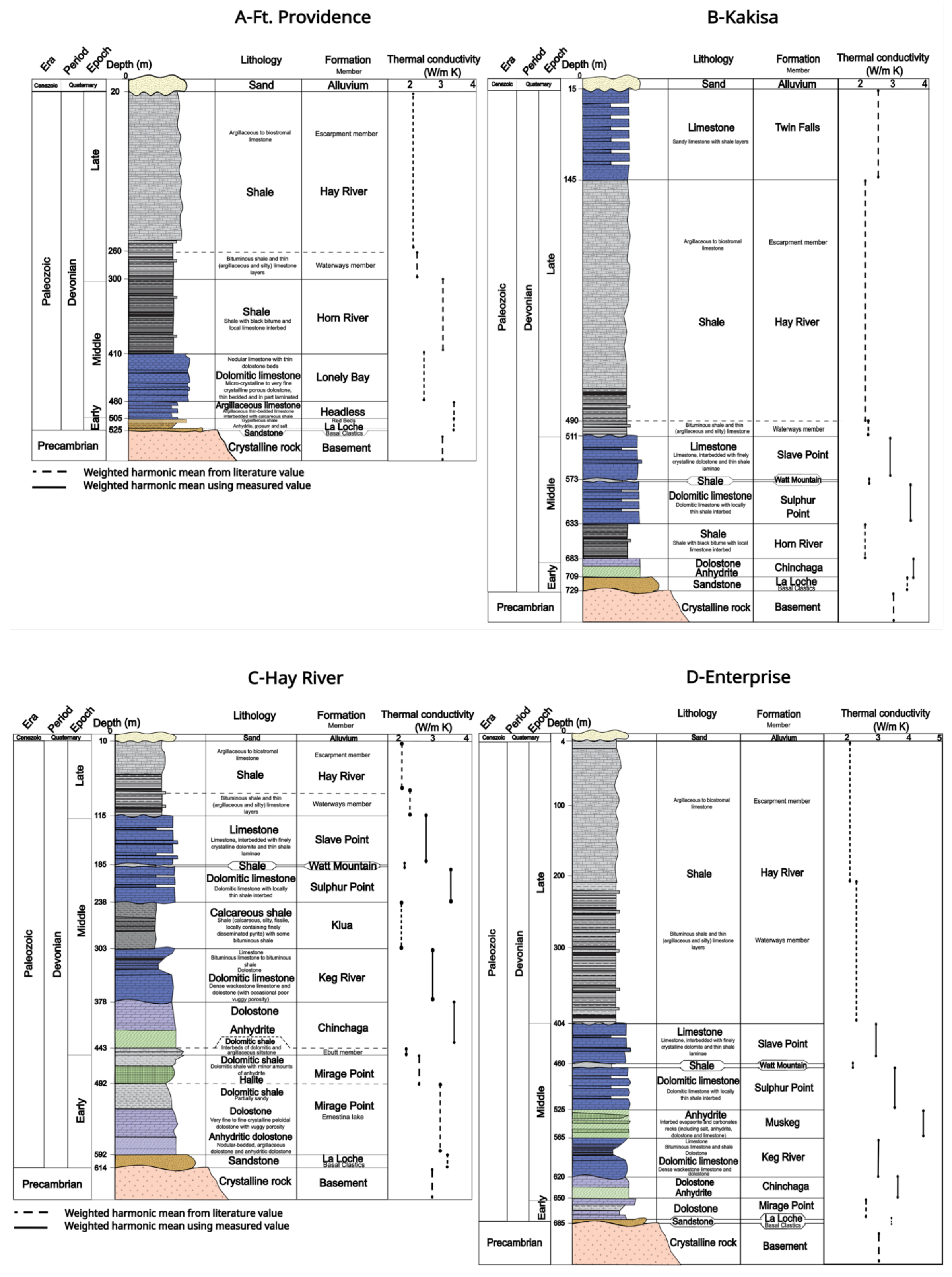

Figure 5.4. Thermostratigraphic log at the location of the four South Slave communities reproduced from Rajaobelison et al. (In press).

5.4.2.2 Cameron Hills

Core materials were not available for the Cameron Hills wells and geological formations encountered here. Thermal conductivity was determined with analogy to thermal conductivity measurements made on core samples for the South Slave Formations from Rajaobelison et al. (In press) (Table 5.2; Figure 5.4).

The internal heat generation rate for rocks *A* (W m^{-3}) intersected by Cameron Hills wells was calculated from the gamma ray log (GR; American Petroleum Institute units) according to (5.2 from Burrus & Foucher (1986):

$$A = 0.0145 \times (GR - 5) \tag{5.2}$$

The average heat production rate for each formation was calculated from the arithmetic average *GR* measured between the top and base of each corresponding formation (Table 5.3).

Table 5.3. Thermal conductivity and heat generation rate of Cameron Hills geological formations.

Well short name	Geological formations	Top	Lithology	*λ*	*GR*	*A*
		(m)		(W m^{-1} K^{-1})	(API)	(W m^{-3})
A-73	Wabamun	443	Dolomitic limestone	3.5	49.0	0.64×10^{-6}
	TwinFalls	809	Limestone	2.5	34.6	0.43×10^{-6}
	Muskwa	1022	Organic-rich shale	2.1	23.5	0.27×10^{-6}
	Waterways	1283	bituminous shale	2.1	11.2	0.09×10^{-6}
E-07	CB SS	461.4	Sandstone	3.4	30.7	0.37×10^{-6}
	Wabamun	471.9	Dolomitic limestone	3.5	32.5	0.40×10^{-6}
	Twin Falls	760	Limestone	2.5	31.8	0.39×10^{-6}
	Hay River	912.5	Shale	2.2	60.6	0.81×10^{-6}
I-10	CBS SS	575.1	Sandstone	3.4	43.3	0.56×10^{-6}
	Wabanum	590.3	Dolomitic limestone	3.5	17.9	0.19×10^{-6}
	Trout River	622	Shale	2.1	15.1	0.15×10^{-6}
	Kakisa	627.9	Limestone	3.0	16.7	0.17×10^{-6}
	RedKnife	665.8	Shale	2.1	57.8	0.77×10^{-6}
	Tathlina	715	Shale	2.1	35.1	0.44×10^{-6}
	Twin Falls	868.3	Limestone	2.5	27.6	0.33×10^{-6}
	Hay River	999.5	Shale	2.1	50.5	0.66×10^{-6}
I-74	BS SS	539.7	Sandstone	3.4	31.5	0.38×10^{-6}
	Wabamun	554.6	Dolomitic limestone	3.5	17.0	0.17×10^{-6}
	Ft.Simpson	717.6	Limestone	3.0	39.2	0.50×10^{-6}
	Twin Falls	829.1	Limestone	2.5	20.4	0.22×10^{-6}
	Hay River	898.8	Shale	2.1	44.5	0.57×10^{-6}
L-44	CB SS	516.8	Sandstone	3.4	30.6	0.37×10^{-6}
	Wabamun	528.2	Dolomitic limestone	3.5	40.6	0.52×10^{-6}
	Twin Falls	855	Limestone	2.2	70.8	0.95×10^{-6}
	Hay River	1022	Shale	2.1	68.3	0.92×10^{-6}
	Beaverhill Lake	1305.2	anhydrite and Limestone	4.3	49.0	0.64×10^{-6}
M-49	CBS SS	471.6	Sandstone	3.4	33.1	0.41×10^{-6}
	Wabanum	478.1	Dolomitic limestone	3.5	33.1	0.41×10^{-6}
	Ft. Simpson	696.5	Shale	3.0	20.2	0.22×10^{-6}
	Twin Falls	812.8	Limestone	2.5	46.5	0.60×10^{-6}
	Hay River	961.9	Shale	2.1	32.2	0.39×10^{-6}
	Beaverhill Lake	1252.6	Anhydrite and Carbonates	4.3	60.5	0.80×10^{-6}
	Slave Point	1301.9	Limestone	2.9	56.6	0.75×10^{-6}

5.5 Methods

Input temperature data were corrected for drilling disturbance and paleoclimates. Then, the geothermal gradient was calculated at the location of each community and for the Cameron Hill wells. The equilibrium temperature profile measured at the Cameron Hills was reproduced to verify if the thermal conductivity for each geological formation was adequately assigned. After the verification, the surface heat flow was calculated for the four communities and the 1D temperature profile below the four South Slave communities was predicted without paleoclimate correction using analytical calculations and assuming one dimensional conductive heat transfer with an internal heat generation in steady state.

5.5.1 Drilling disturbance correction for BHTs

Of the 75 wells, only 42 had one to two BHTs from wireline logs and mud circulation time was not provided. This is insufficient to meet the criteria for Peters & Nelson (2012). Empirical corrections were therefore applied to the BHTs following the work of Crowell et al. (2012). The Harrison equation (Harrison et al., 1983), the Kehle equation (Richards & Crowell, 2012), the Förster (a) equation (Förster et al., 1997) and the Förster (b) equation (Mareschal & Jaupart, 2004) were considered for corrections, because the lithology of the South Slave Region is similar to that of the basins in which these corrections were developed (e.g., Blackwell et al., 2010; Blackwell & Steele, 1992; Crowell et al., 2012; Förster et al., 1997; Gregory et al., 1980):

$$T_{cf}(°C) = -16.51 + 0.018 \times TVD - 2.345 \times 10^{-6} \times TVD^2 \quad (5.3)$$

$$T_{cf}(°F) = -8.819 \times 10^{-12} \times TVD - 2.143 \times 10^{-8} \times TVD^2 + 4.375 \times 10^{-3} \times TVD - 1.018 \quad (5.4)$$

$$T_{cf}(°C) = 0.012 \times TVD - 3.68 \quad (5.5)$$

$$T_{cf}(°C) = 0.017 \times TVD - 6.58 \quad (5.6)$$

where T_{cf} (°C/°F) is the temperature coefficient correction added to the BHT and *TVD* (m/in feet for Kehle equation) is the true vertical depth at which the BHT was measured.

Then, the best correction method was chosen based on the best fit to the geothermal gradient calculated from DST temperatures (Förster et al., 1997). The corrections were established for depths from 600 m to 3 km, thus temperatures recorded in South Salve wells at depths shallower than 600 m were not corrected. However, uncorrected temperatures at depth between 300 m and 600 m were retained when the gradient was evaluated at the community scale to improve the accuracy of the evaluation where data is limited.

5.5.2 Paleoclimate correction

Quaternary glaciation periods are expected to have disturbed the subsurface temperature in the South Slave Region, as paleoclimate perturbations were recorded in the temperature signal of deep boreholes over more than 3 km depth in other nearby regions of

Canada (e.g., Bédard et al., 2018; Beltrami et al., 2003; Majorowicz et al., 2012, 2014a). BHT and DST temperatures are assumed to have recorded significant Holocene and Pleistocene climatic perturbations. Based on the ground temperature history and the method of Birch (1948), the temperature during the Pleistocene glacial cycles in Canada has been considered to be 5 °C colder during the glaciations (Jessop, 1971, 1990). At the beginning and end of each glaciation, this is the magnitude of temperature change or the temperature step (*T*i) that was assumed for the ground surface below the ice sheets (Jessop, 1971; Figure 5.5).

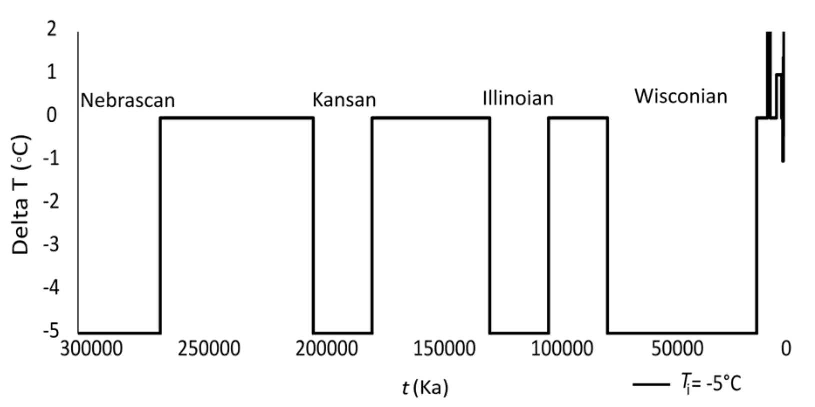

Figure 5.5. Timeline of Pleistocene and Holocene climate events according to a relative change of temperature of 5 °C modified from Bédard et al. (2018).

The temperature at any depth corrected for paleoclimate effects is (e.g., Jessop, 1990):

$$T_{z(eq)} = T_m + \sum_i (T_i)\left[erf\left(\frac{z}{2\sqrt{\alpha\, t_1}}\right) - erf\left(\frac{z}{2\sqrt{\alpha\, t_2}}\right)\right] \tag{5.7}$$

where $T_{z(eq)}$ (°C) is the temperature corrected for paleoclimate, T_m (°C) is the temperature measured at depth, T_i (°C) is the temperature step between glaciations, erf is the error function, α ($m^2\ s^{-1}$) is the rock thermal diffusivity (estimated to be ~1.44×10^{-6} considering the laboratory and thermostratigraphic assessments), t_1 (s) is the end of the ice age, t_2 (s) is the beginning of the ice age and z (m) is the depth of the temperature measurement.

5.5.3 Geothermal gradient calculation

Below each community, the average geothermal gradient g (°C m^{-1}) was calculated from the corrected temperature data of the nearest wells (Figure 5.3) using:

$$g = \frac{\Delta T}{\Delta z} = \frac{T_c - T_s}{\Delta TVD} \tag{5.8}$$

where ΔT (°C) is the difference between the corrected and the undisturbed ground temperature (T_s = 2.1 °C) divided by Δz (m), the true vertical depth difference. Depending on the purpose of the calculation, the corrected temperature can be BHT corrected for the drilling disturbance and paleoclimates when required or DST corrected for paleoclimates when required.

The geothermal gradient for Cameron Hills wells was determined from the slope calculation method using the temperature regression line of the measured profile. The average geothermal gradient *g* is the reverse of the slope.

5.5.4 Verification with temperature profiles from Cameron Hills

We used the equilibrium temperature profiles collect from the six wells in Cameron Hills to verify our thermostratigraphic model (Table 5.3 and Figure 5.4). This verified approached is then used to evaluate the heat flow (Q_0, W m-^{2}) and to predict temperature below the four South Slave communities where there are no equilibrium temperature profiles available. The heat flow at Cameron Hills was first calculated considering the equilibrium temperature at the bottom of the well. Then, temperature profiles recorded at the six Cameron Hills wells were recalculated according to the thermostratigraphic assessment made in South Slave communities. This temperature-depth model is to verify if the selected thermal properties for the geological formations are appropriate for the computed temperature to reproduce the observed temperature. The measured equilibrium temperature at the Cameron Hills wells are perturbed by paleoclimate effects. Therefore, no paleoclimate correction was made here to predict the ground temperature.

5.5.4.1 Heat flow evaluation for Cameron Hills

Equation (5.9) (e.g., Beardsmore & Cull, 2001; Eppelbaum et al., 2014; Jaupart & Mareschal, 2010) allowed to calculate the surface heat flow Q_0 for Cameron Hill wells:

$$Q_0 = \lambda g + A\frac{z}{2} \tag{5.9}$$

where the thermal conductivity λ (W m^{-1} K^{-1}) is the weighted harmonic mean calculated from the lithological units, A (W m^{-3}) is the weighted arithmetic average heat generation in the sedimentary rock cover, z (m) is the thickness between the ground surface and measured temperature at both ends of the temperature profile and *g* (°C m^{-1}) is the geothermal gradient identified previously.

5.5.4.2 Temperature-depth models for Cameron Hills

The 1D calculation was made considering conductive heat transfer in steady-state conditions following (e.g., Jessop, 1990; Stein, 1995; Turcotte & Schubert, 2002):

$$T_z = T_s + \frac{Q_0\, z}{\lambda} + A\frac{z^2}{2\lambda} \tag{5.10}$$

where T_z is the temperature at the depth *z* (m) in the sedimentary rock formations and

Q_0 (W m^{-2}) was determined in the previous step, used as boundary conditions.

5.5.5 Prediction of temperature profiles for South Slave Communities

After verifying that our thermal conductivity assessment could accurately evaluate the temperature at depth for the Cameron Hills, the same approach was used to predict the temperature below the South Slave communities where no equilibrium temperature profile exists.

5.5.5.1 Heat flow evaluation for South Slave Communities

The surface heat flow Q_0 at the location of each community was then calculated using Equation (5.9. The stratigraphic column thickness z (m) was calculated from the surface to the top of the basement.

5.5.5.2 Temperature-depth model

1D temperature profiles below the four South Slave communities were calculated using Equation (5.10) and thermal conductivity was validated with the data from the Cameron Hills wells. The temperature profiles predicted in the sedimentary rock cover overlying the crystalline basement assumes steady state conductive heat transfer and considers internal heat generation at the location of the communities. The boundary conditions are the undisturbed ground temperature (T_s = 2.1 °C) and the surface heat flow Q_0.

The paleoclimate correction was not applied to the ground temperatrure calculation as it reflects the temperature that can be measured in sedimentary rocks below the South Slave communities. Thus, the predicted temperature is perturbed by paleoclimates, as can be expected when measurements are taken at depths of less than a kilometer.

5.6 Results

5.6.1 Corrected BHTs

Six of the 42 BHTs were not corrected because the temperature was recorded at depth less than 600 m. The Förster (a) correction revealed corrected BHTs closer to DST temperatures and a smaller standard deviation when compared to other correction methods (Figure 5.6). The correction factor T_{cf} (°C) obtained with Förster (a) method varied from 3.8 °C to 16.2 °C, resulting in corrected BHTs from 30.6 °C to 89.9 °C from 625.8 m to 1657 m depth.

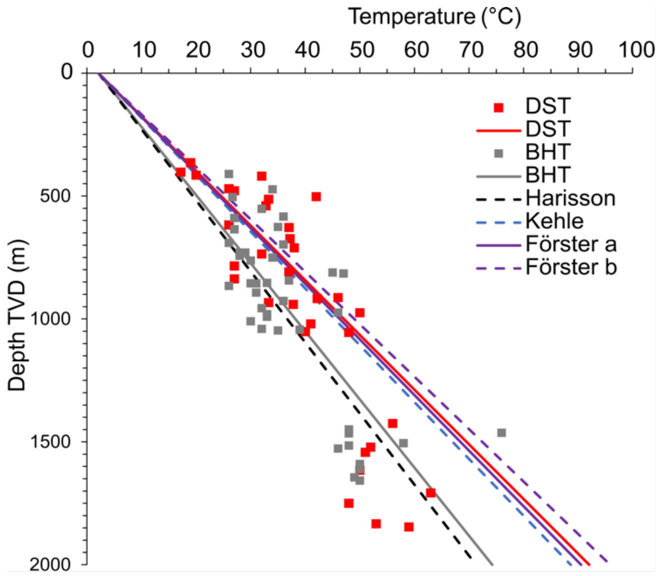

Figure 5.6. Uncorrected BHTs for the South Slave Region showing linear regression for corrected BHT compared to DST temperature and its trendline.

Due to the depth for which the correction method is developed, only one BHTs out of four in Ft. Providence and two out of the three in Enterprise could be corrected for the drilling disturbances (Table 5.4). Nevertheless, the non-corrected BHTs above minimum correction depth were kept to calculate the average geothermal gradient since measurements are relatively shallow and drilling disturbances expected to be less important. Only DST temperatures were available for Hay River.

Table 5.4. Temperature corrected for paleoclimates in each community.

		DST (*n*=5)	Paleoclimate T_i=-5°C	BHT (*n*=4)	Förster (b)	Paleoclimate T_i=-5°C
Fort-Providence	Min	20.0	21.4	26.7	41.3	43.1
	Max	37.0	38.8	36	41.3	43.1
		DST (*n*=7)	**Paleoclimate T_i=-5°C**	**BHT (*n*=14)**	**Khele**	**Paleoclimate T_i=-5°C**
Kakisa	Min	28.0	30.0	28.0	33.2	35.2
	Max	42.2	44.3	45.0	50.7	52.8
		DST (*n*=5)	**Paleoclimate T_i=-5°C**	**BHT (*n*=0)**		
Hay River	Min	19.0	20.3			
	Max	42.0	43.6			
		DST (*n*=2)	**Paleoclimate T_i=-5°C**	**BHT (*n*=3)**	**Harisson**	**Paleoclimate T_i=-5°C**
Enterprise	Min	17.2	18.6	27.0	23.6	25.5
	Max	56.0	58.5	34.0	21.2	22.9

n= number of temperature measurements

The most accurate correction method when analyzing each community individually is Förster (b) in Ft. Providence and Khele in Kakisa. Harisson method provided a better correlation with DST temperatures in Enterprise (Figure 7). It should be noted that the

Harisson correction lowers the corrected temperature when the depth is less than 1000 m. The corresponding corrected temperature range is given in the Table 5.4.

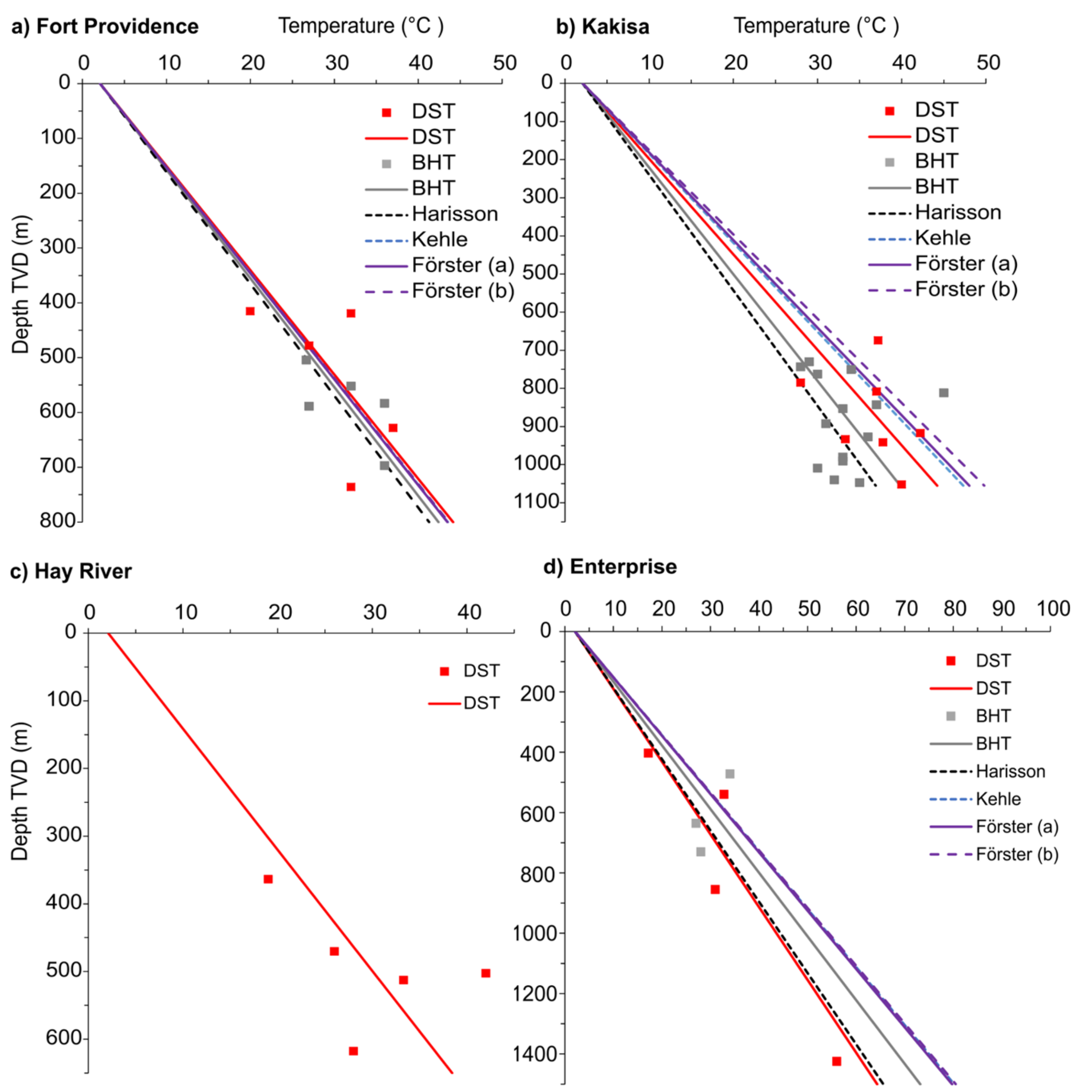

Figure 5.7. Uncorrected BHTs with the regression lines from corrected BHTs compared to DSTs temperature trendline for each community of the South Slave Region.

5.6.2 Paleoclimate correction

The temperature correction varies between 1.1 °C and 2.5 °C from 364 m to 1846 m depth (Figure 5.8). The temperature ranges at each community are presented in Table 5.4.

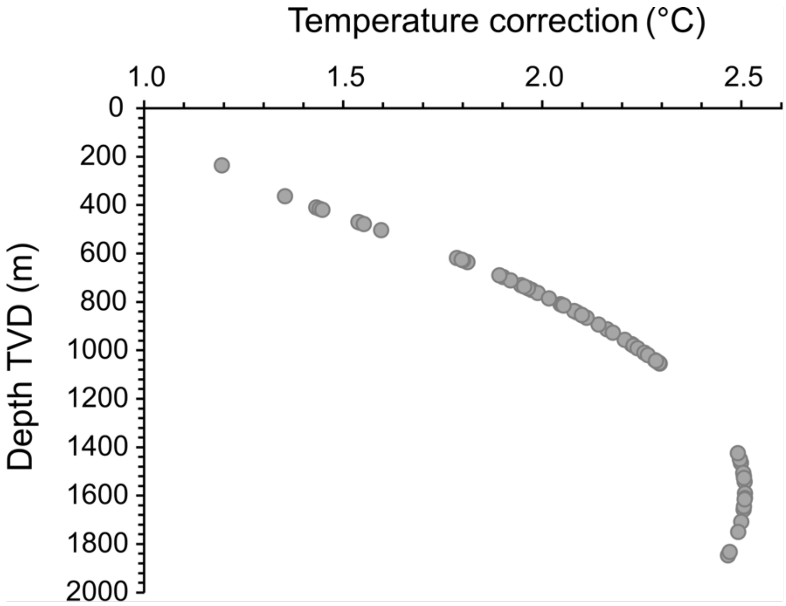

Figure 5.8. Paleoclimate temperature correction calculated as a funcion of depth at which DST and BHT were measured in the South Slave Region.

5.6.3 Geothermal gradient

The geothermal gradients calculated from the BHTs recorded in 42 wells are from 27.6 °C km^{-1} to 55.1 °C km^{-1} with a mean of 36.1 ± 7.7 °C km^{-1}. After the drilling correction, the range of geothermal gradient is from 35.4 °C km^{-1} to 62.6 °C km^{-1} with an average of 44.3 ± 7.2 °C km^{-1}. The paleoclimate correction on DST temperatures and corrected BHTs revealed an average geothermal gradient of 45.6 ± 12.8 °C $km^{-1}$and 46.4 ± 7.5 °C km^{-1}, respectively (Table 5.5).

Table 5.5. Geothermal gradient (°C km^{-1}) in the South Slave Region.

	DST (*n*=33)	Paleoclimate T_i=-5°C	BHT (*n*=42)	Förster (a)	Paleoclimate T_i=-5°C
Min	26.2	27.7	27.6	35.4	37.8
Mean	43.1	45.6	36.1	44.2	46.4
Max	79.4	82.5	55.1	62.6	65.1
St.Dev.	12.3	12.8	7.7	7.2	7.5

n= number of temperatures

The temperature gradients are summarized per community. After applying the paleoclimate correction, the most reliable estimate of the geothermal gradient under Ft. Providence was determined from DST temperatures and is 55.7 ± 12.3 °C km^{-1}. Despite the fact that the number of BHTs and DST temperatures was the same, only one of the four BHT data points is deep enough to be corrected, and resulted in a lower geothermal gradient of 54.8 ± 6.4 °C km^{-1}. In Kakisa, twice as many BHTs are available than DSTs; these corrected BHTs provide the most reliable estimate of the geothermal gradient of 45.2 ± 6.6 °C km^{-1}. Hay River showed the highest mean geothermal gradient of 59.1 ± 14.9 °C km^{-1} calculated from DST temperatures only. In Enterprise, the most reliable estimate for the geothermal gradient of 44.1 ± 10.6 °C km^{-1} was obtained from the corrected DST temperatures. Despite the fact that the corrected BHTs gave higher values, it is noted that only two BHTs out of the three could be corrected for drilling disturbances due to their shallow depth and the shallow non-corrected temperatures are kept for paleoclimate correction (Table 5.6 and Figure 5.9).

Table 5.6. Geothermal gradient g (°C km^{-1}) in each community.

		DST (*n*=4)	Paleoclimate T_i=-5°C	BHT (*n*=5)	Forster (b)	Paleoclimate T_i=-5°C
Fort-Providence	Min	40.6	43.3	42.3	42.3	45.2
	Mean	52.6	**55.7**	50.4	51.9	54.8
	Max	71.3	74.8	58.1	58.1	61.0
	St.Dev	12.2	12.3	6.0	6.4	6.4
		DST (*n*=7)	**Paleoclimate T_i=-5°C**	**BHT (*n*=14)**	**Khele**	**Paleoclimate T_i=-5°C**
Kakisa	Min	33.0	35.6	27.6	34.8	37.0
	Mean	39.9	42.6	35.8	42.8	**45.2**
	Max	60.9	35.6	52.9	59.9	62.4
	St.De	6.9	7.0	6.6	6.5	6.6
		DST (*n*=5)	**Paleoclimate T_i=-5°C**	**BHT (*n*=0)**		
Hay River	Min	41.9	44.8			
	Mean	55.9	**59.1**			
	Max	79.4	82.5			
	St.Dev	14.9	14.9			
		DST (*n*=4)	**Paleoclimate T_i=-5°C**	**BHT (*n*=3)**	**Harisson**	**Paleoclimate T_i=-5°C**
Enterprise	Min	33.8	36.2	35.5	29.4	32.8
	Mean	41.5	**44.1**	47.4	42.3	45.7
	Max	56.8	59.8	67.5	67.5	70.8
	St.Dev	10.4	10.6	17.5	21.8	20.8

n= number of temperature measurements. The most reliable estimate of the geothermal gradient is in bold.

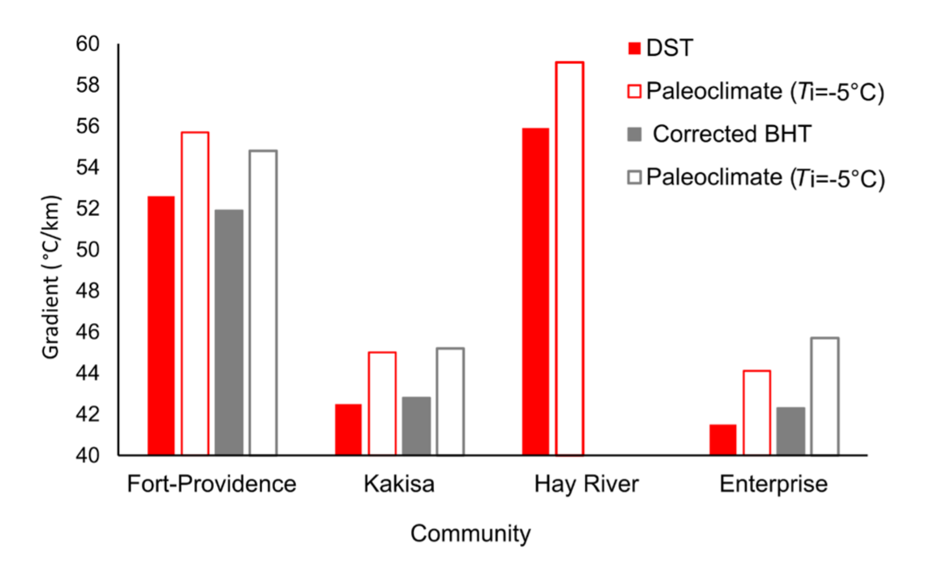

Figure 5.9. Geothermal gradient estimates of the four South Slave communities.

The average geothermal gradient measured which was affected by the glaciations, in the six Cameron Hill wells is from 35.4 °C km^{-1} to 43.7 °C km^{-1}, and the paleoclimate correction increases the geothermal gradient from 36.4 °C km^{-1}to 44.6 °C km^{-1} (Table 5.7).

Table 5.7. Geothermal gradient g (°C km^{-1}) from Cameron Hills wells.

Well short name	Measured gradient (°C km^{-1})	Gradient paleoclimate T_i=-5°C (°C km^{-1})
A-73	39.2	40.2
E-07	43.7	44.6
I-10	35.4	36.4
I-74	42.5	43.5
L-44	37.8	38.8
M-49	43.5	45.3

5.6.4 Verification with temperature profiles from Cameron Hills

5.6.4.1 Heat flow evaluation for Cameron Hills

Table 5.8 shows the evaluation of the heat flow considering the thermal conductivity from Table 5.3. The heat flow is from 80.6 mW m^{-2} to 115.8 mW m^{-2} and the paleoclimate correction increased the range to 83.0 mW m^{-2} to 120.6 mW m^{-2}.

Table 5.8. Surface heat flow from Cameron Hills wells.

Well short name	Q_o (mW m^{-2})	Q_o paleoclimate T_i=-5°C (mW m^{-2})
A-73	104.1	106.8
E07	113.8	116.0
I-10	80.6	83.0
I-74	105.7	108.3
L-44	102.5	105.1
M-49	115.8	120.6

5.6.4.2 Temperature-depth model

Calculated temperature is compared to measured temperature in the Cameron Hills (Figure 5.10). The maximum difference is 3.6 °C. Thermal conductivity assigned to the Cameron Hills formations seems logical and allows for observed temperatures to be reproduced.

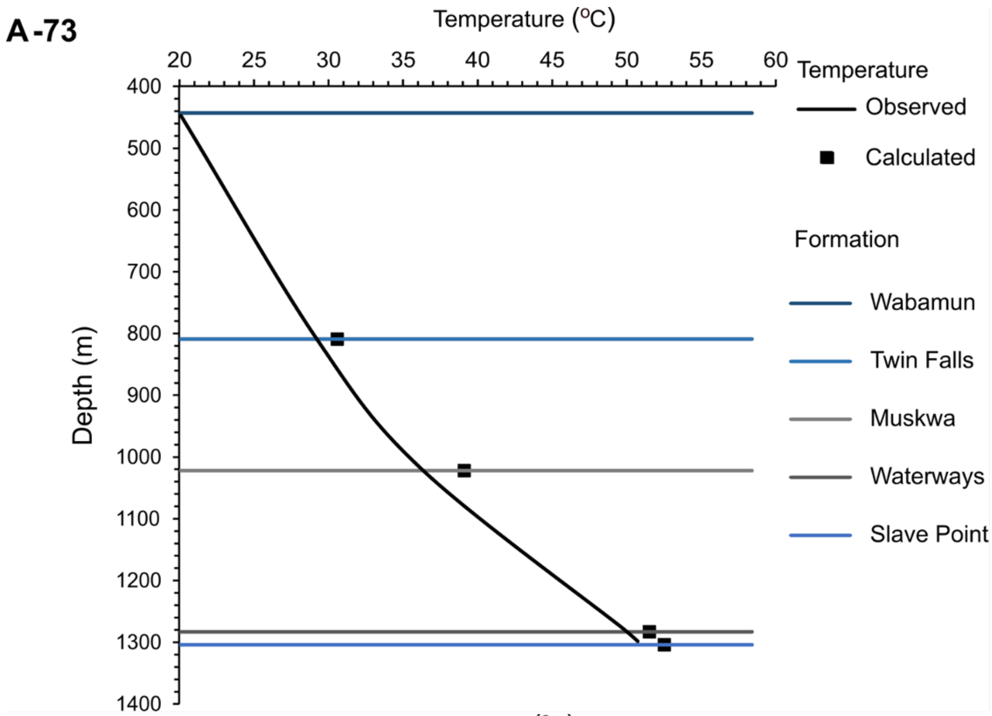
A -73
Temperature (°C)
20 25 30 35 40 45 50 55 60
Depth (m)
400 500 600 700 800 900 1000 1100 1200 1300 1400
Temperature
Observed
Calculated
Formation
Wabamun
Twin Falls
Muskwa
Waterways
Slave Point

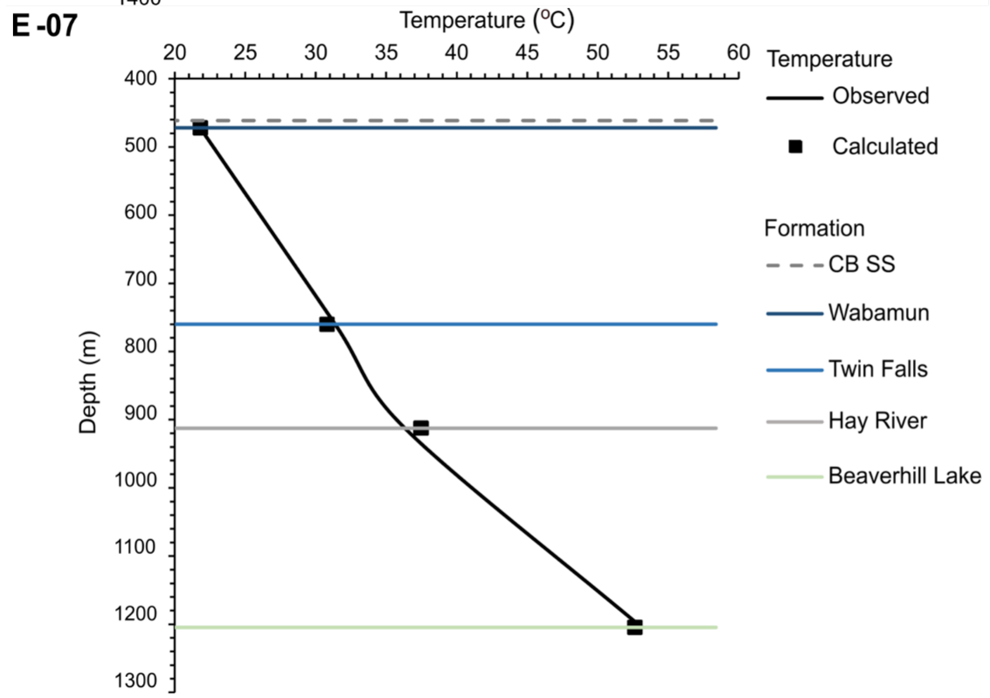
E -07
Temperature (°C)
20 25 30 35 40 45 50 55 60
Depth (m)
400 500 600 700 800 900 1000 1100 1200 1300
Temperature
Observed
Calculated
Formation
CB SS
Wabamun
Twin Falls
Hay River
Beaverhill Lake

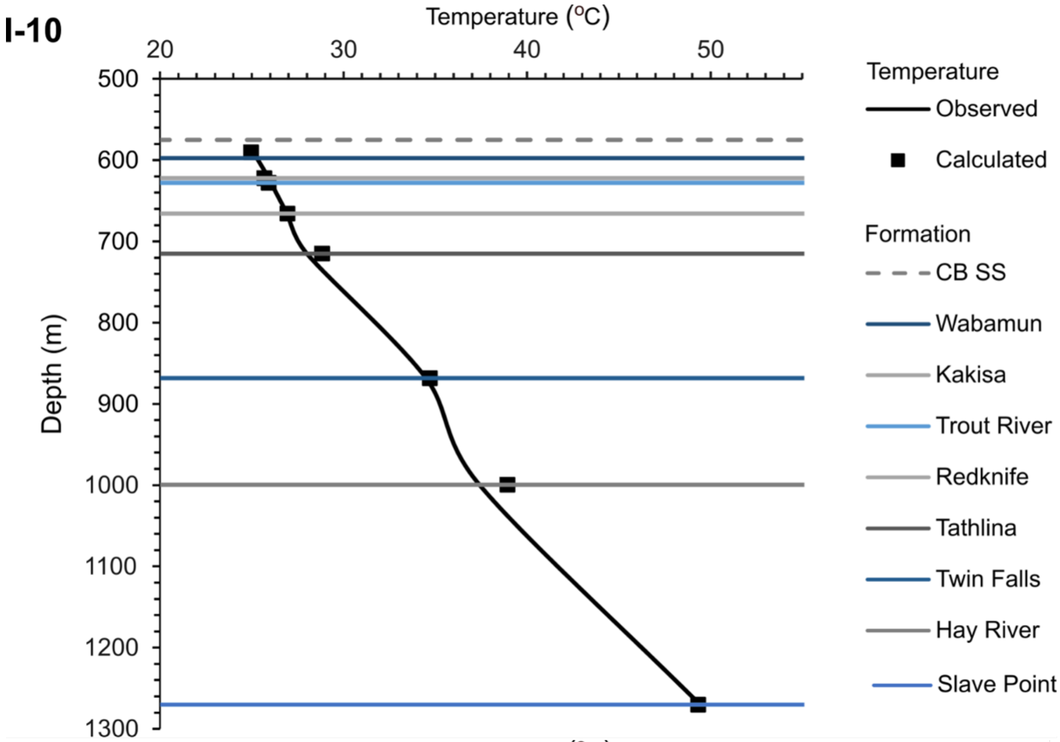
I-10
Temperature (°C)
20
30
40
50
500
600
700
800
900
1000
1100
1200
1300
Depth (m)
Temperature
Observed
Calculated
Formation
CB SS
Wabamun
Kakisa
Trout River
Redknife
Tathlina
Twin Falls
Hay River
Slave Point

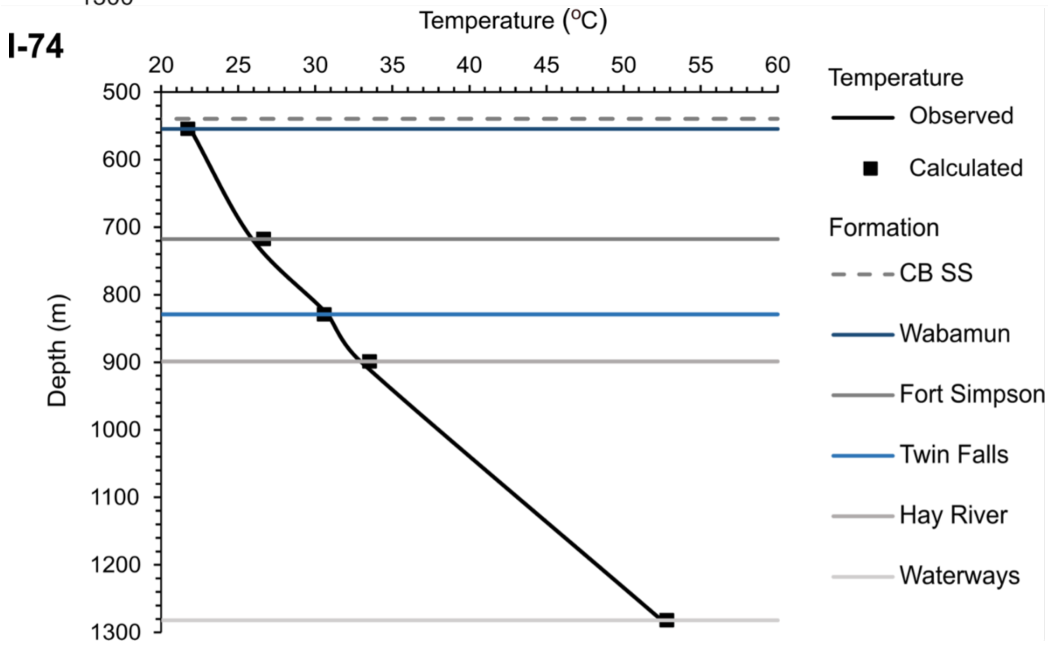
I-74
Temperature (°C)
20
25
30
35
40
45
50
55
60
500
600
700
800
900
1000
1100
1200
1300
Depth (m)
Temperature
Observed
Calculated
Formation
CB SS
Wabamun
Fort Simpson
Twin Falls
Hay River
Waterways

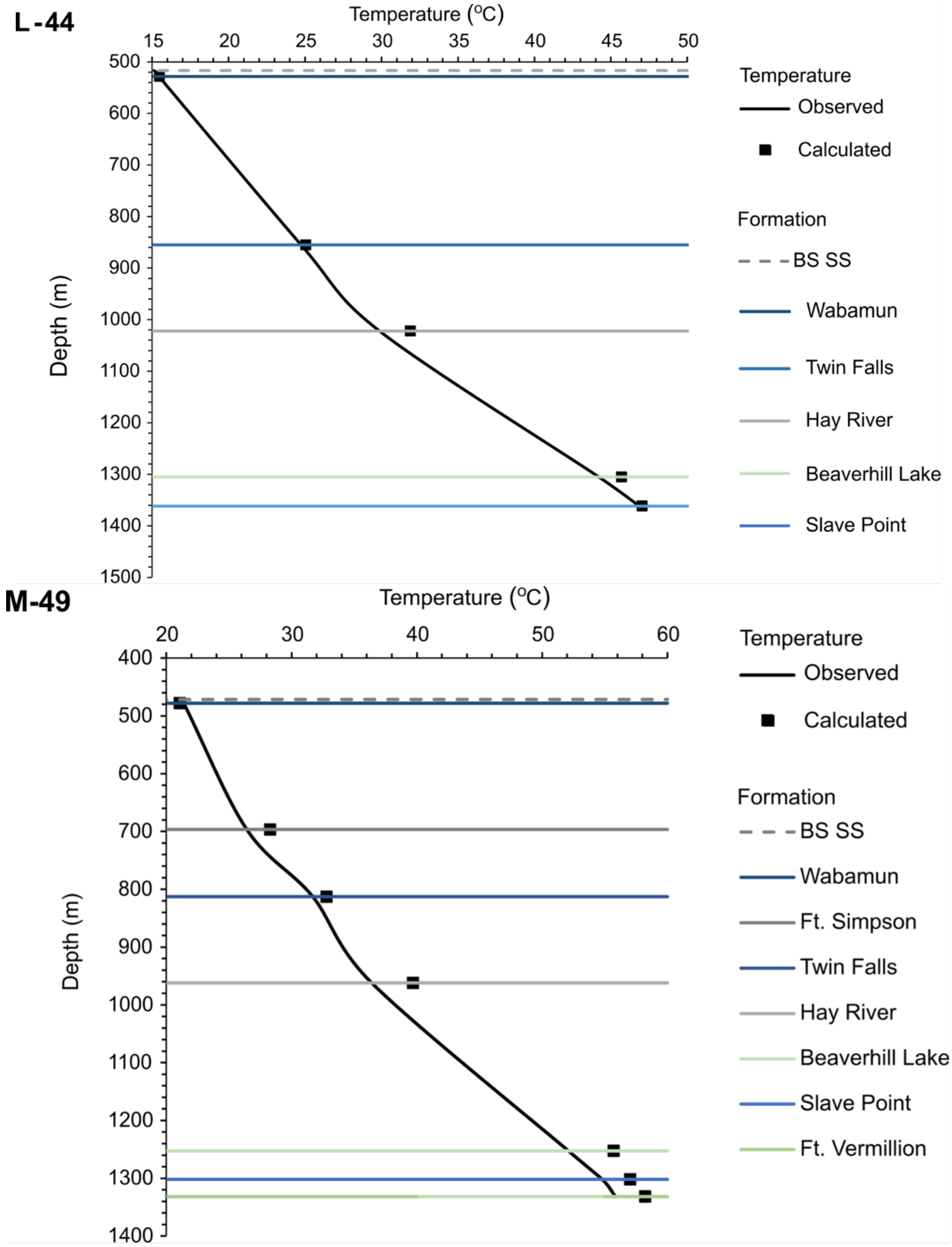

Figure 5.10. Calculated temperature plotted against observed temperature recorded in the six wells of Cameron Hills region.

5.6.5 Prediction of temperature profiles for South Slave Communities

5.6.5.1 Heat flow evaluation for South Slave Communities

At the community level, the most logical estimation of the heat flow was determined from the most reliable estimate of the geothermal gradient, presented in Table 5.5. Heat flow assessments are either based on DST or BHT corrected for drilling disturbances, and both temperature data were corrected for paleoclimate effects. The estimate of the surface heat flow in Ft. Providence is 131.5 mW m^{-2}, 105.5 mW m^{-2} in Kakisa, 160.2 mW m^{-2} in Hay River, and 109.3 mW m^{-2} in Enterprise (Figure 5.11).

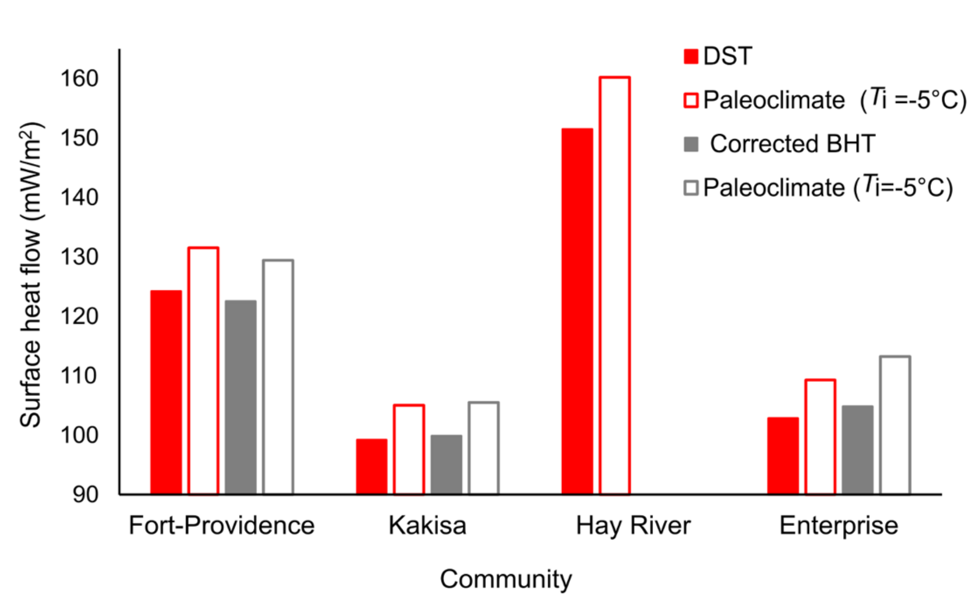

Figure 5.11. Heat flow estimated for communities of the South Salve Region.

5.6.5.2 Temperature depth model

For all communities, the temperature varies from ~3.2 °C under the Quaternary cover to 33.3 °C at the basement top, with the maximum of 36.5°C in Hay River where the basement top is at 614 m depth. Temperature profiles for Fort Providence, Kakisa, and Enterprise are similar to each other due to the thick shale formations underlying the communities. The maximum temperature reached for these communities is 33.1 °C at the top of the crystalline basement (Figure 5.12).

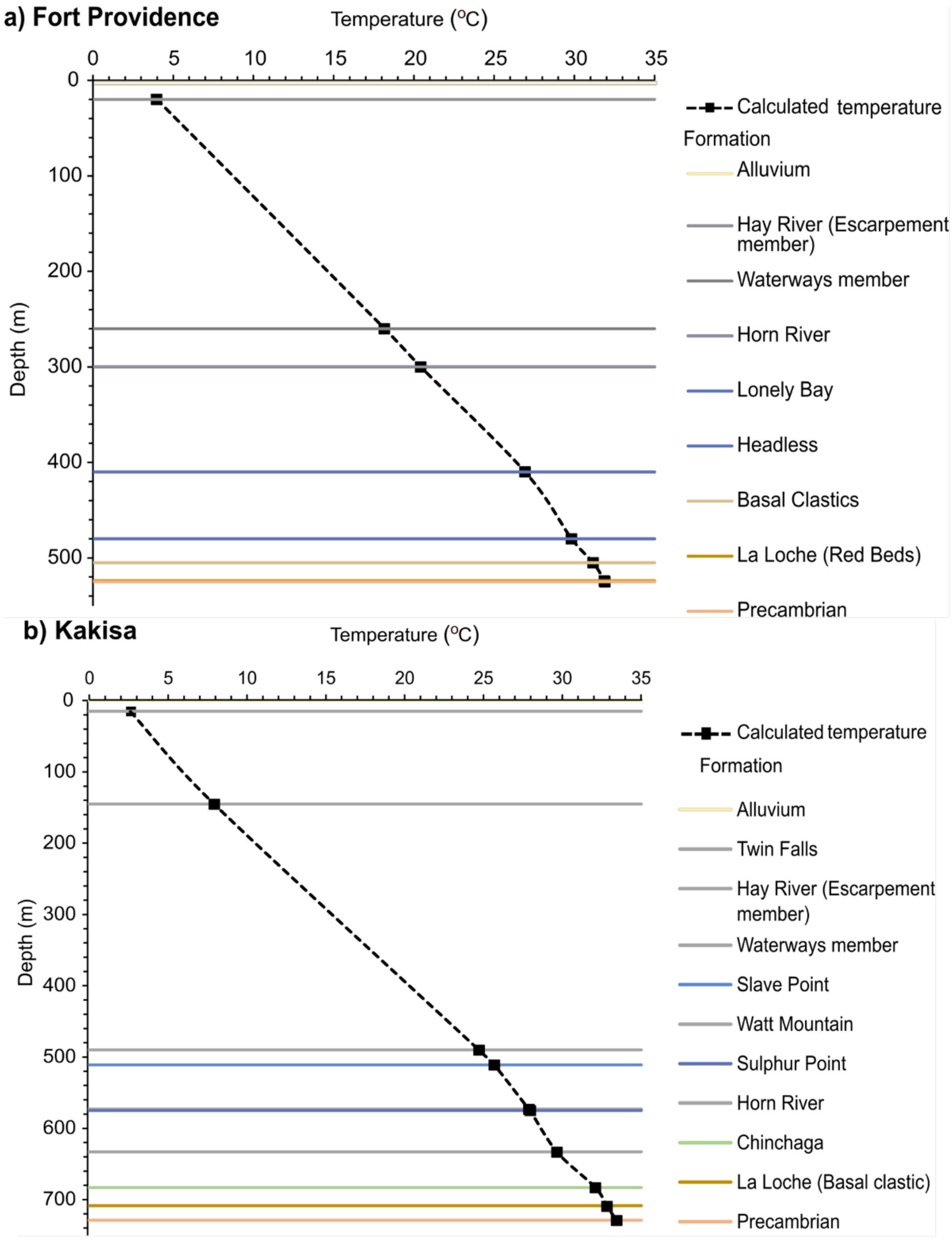
a) Fort Providence
Temperature (°C)
0
5
10
15
20
25
30
35
Depth (m)
0
100
200
300
400
500
Calculated temperature
Formation
Alluvium
Hay River (Escarpement member)
Waterways member
Horn River
Lonely Bay
Headless
Basal Clastics
La Loche (Red Beds)
Precambrian
b) Kakisa
Temperature (°C)
0
5
10
15
20
25
30
35
Depth (m)
0
100
200
300
400
500
600
700
Calculated temperature
Formation
Alluvium
Twin Falls
Hay River (Escarpement member)
Waterways member
Slave Point
Watt Mountain
Sulphur Point
Horn River
Chinchaga
La Loche (Basal clastic)
Precambrian

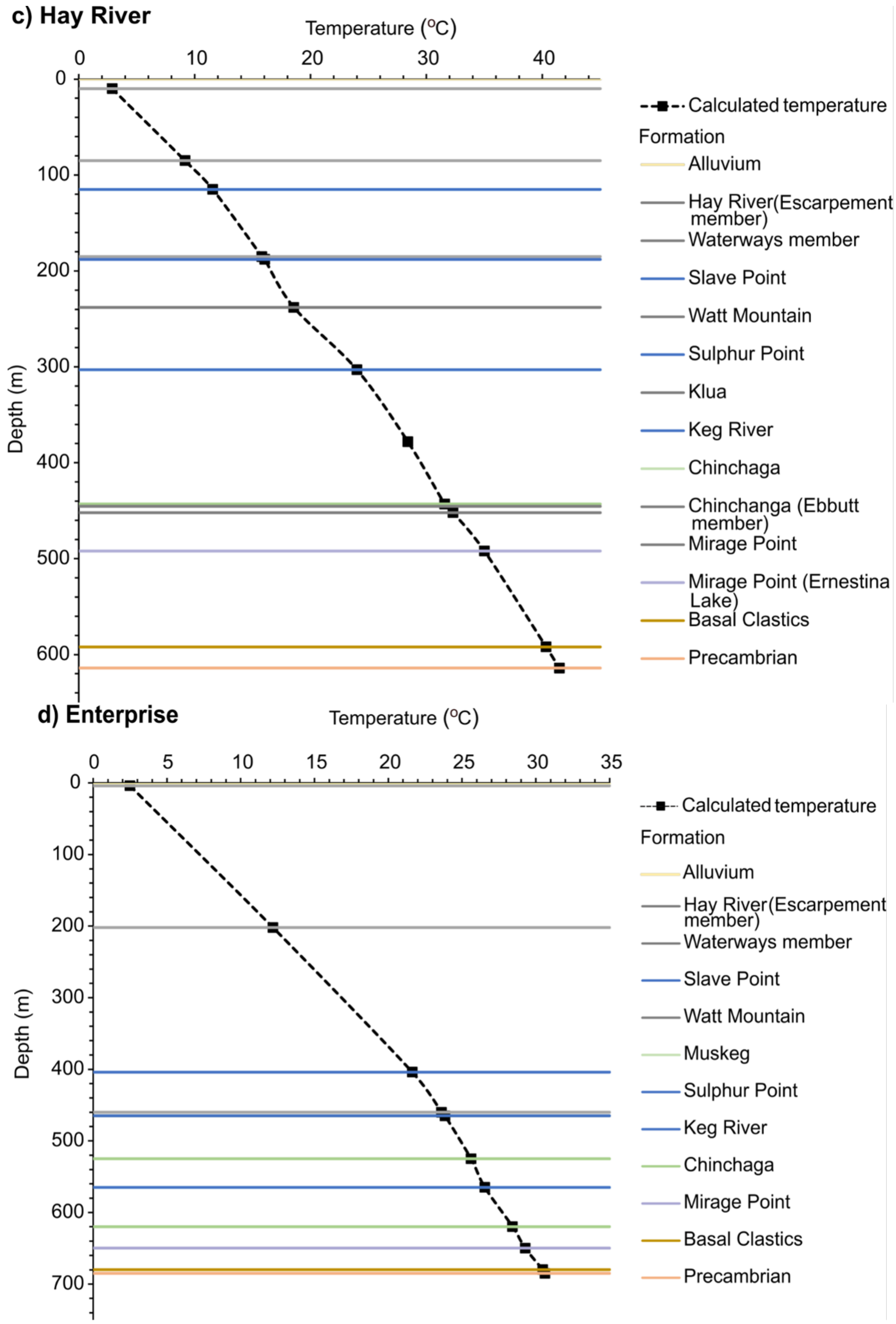

Figure 5.12. Predicted temperature profiles superposed to the formation tops below each South Slave community.

5.7 Discussion

Analyses of BHT and DST data (75 readings) from the South Slave Region yielded a local geothermal gradient varying from 45.2 ± 6.6 °C km^{-1} to 59.1 ± 14.9 °C km^{-1} below the communities of Ft. Providence, Kakisa, Hay River, and Enterprise. Heat flow estimates varies from 105.7 mW m^{-2} to 160.2 mW m^{-2} under these communities. These values are comparable to heat flow calculated in the Cameron Hills region where equilibrium temperature profiles were used for verification (Table 5.8 and Figure 5.11). The regional temperature distribution throughout the WCSB was previously mapped by other researchers (e.g., Gray et al., 2012; Majorowicz & Grasby, 2010a). High geothermal gradients (>35 °C km^{-1}) were estimated in the NWT North of 65° latitude with values of 40 °C km^{-1} to 50 °C km^{-1} East of the Mackenzie Mountains (Grasby et al., 2013). Our work suggest elevated geothermal gradients and heat flows under four communities in the Southern NWT, and confirmed the previous elevated geothermal gradient estimates. These results indicate significant geothermal potential in the communities of Ft. Providence and Hay River. The geothermal gradient in Kakisa and Enterprise is expected to be > 40 °C km^{-1}, which is highly favourable, but the small population of those communities could be a challenge for economic exploitation of the geothermal resource.

For this study, no information on the quality of the temperature readings was available, since this relates to the flow rate during the DST and to the mud circulation time for BHT measurements (Grasby et al., 2013). Limited temperature data was available for each community as they are located in a remote Northern region. The number of temperature data points available in each community was the criterion to determine the most reliable type of data to estimate the geothermal gradient from the group of wells near each community. A large number of BHTs were favoured when possible, but the number of DST temperature was more important for three communities (Ft. Providence, Hay River, and Enterprise).

Measured temperatures from six wells in Cameron Hills was used to verify our thermostratigraphic approach for temperature predictions. A similar approach that uses equilibrium temperature was done for several basins in the USA (e.g., Crowell et al., 2012; Crowell & Gosnold, 2011). Majorowicz et al. (1999) concluded that even corrected BHTs tend to be systematically higher compared to equilibrium temperature measurements of shallow basins (from 500 to 900 m depth) for wells in the Rocky Mountain Foothills and at the Western edge of the WCSB, and that shallow BHTs contain systematic errors. This was also confirmed and discussed by the works of Gray et al. (2012) who estimated the geothermal gradient and regionally mapped the geothermal anomalies of the WCSB. The discrepancies between calculated and observed temperature can be explained by many factors, but the input temperature remains the parameter that has the highest impact on the final geothermal gradient and heat flow estimation (Bédard et al., 2018). It should also be noted that only Kakisa and Enterprise have temperature data recorded at depth greater than 1 km (Figure 5.7), resulting in the two communities having the lowest gradient, but one comparable to the values of Cameron Hills. It is therefore possible that considering data from a shallow depth, like Hay River, resulted in overestimating the geothermal gradient.

Our analyses have demonstrated that the temperature predicted below the four communities present similar trends to that measured for Cameron Hills. The range of thermal conductivity is a source of uncertainty, but verification with temperature profiles in Cameron Hills resulted in small differences of 3.61 °C between calculated and measured temperatures (Figure 5.10). The radiogenic heat production is part of the assessable intrinsic property of the rock that cannot be ignored in the equation of the heat flow. However, it had a relatively minor impact for the calculation made in this study since the total thickness of the sedimentary rock formations is less than 1 km and temperature predictions are for a relatively shallow depth. The heat production rate calculated from either radiogenic element content (determined with inductively coupled plasma techniques) or gamma ray is similar for the geological formations common to the South Slave communities (Table 5.2) and the

Cameron Hills (Table 5.3).

The thermal conductivity is assumed to be uniform in each geological formation, and is responsible for changes in geothermal gradient at geological formation contacts. Lithologies with a lower thermal conductivity shows a relatively more rapid increase in temperature with depth (Figure 5.12). The most prominent lithologies below the South Slave communities are shales and carbonates. Their estimated thermal conductivity is consistent with thermal conductivity of the typical sedimentary rocks in the WCBS, and have values from 1.4 ± 0.4 W m^{-1}K^{-1} to 2.1 ± 0.4 W m^{-1} K^{-1} in shale, 2.4 ± 0.9 W m^{-1} K^{-1} to 3.4 ± 3.0 Wm^{-1} K^{-1} in limestone, 3.1 ± 1.4 W m^{-1} K^{-1} to 5.0 ± 0.6 Wm^{-1}K^{-1} in dolomite and 2.8 W m^{-1} K^{-1} to 4.7 ± 2.8 W m^{-1} K^{-1} in sandstone (e.g., . The low harmonic average of thermal conductivity estimated for sedimentary rocks below the four communities (~2.5 W m^{-1} K^{-1}) reveal its blanketing effect and can partially explain the high geothermal gradient given by the significant thickness of shales in this high heat flow region (Figure 5.4, Figure 5.12). Furthermore, the area of interest is located at the edge of the platform where major faults and shear zones affected the basement in an extensional tectonic regime (Figure 5.3). Majorowicz (1996) proposed that this heat flow anomaly is due to an increased mantle upflow beneath the region, coinciding with crustal faults such as the Great Slave Lake shear zone that separates the Churchill and Salve Provinces and potentially continues under the sedimentary basin (e.g., Eaton & Hope, 2003; Yin et al., 2014, Figure 5.3).

This study improved the geothermal knowledge of the South Slave Region by using recently acquired information on thermal properties to evaluate heat flow and interpolate subsurface temperature from the surface to the top of the crystalline basement. The regional and deep basement faults that cross the communities (Figure 5.2) could have an influence on the permeability and convective heat transfer. However, an analysis of the structural context was not addressed in this study. Natural hydrothermal systems are commonly present in fractured rocks, and typically associated with extensional faulting (e.g., Faulds et al., 2010; Moeck, 2012; Rajaobelison et al., 2022). This is a limitation of our study that focused on conductive heat transfer mechanisms only.

5.8 Conclusions

Compilation of DST temperature and BHT that were corrected for drilling disturbances allowed evaluation of the geothermal gradient and heat flow below communities of the South Slave Region to subsequently predict the temperature-depth distribution in the sedimentary basin formations. The current estimation of the geothermal gradient is > 40 ˚C km^{-1} and up to 100 mW m^{-2} for heat flow.

The result indicates high geothermal gradient and high surface heat flow suitable for direct use of geothermal resources at the depth of sedimentary rock formations according to the Lindal diagram (Lindal, 1973). The communities, particularly Hay River, could potentially exploit the geothermal resource. Here, the high geothermal gradient could facilitate exploitation at shallow drilling depth and result in potentially economic projects.

Based on these models, the heat flow in the South Slave Region would be the highest of all the WCSB, but geothermal exploration boreholes will have to be drilled to confirm these results. Drilling exploration wells and measuring equilibrium temperature profiles are the next steps to confirm our finding and eventually exploit geothermal resources. The use of thermally equilibrated temperature measurement data from wells in the Cameron Hills allowed verification of our model to determined if the thermal conductivities assigned to the geological formations underlying the South Slave communities is logical, using formations common to both areas (Twin Falls, Hay River, and Slave Point Formations). The thermal conductivity values of the sedimentary rocks varies from 1.4 W m-1 K^{-1} to 3.5 W m-1 K^{-1}. However, the nature and the thermal properties of the Precambrian basement below the sedimentary basin at the location of the South Slave communities need to be defined in future work in order to extrapolate the temperature at depth below the basin. Evaluating the thermal conductivity of the crystalline basement will be crucial to get a reliable estimate of temperature in deep basement rocks.

In the Northwest Territories, other communities like Fort Simpson, Jean Marie River, Nahanni Butte and Fort Liard also have a high geothermal potential and are situated in a similar geological setting. The methodology presented in this article could be applied for a better evaluation of the geothermal potential at these locations.

5.9 Supplementary data

DST and uncorrected BHT are presented as a Supplementary data. The following supporting information can be downloaded at: https://www.mdpi.com/article/10.3390/en17164165/s1, Table S1: DSTs and uncorrected BHTs.

5.10 Acknowledgements

We would like to thank Hickson C. J. (Smejkal et al., 2023) who made available the temperature data of Cameron Hills wells through the collaborative work of geothermal development and energy sustainability decisions in the Dehcho Region. This project was funded by GEM-GeoNorth program of Natural Resources Canada.